UNIVERSITY OF CALIFORNIA

Santa Barbara

Developing Methods for Discovering Non-Natural and pH Switching Aptamers

A dissertation submitted in partial satisfaction of the
requirements for the degree Doctor of Philosophy
in Materials

by

Chelsea Kathleen Lyons Gordon

Committee in charge:

Professor H. Tom Soh, Chair

Professor Craig Hawker

Professor Cyrus Safinya

Professor Erkki Ruoslahti

March 2018

The dissertation of Chelsea Kathleen Lyons Gordon is approved.

_____

Craig Hawker

_____

Cyrus Safinya

_____

Erkki Ruoslahti

_____

H. Tom Soh, Committee Chair

March 2018

Developing Methods for Discovering Non-Natural and pH Switching Aptamers

by

Chelsea Kathleen Lyons Gordon

ACKNOWLEDGEMENTS

First, I would like to acknowledge all of those who contributed to different parts of these projects: Jia Niu, Andrew Csordas, Anusha Pusuluri, Elizabeth Bagley, Diana Wu, Trevor Feagin, Margaret Nakamoto, Peter Mage, Gary Braun, and Aman Mann. This work would not have been possible without their help. I would like to thank Andrew Csordas and JP Wang for training me when I joined the lab and for lots of valuable advice. Jia Niu has also been a wonderful mentor, and it has been a privilege to work with him. I also want to thank all my other labmates past and present for countless helpful ideas and conversations. My advisor, Prof. Tom Soh, has given me his support and guidance over the past several years, and I am so grateful for the opportunity I have had to work in his lab. I also want to thank the other members of my committee for their guidance: Prof. Craig Hawker, Prof. Cyrus Safinya, and Prof. Erkki Ruoslahti. I also need to thank all of my friends and family who have supported me in my life outside the lab. My parents, Michael and Christine Lyons, have been a constant source of encouragement, and I will be forever grateful for their love and support. I have too many incredible family members to list them all here, but I particularly want to recognize my brothers, Nate, Zach, and Luke Lyons; my grandparents, Clem and Bea Clement, Walt and Patty Lyons, and Kathy Lyons; and my in-laws, Stephanie, Robert, Maeve, and Anna Gordon. Finally, I want to thank my husband Luke and my daughter Lucy, who fill my life with so much joy.

VITA OF CHELSEA KATHLEEN LYONS GORDON
March 2018

EDUCATION

Bachelor of Science in Materials Science and Engineering, MIT, June 2012
Doctor of Philosophy in Materials Engineering, University of California, Santa Barbara, March 2018

PROFESSIONAL EMPLOYMENT

Summer 2010: Internship, Harris Orthopaedic Biomechanics and Biomaterials Laboratory, Massachusetts General Hospital
Summer 2011: Internship, International Iberian Nanotechnology Laboratory, Braga, Portugal
Summer 2012: Process engineering internship, Xerox, Webster, NY

PUBLICATIONS

Niu, J.,*** Gordon, C. K. L**,***** Bagley, E. R., Wu, D., Pusuluri, A., Feagin, T. A., Csordas, A. T., Nakamoto, M., Eisenstein, M., Hawker, C. J., Soh, H. T. "Rapid Screening of Carbohydrate-Nucleic Acid Hybrid Reagents for Highly Specific Lectin Recognition," in revision, 2018.

Oral, E., Neils, A. L., **Lyons, C**., Fung, M., Doshi, B. and Muratoglu, O. K. (2013), Surface cross-linked UHMWPE can enable the use of larger femoral heads in total joints. J. Orthop. Res., 31: 59–66. doi:10.1002/jor.22195

ABSTRACT

Developing Methods for Discovering Non-Natural and pH Switching Aptamers

by

Chelsea Kathleen Lyons Gordon

Molecular recognition of disease biomarkers is essential for the detection, monitoring, and treatment of disease. Antibodies, which detect target antigens, have enabled the rapid growth of molecular detection assays and targeted therapies. Despite this, antibodies remain time- and cost-intensive to produce and often have severe limitations in specificity and reproducibility. Aptamers, single stranded DNA or RNA affinity reagents, are a promising alternative. Aptamers are produced *in vitro*, and they can be chemically synthesized reliably. However, traditional aptamer discovery methods suffer from low enrichment of high affinity aptamers, and aptamer selections frequently fail or yield poor aptamers. Most methods are also constrained by the limited chemical diversity of natural DNA, limiting targets to those with affinity to DNA. Additionally, traditional methods isolate aptamers based only on binding affinity, and it is difficult to generate aptamers with desired functions beyond binding.

Our lab has developed a method called particle display that uses high-throughput, quantitative screening to efficiently isolate high affinity aptamers. Here, we discuss three projects that build on this method to address critical limitations of existing aptamer discovery methods. First, we used this platform to identify an aptamer for p32, a tumor biomarker, with low nanomolar affinity. Next, we extended this method to screen for non-natural DNA

aptamers, expanding the chemical diversity of DNA without complex synthesis or polymerase engineering. We generated a mannose-modified DNA aptamer with high affinity and specificity to its target, concanavalin A. Finally, we developed a method to generate pH switching aptamers, for potential use in drug delivery or intracellular sensing. A streptavidin aptamer with pH dependent binding was discovered, and its pH active domain was identified. Together, these methods enable the development of highly functional aptamers for the detection of important biological targets.

TABLE OF CONTENTS

LIST OF FIGURES

LIST OF TABLES

Chapter I. Introduction

A. Antibodies—paving the way for molecular recognition

Monoclonal antibodies (mAbs), developed in 1975,[1] were a breakthrough technology in biology and medicine. By specifically detecting target antigens, mAbs have enabled countless developments in biomedical research, including targeted therapies and molecular diagnostics.[2,3] However, mAbs have some critical limitations. Generating mAbs is a time-, cost-, and labor-intensive process, and targets are limited to those that produce an appropriate immune response in the host animal.[4,5] Monoclonal antibodies have better reproducibility than polyclonal antibodies, but even monoclonal antibodies require ongoing validation because of variation between batches. On top of that, studies have shown that over half of commercial antibodies have severe performance issues, including poor specificity, cross-reactivity, or even no activity at all.[6]

B. Aptamers—synthetic nucleic acid affinity reagents

Aptamers, synthetic nucleic acid affinity reagents,[7] offer several advantages over mAbs. One central advantage is that aptamers are produced by *in vitro* directed evolution (systematic evolution of ligands by exponential enrichment, or SELEX) rather than *in vivo* processes, eliminating the batch-to-batch variability that plagues antibodies. Once an aptamer has been discovered, it can be chemically synthesized easily and reproducibly given only its sequence information. Although aptamers have been generated for a variety of targets, issues with aptamer discovery remain. First, traditional SELEX methods suffer from a low enrichment rate, a measure of how efficiently high affinity aptamers are enriched in each round. The enrichment rate determines the outcome of the experiment—success or failure, and the quality of the discovered aptamers. Ten or more rounds of selection are often required due to high background and inefficient partitioning. This can lead to PCR bias and

the emergence of artifacts, enriching sequences that amplify easily or bind to the solid support rather than true target binders. Second, many SELEX experiments have little or no selection for specificity. This leads to aptamers with poor or unreported specificity, greatly limiting their utility. Third, SELEX is designed to isolate high affinity aptamers, but there typically is not a way to evolve other desired functions. Finally, many traditional SELEX methods are constrained by the limited chemical diversity of natural DNA. Incorporating chemical modifications is desirable because natural DNA has low affinity to several important classes of targets, such as glycans and other small molecules. However, synthesizing nucleotides with all modifications of interest and the polymerase engineering often required to incorporate them are serious hurdles to the use of non-natural DNA in aptamer selections. Better aptamer discovery methods are required to develop highly functional aptamers for a wide range of targets.

C. Particle Display—overcoming the limitations of SELEX

Our lab has developed an aptamer discovery platform called particle display to overcome the limitations of SELEX. Here, we will describe methods developed to address three of the problems discussed above: (1) low enrichment of high affinity aptamers, (2) limited selection for specificity, and (3) minimal capacity to evolve functions other than binding. Particle display uses high-throughput, quantitative screening of monoclonal aptamer particles to efficiently enrich high affinity aptamers. This section will describe this method and its evolution to date. Our lab has extended the particle display platform to include simultaneous screening for affinity and specificity, using a method called multiparameter particle display. Two methods for functional screening have also been developed to directly

generate “assay ready” aptamers: particle display of aptamer pairs and structure-switching particle display. These methods demonstrate the versatility of the particle display platform.

1. Particle display—efficient enrichment of high affinity aptamers

The fundamental limitation of traditional SELEX is poor efficiency of aptamer enrichment. Analysis has shown that the theoretical maximum enrichment of a given aptamer relative to a lower affinity aptamer in one round of SELEX is equal to the ratio of their equilibrium dissociation constants (K_d).[8,9] This ratio varies depending on the distribution of the K_d values of the aptamers in the pool, but typical estimates predict a theoretical limit of 100- to 1000-fold enrichment per round. This means that many rounds of selection are required to enrich a sufficient fraction of high affinity aptamers and to identify successful binders, while also increasing the risk of lowering the pool quality through emergence of biases and artifacts as described above.

The particle display method (**Fig. 1.1**) overcomes this inherent limitation in enrichment. By individually characterizing the binding characteristics of aptamers in high-throughput, we can screen for high affinity binders rather than relying on washing to discard low affinity binders.[10] Particle display begins with the conversion of a library of aptamer candidates into monoclonal aptamer particles that each display ~10^5 copies of the same sequence using emulsion polymerase chain reaction (PCR). A water-in-oil emulsion is created, and each droplet contains PCR reagents, a polymer bead coated with forward primers, and a DNA template (**Fig. 1.1**, step 1). The number of DNA molecules in each droplet follows a Poisson distribution, and the concentration of DNA in the reaction is tuned so that the majority of droplets contain no more than one template. This ensures that each aptamer particle displays a single sequence. The reactions are subjected to PCR amplification

(**Fig. 1.1**, step 2), after which the emulsions are broken and the aptamer particles are recovered (**Fig. 1.1**, step 3). The pool of aptamer particles is then incubated with a fluorescently-labeled target molecule (**Fig. 1.1**, step 4), such that the affinity of each aptamer sequence can be directly measured using FACS (**Fig. 1.1**, step 5). The fluorescence intensity of each aptamer particle is directly proportional to the target affinity of the displayed aptamer, enabling the identification and collection of the individual aptamer particles with the highest fluorescence. The collected aptamer particles are then amplified by PCR to produce the starting pool for the next round (**Fig. 1.1**, step 6). Once the pool has reached a point where there is no longer meaningful enrichment of the target-binding subpopulation of aptamer particles, the resulting pool is sequenced to identify aptamer candidates (**Fig. 1.1**, step 7) for further characterization.

Particle display introduces several innovations to aptamer discovery. First, particle display overcomes the theoretical enrichment limit described above for SELEX by changing aptamer selection into screening. Each sequence is individually measured and sorted based on its affinity to the target, so greater enrichment rates are achieved in each round. Theoretically, an aptamer with a K_d of 100 pM within a pool of aptamers with a K_d of 1 nM can be enriched by a factor of 1.7×10^9-fold in a single round of particle display screening.[10] In contrast, the extent of enrichment that can be achieved in conventional SELEX is 10-fold, based on the K_d ratio limitation described above. This means that particle display can isolate high affinity aptamers with dramatically improved efficiency. Second, particle display prevents the unwanted enrichment of low-affinity sequences based on stochastic binding events, because these rare events do not produce a strong enough fluorescent signal for FACS separation to occur. Instead, only the strong fluorescent signals generated by the

binding of multiple labeled target molecules to multiple aptamer copies on a given particle will register as true positives. Each particle displays roughly the same number of aptamer sequences, so differences in fluorescence are due to differences in affinity rather than avidity. Finally, the progress of the screen is directly visualized using FACS. This allows precise adjustment the stringency from round to round by modulating the target concentration and placement of the sort gate (as shown in **Fig. 1.2a**).

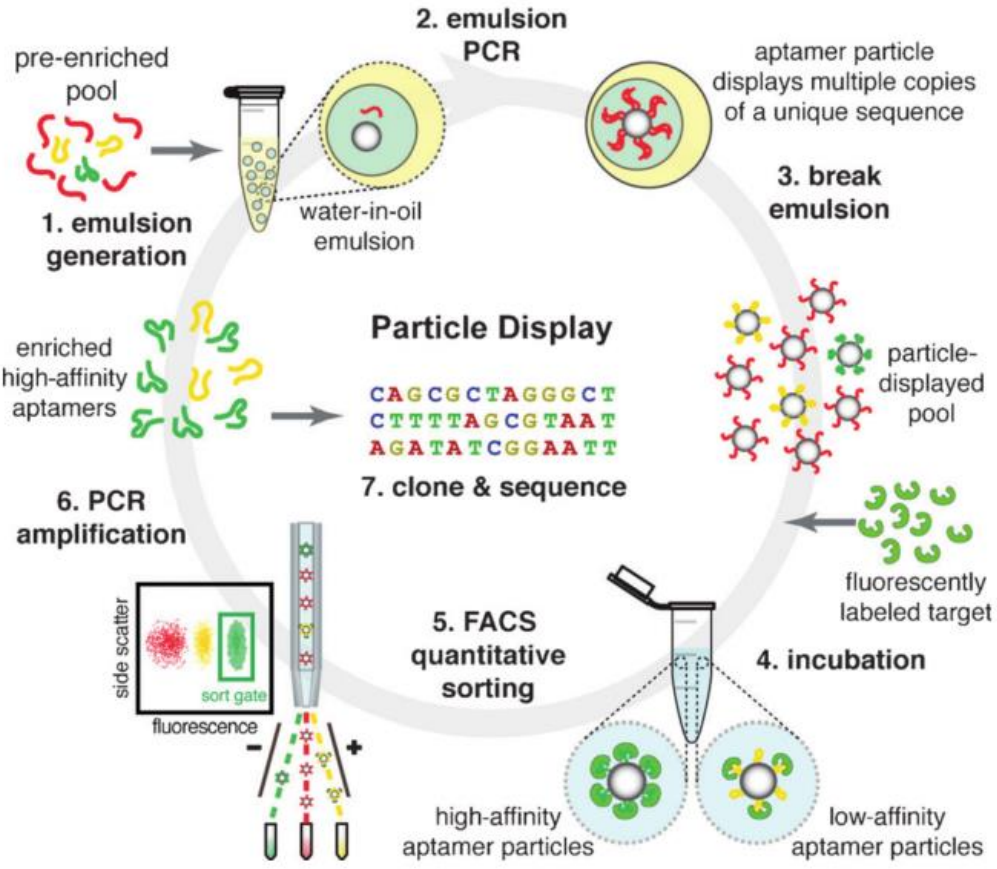

Figure 1.1. Overview of particle display. After one round of conventional selection, the pre-enriched aptamer pool is converted into a pool of monoclonal aptamer particles using emulsion PCR. The aptamer particles are incubated with fluorescently labeled target, and high affinity aptamers are collected using FACS. After three rounds of particle display screening, the resulting aptamer pools are sequenced. Reprinted with permission from Wang J, Gong Q, Maheshwari N, et al. Particle Display: A Quantitative Screening Method for Generating High-Affinity Aptamers. *Angew Chemie.* 2014;126(19):4896-4901. doi:10.1002/ange.201309334. Copyright 2014 WILEY-VCH Verlag GmbH & Co. KGaA, Weinheim.

Initial work with particle display demonstrated rapid isolation of high-quality DNA aptamers against a diverse range of proteins, including some highly challenging targets.[10] Four different protein targets were used as a proof of concept. Thrombin and apolipoprotein E (ApoE) were chosen because well-characterized DNA aptamers had previously been generated for these proteins via SELEX.[11–13] For PAI-1 and 4-1BB, on the other hand, previous attempts to generate natural DNA aptamers had failed.[14] However, RNA aptamers exist for both proteins.[15,16] After just three rounds of particle display, high affinity natural DNA aptamers were discovered for all four targets.

As described above, the use of FACS made it possible to observe the target-binding fraction of the aptamer pool in each round (**Fig. 1.2a**). The sort gates were positioned each round to isolate only the particles that exhibited the highest fluorescence, and therefore strongest target binding. Critically, the target concentration was decreased from round to round, resulting in more stringent selection of the highest affinity aptamers in each round. In only three rounds of screening, aptamers were isolated for all four targets. The resulting thrombin and ApoE aptamers exhibited far superior affinity to previously generated aptamers;[11–13] for example, the thrombin aptamer had a K_d of ~7 pM (**Fig. 1.2b**), an improvement of 2–3 orders of magnitude compared to previously published thrombin aptamers as measured using the same binding assay. This experiment also generated the first reported natural DNA aptamers for PAI-1 and 4-1BB, with affinities (K_d of 339 pM and 2.32 nM, respectively) that were comparable to previously reported aptamers with non-natural bases. This work shows that particle display can isolate higher affinity aptamers against a broad range of targets in far fewer rounds than traditional SELEX methods.

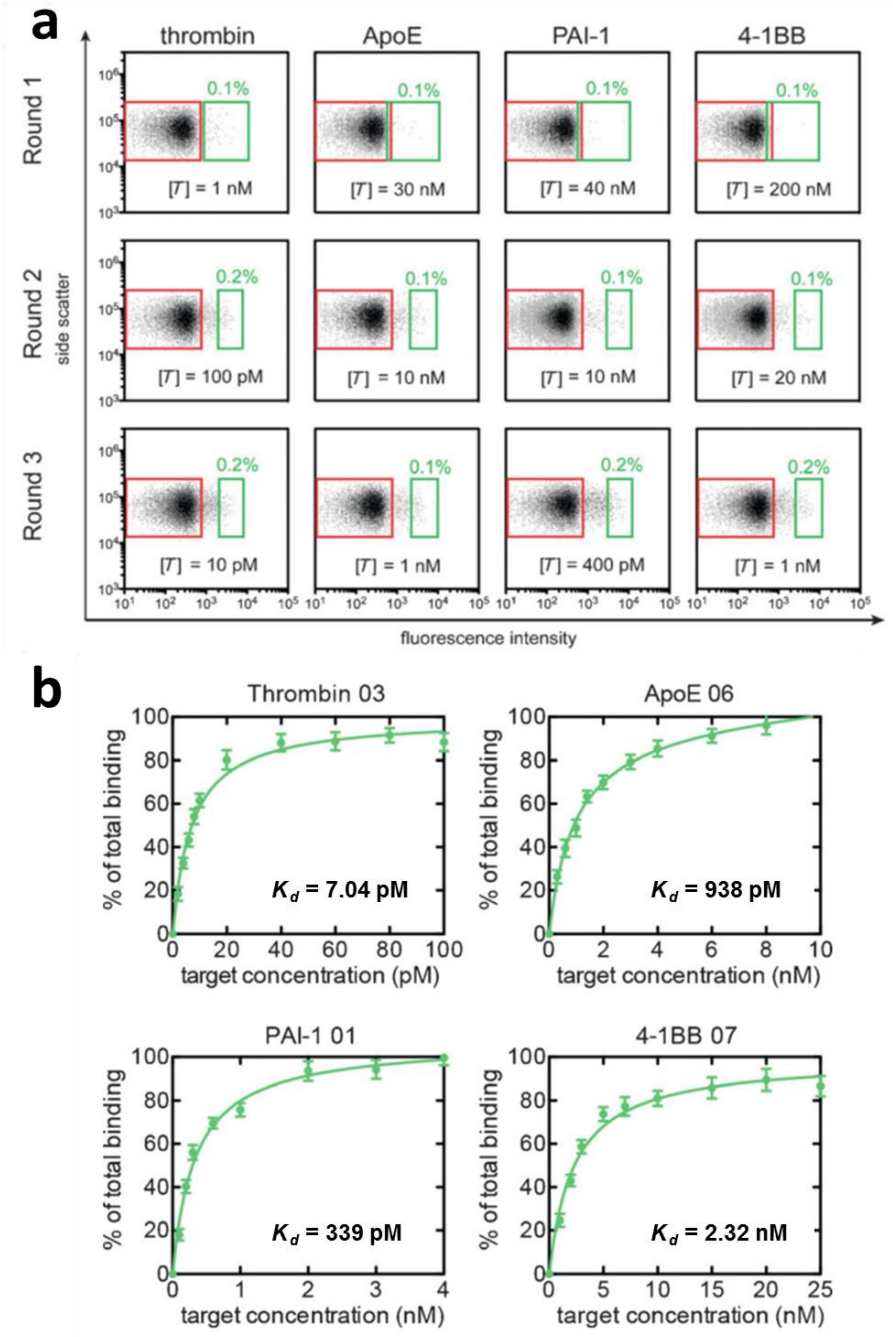

Figure 1.2. (a) Reference (red) and sort (green) gates for multiple rounds of screening against four protein targets: thrombin, ApoE, PAI-1, and 4-1BB. In each round, a larger proportion of the aptamer particles binds to the target despite decreasing the target concentration. (b) Binding curves for the highest affinity aptamers from our particle display screening experiments. Adapted with permission from Wang J, Gong Q, Maheshwari N, et al. Particle Display: A Quantitative Screening Method for Generating High-Affinity Aptamers. *Angew Chemie.* 2014;126(19):4896-4901. doi:10.1002/ange.201309334. Copyright 2014 WILEY-VCH Verlag GmbH & Co. KGaA, Weinheim.

2. Multiparameter particle display—simultaneous screening for affinity and specificity

One critical limitation of SELEX is that a high affinity aptamer may still lack specificity and be prone to excessive off-target binding. One widely-used solution is an additional multi-round "counter-SELEX" procedure, which eliminates aptamers with cross-reactivity to non-target or interferent molecules. However, this strategy is problematic for multiple reasons. First, the addition of even more rounds of amplification and screening exacerbates the risk of PCR and other biases. More importantly, each SELEX procedure is focused entirely on only a single dimension of aptamer function—affinity in the first stage, specificity in the second. This creates opportunities to unwittingly discard aptamers that strike an optimal balance between affinity and specificity by not maintaining continuous selection pressure for both characteristics throughout the screening process.

By exploiting the multi-color sorting capabilities of FACS, our lab devised an enhanced version of particle display to screen aptamer libraries for both affinity and specificity simultaneously.[17] For the multiparameter particle display (MPPD) screening method, target and non-target proteins are labeled with two different colored fluorophores. Using flow cytometry, aptamers that exhibit both strong target fluorescence (high affinity) and low non-target fluorescence (high specificity) can be detected and isolated (**Fig. 1.3a**). As proof of concept, MPPD was used to screen for DNA aptamers for tumor necrosis factor α (TNF-α) in a background of diluted human serum. TNF-α is an important mediator of inflammation that plays a role in many diseases, including rheumatoid arthritis, psoriasis, and the development of insulin resistance.[18–20] TNF-α was labeled with Alexa Fluor 488 (green), while serum proteins were non-specifically labeled with Alexa Fluor 647 (red). By screening

for aptamers with high green and low red fluorescence (**Fig. 1.3a**, quadrant IV), aptamers with high affinity to TNF-α and minimal affinity to background proteins were enriched in just four rounds.

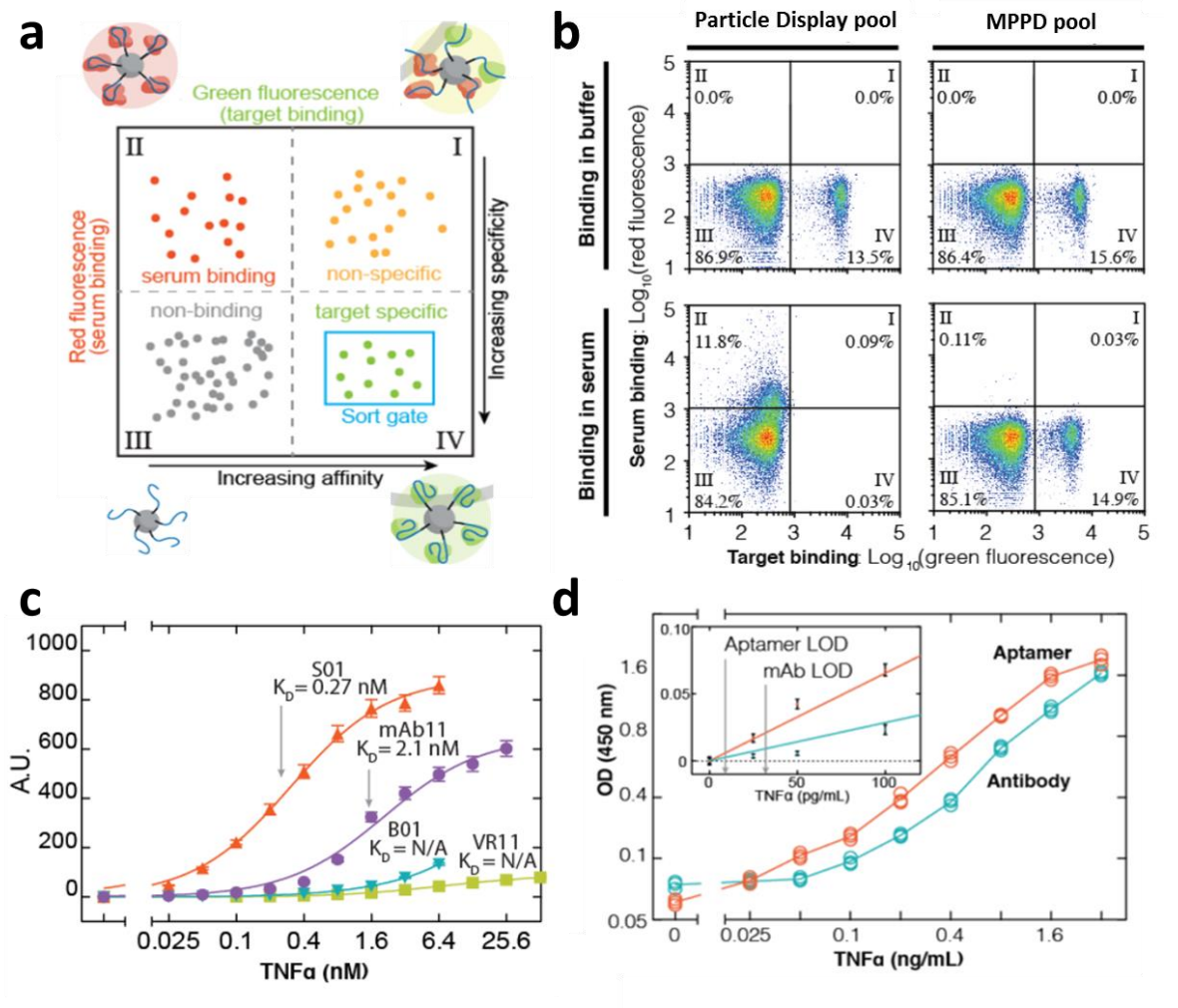

Figure 1.3. (a) Two-color FACS screening for multiparameter particle display (MPPD). The target is labeled with a green fluorescent tag, and non-target serum proteins are nonspecifically labeled with a red fluorescent tag. Those aptamer particles residing in quadrant IV display sequences with high target affinity (high green fluorescence) and high target specificity (low red fluorescence). (b) Aptamers isolated via standard particle display (left) bind poorly in serum, indicating limited specificity, whereas those isolated via MPPD (right) perform equally well in both buffer and serum. (c) TNF-α binding curves in serum for the top-performing MPPD (S01) and particle display (B01) aptamers relative to a previously published TNF-α aptamer (VR11) and a commercial TNF-α antibody (mAb11). (d) In ELISA assays performed in serum, S01 achieves a superior limit of detection to mAb11. Adapted with permission from Wang J, Yu J, Yang Q, et al. Multiparameter Particle Display (MPPD): A Quantitative Screening Method for the Discovery of Highly Specific Aptamers. *Angew Chemie Int Ed*. 2017;56(3):744-747. doi:10.1002/anie.201608880. Copyright 2017 WILEY-VCH Verlag GmbH & Co. KGaA, Weinheim.

The enhanced specificity of aptamers isolated via MPPD was demonstrated by performing a parallel screen for TNF-α with conventional particle display, which selects exclusively on the basis of affinity. The aptamers isolated by MPPD achieved equally strong and specific binding to TNF-α in both serum and buffer (Quadrant IV in **Fig. 1.3b**, right panels). In contrast, although the aptamers isolated via particle display exhibited strong binding to TNF-α in buffer (**Fig. 1.3b**, top left), these aptamers also exhibited poor specificity, with extensive off-target binding to serum proteins (Quadrant II in **Fig. 1.3b**, bottom left) and almost no meaningful signal from TNF-α binding in serum. This was confirmed by analyzing the highest affinity aptamer from the particle display (B01) and MPPD (S01) screens. As with the FACS analysis, both S01 and B01 exhibited excellent affinity for TNF-α in buffer, considerably outperforming a previously reported aptamer (VR11) and a commercial antibody (mAb11) for the same target. However, B01 target affinity essentially disappeared in the complex medium of serum, presumably due to extensive off-target binding to interferent proteins (**Fig. 1.3c**). In contrast, the affinity of S01 was virtually unchanged in 10% serum (K_d of 0.27 nM vs 0.19 nM in buffer). Finally, the performance of S01 was tested in an ELISA relative to a commercial kit, and the S01-based assay achieved a LOD that was more than three-fold lower than the commercial assay (**Fig. 1.3d**).

These results demonstrate the clear advantages of using MPPD to actively select for aptamer specificity in parallel with affinity-based selection. Aptamers selected only for high affinity may have poor specificity, greatly limiting their usefulness in applications such as biosensing, imaging, and affinity purification.[21]

3. Particle display of aptamer pairs—screening for function

Once high affinity and specificity aptamers are identified, significant challenges to incorporating them into relevant assays remain. A readout (fluorescent, electrochemical, or another method) is required to transduce the target binding signal. Post-selection modification is possible, but this frequently disrupts the binding of the aptamer to the target. By screening for aptamers in the desired assay format, we can directly identify aptamers that are ready to use. Our lab has developed one such method: particle display of aptamer pairs (PDAP).

In molecular detection assays, it is advantageous to have multiple affinity reagents that bind to the same target to minimize false signals from non-specific binding. For example, the widely used enzyme-linked immunosorbent assay (ELISA) employs pairs of antibodies that bind to distinct epitopes on a given target in a "sandwich assay" format, such that a signal is only achieved through simultaneous binding by both antibodies. Unfortunately, the discovery of antibody pairs is greatly constrained by the "hot spot" problem, wherein most antibodies are raised against the most immunogenic site of the target, while antibodies that bind to other, secondary sites are relatively rare and thus difficult to isolate.[22]

Several methods have been described for the generation of aptamer pairs that overcome this hot spot problem, but these are generally inefficient and low-throughput.[23,24] Building off of particle display, our lab developed an efficient screening strategy for the rapid discovery of high-affinity aptamer pairs, called particle display of aptamer pairs (PDAP).[25] PDAP uses quantitative FACS-based screening of a library of monoclonal aptamer particles to identify sequences that can bind to the target at the same time as a

fluorescently-tagged detection aptamer with known affinity for that particular target (**Fig. 1.4a**).

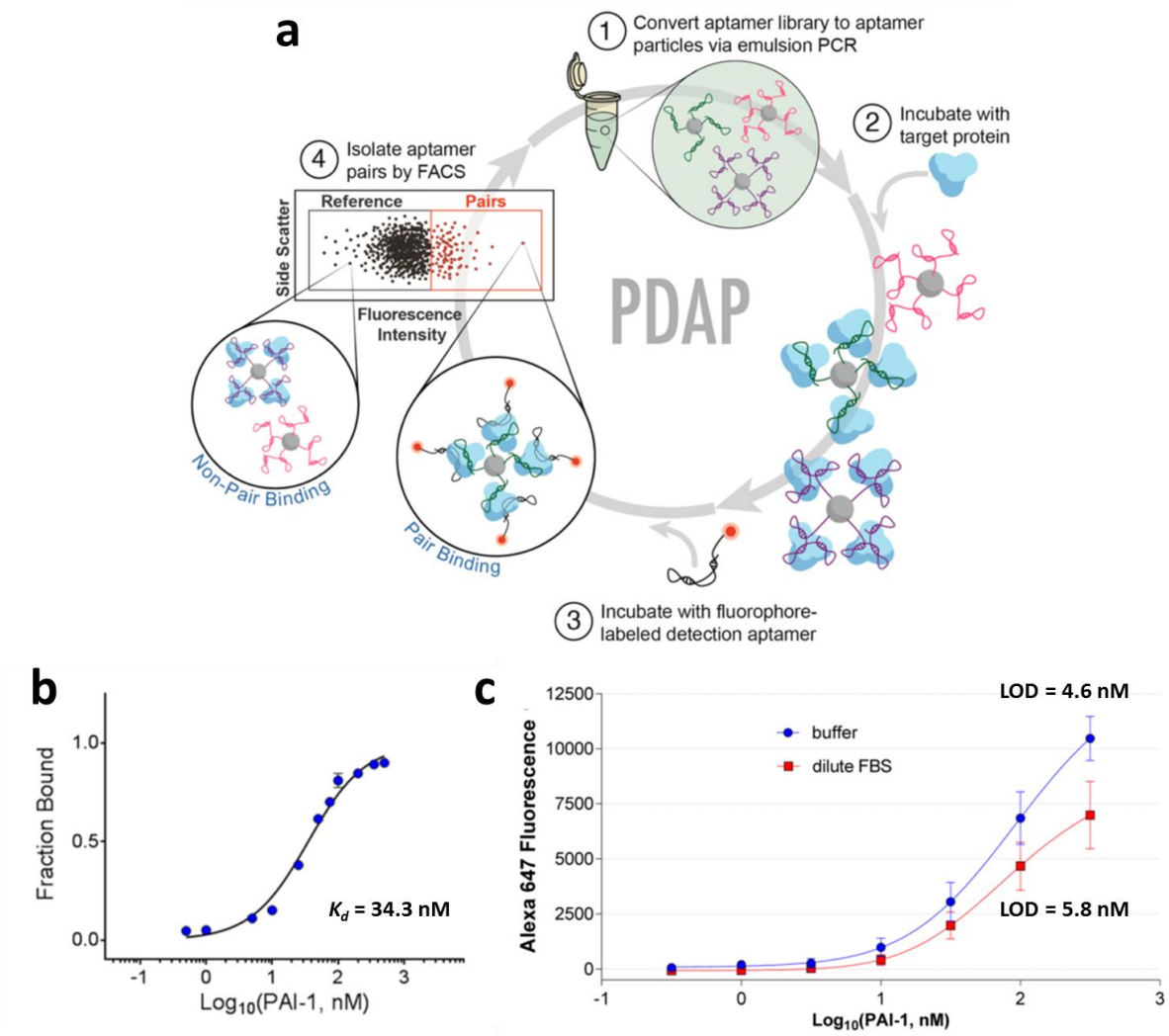

Figure 1.4. (a) Overview of particle display of aptamer pairs (PDAP). (b) The K_d of the highest-affinity capture aptamer, CA-1, was measured by incubating monoclonal CA-1 particles with fluorescently labeled PAI-1. (c) Flow cytometry assay to measure aptamer pair sensitivity for CA-1 and the detection aptamer. Adapted with permission from Csordas AT, Jørgensen A, Wang J, et al. High-Throughput Discovery of Aptamers for Sandwich Assays. *Anal Chem*. 2016:acs.analchem.6b03450. doi:10.1021/acs.analchem.6b03450. Copyright 2016 American Chemical Society.

If the aptamer displayed on a given particle recognizes the same protein site as the detection aptamer, the particle will remain unlabeled—or alternately, the target will be

displaced from the particle through higher affinity binding to the detection aptamer. On the other hand, if the aptamer particle and detection aptamer simultaneously bind distinct sites on the target, the high fluorescence of the aptamer particle can be detected via FACS and isolated by sorting. Importantly, because the fluorescent signal is generated by the detection aptamer, no labeling or modification of the target is required.

As a proof of concept, plasminogen activator inhibitor-1 (PAI-1) was selected as the target. PAI-1 is an important biomarker of thrombosis and atherosclerosis.[26,27] After two rounds of PDAP screening, an aptamer (CA-1) was discovered that bound to PAI-1 with high affinity in parallel with the detection aptamer, exhibiting a K_d of 34.3 nM (**Fig. 1.4b**). In order to maximize the specificity of the resulting aptamer pairs, all particle display screens were performed in the complex medium of diluted fetal bovine serum rather than buffer. As a result of this rigorous selection procedure, the aptamer exhibited excellent sensitivity in a sandwich-style molecular detection assay, with a limit of detection (LOD) of 5.8 nM PAI-1 in diluted fetal bovine serum (**Fig. 1.4c**). Notably, this was only slightly higher than the LOD observed when a similar assay was conducted in buffer (4.6 nM). Thus, PDAP can rapidly isolate aptamer pairs that are distinctly well-suited for performing sensitive molecular detection even in complex sample matrices.

4. Structure-switching particle display—screening for function

Our lab developed structure-switching particle display (SS-PD) to directly identify aptamers that change conformation upon target binding.[28] Structure-switching is a valuable property for aptamers. Such aptamers can be modified in order to transduce a signal upon binding, making them immediately useful in the context of platforms such as biosensors. SS-PD has been used to identify binding-induced conformational change by detecting the

displacement of a fluorescently-labeled complementary DNA strand from a given aptamer particle.[28]

The SS-PD library includes two 10 nucleotide (nt) random domains separated by a 21 nt constant domain (**Fig. 1.5a**). A fluorescently-labeled "red reporter" strand is initially hybridized to the constant domain; however, sufficiently strong binding between the target and the random domains destabilizes reporter binding, resulting in a loss of fluorescence (**Fig. 1.5b**). Because the binding signal comes from the release of the reporter strand, screening is "label-free"—the target molecule does not need to be modified. A secondary fluorescently-labeled "green reporter" strand is hybridized to the reverse primer-binding domain to confirm that particles lacking a red reporter signal are in fact displaying aptamers. Each round of SS-PD consists of a "binding screen" to collect aptamer particles with reduced red fluorescence, and a "folding screen" in the absence of the target to collect aptamer particles with both red and green fluorescence. The folding screen confirms that aptamers selected in the binding screen represent true target binding-induced structure-switching events, eliminating any sequences that release the red reporter spontaneously.

SS-PD was used to screen for aptamers for two challenging targets: a pair of metal ions, Hg^{2+} and Cu^{2+}. These molecules are not amenable to modification, which can dramatically change their structure and properties,[29] making a label-free assay ideal. Aptamers for Hg^{2+} have proven useful for the detection of mercury in serum and in environmental water samples.[30–32] In contrast, no aptamers had been described to date for Cu^{2+}, although this ion is also a pollutant with toxic effects.[33] Structure-switching aptamers were identified after four rounds of screening for Hg^{2+} and three rounds of screening for Cu^{2+}. Binding was measured in terms of IC_{50} rather than K_d because the red reporter acts as a

binding competitor, and it was subsequently determined that the K_d is smaller than the measured IC_{50} values by about one order of magnitude. The highest affinity aptamer for Hg^{2+} had an IC_{50} of 2.27 μM, with a K_d of 1.49 μM measured by microscale thermophoresis—about 30-fold higher affinity than a previously published Hg^{2+} aptamer.[34] The first reported aptamer was generated for Cu^{2+}, with an IC_{50} of 47.15 μM (**Fig. 1.5c**). Given the clear difficulty of isolating aptamers for metal ions, SS-PD should be readily applicable for the generation of structure-switching aptamers for a variety of unmodified small-molecule targets, making it a valuable tool for biosensor development.

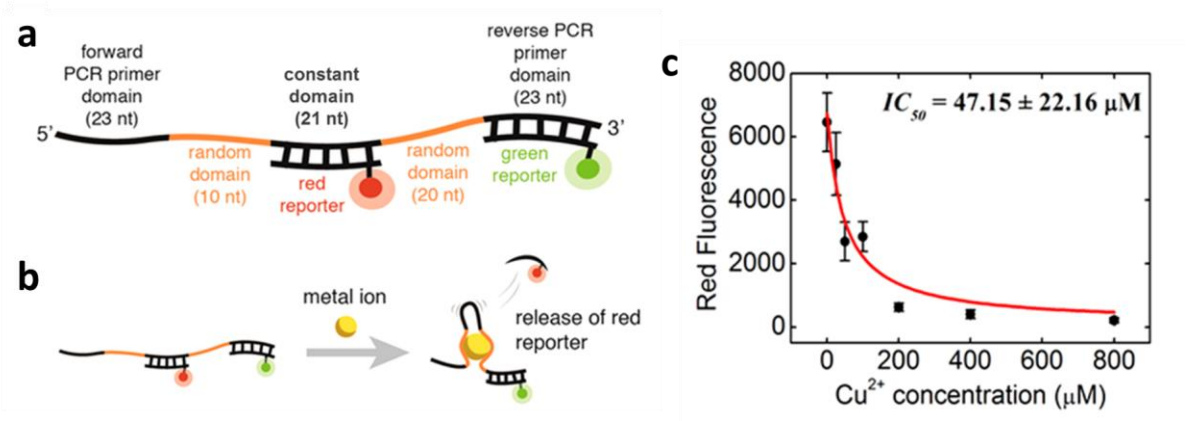

Figure 1.5. (a) Library design for structure-switching particle display (SS-PD). (b) The red reporter is released in response to binding between the aptamer and the metal ion. The green reporter verifies the presence of aptamers on the particle surface. (c) IC_{50} measurement of the Cu^{2+} aptamer with the strongest binding. Adapted with permission from Qu H, Csordas AT, Wang J, Oh SS, Eisenstein MS, Soh HT. Rapid and Label-Free Strategy to Isolate Aptamers for Metal Ions. *ACS Nano*. 2016;10(8):7558-7565. doi:10.1021/acsnano.6b02558. Copyright 2016 American Chemical Society.

D. Outline

Our lab has made substantial progress in aptamer discovery methods, but limitations and unexplored areas of critical importance remain. In this thesis, I will describe three projects that improve different parts of the aptamer discovery process. First, we used particle

display to discover the first reported aptamers for tumor marker, p32. By efficiently enriching aptamers for important biological targets, we create tools that can potentially be used for critical therapeutic or diagnostic functions. Next, we expanded the particle display platform to screen for non-natural DNA aptamers. This method, called click-PD, enables the incorporation of a huge variety of chemical modifications into aptamer selections, without complex synthesis or polymerase engineering. Finally, we developed a new functional screening method to isolate pH switching aptamers. There are no previously reported methods of selecting aptamers with pH switching functions. Aptamers with pH tunable behavior are of great interest for drug delivery, pH-sensitive imaging, and pH-gated nanostructures. Together, these methods are a step forward in developing useful, high quality aptamers for important biological targets.

E. References

1. Köhler G, Milstein C. Continuous cultures of fused cells secreting antibody of predefined specificity. *Nature*. 1975;256(5517):495-497. doi:10.1038/256495a0.
2. Slamon DJ, Leyland-Jones B, Shak S, et al. Use of Chemotherapy plus a Monoclonal Antibody against HER2 for Metastatic Breast Cancer That Overexpresses HER2. *N Engl J Med*. 2001;344(11):783-792. doi:10.1056/NEJM200103153441101.
3. Demerdash ZA, Diab TM, Aly IR, et al. Diagnostic efficacy of monoclonal antibody based sandwich enzyme linked immunosorbent assay (ELISA) for detection of Fasciola gigantica excretory / secretory antigens in both serum and stool. *Parasit Vectors*. 2011;4(1):1-7. doi:10.1186/1756-3305-4-176.
4. Liu JKH. The history of monoclonal antibody development - Progress, remaining challenges and future innovations. *Ann Med Surg*. 2014;3(4):113-116. doi:10.1016/j.amsu.2014.09.001.
5. Chames P, Van Regenmortel M, Weiss E, Baty D. Therapeutic antibodies: Successes, limitations and hopes for the future. *Br J Pharmacol*. 2009;157(2):220-233. doi:10.1111/j.1476-5381.2009.00190.x.
6. Berglund L, Björling E, Oksvold P, et al. A Genecentric Human Protein Atlas for Expression Profiles Based on Antibodies. *Mol Cell Proteomics*. 2008;7(10):2019-2027. doi:10.1074/mcp.R800013-MCP200.

7. Keefe AD, Pai S, Ellington A. Aptamers as therapeutics. *Nat Rev Drug Discov*. 2010;9(7):537-550. doi:10.1038/nrd3141.

8. Irvine D, Tuerk C, Gold L. Selexion. Systematic evolution of ligands by exponential enrichment with integrated optimization by non-linear analysis. *J Mol Biol*. 1991;222(3):739-761. doi:10.1016/0022-2836(91)90509-5.

9. Wang J, Rudzinski JF, Gong Q, Soh HT, Atzberger PJ. Influence of Target Concentration and Background Binding on In Vitro Selection of Affinity Reagents. *PLoS One*. 2012;7(8):1-8. doi:10.1371/journal.pone.0043940.

10. Wang J, Gong Q, Maheshwari N, et al. Particle Display: A Quantitative Screening Method for Generating High-Affinity Aptamers. *Angew Chemie*. 2014;126(19):4896-4901. doi:10.1002/ange.201309334.

11. Bock LC, Griffin LC, Latham J a, Vermaas EH, Toole JJ. Selection of single-stranded DNA molecules that bind and inhibit human thrombin. *Nature*. 1992;355(6360):564-566. doi:10.1038/355564a0.

12. Tasset DM, Kubik MF, Steiner W. Oligonucleotide inhibitors of human thrombin that bind distinct epitopes. *J Mol Biol*. 1997;272(5):688-698. doi:10.1006/jmbi.1997.1275.

13. Ahmad KM, Oh SS, Kim S, McClellen FM, Xiao Y, Soh HT. Probing the limits of aptamer affinity with a microfluidic SELEX platform. *PLoS One*. 2011;6(11). doi:10.1371/journal.pone.0027051.

14. Gold L, Ayers D, Bertino J, et al. Aptamer-based multiplexed proteomic technology for biomarker discovery. *PLoS One*. 2010;5(12). doi:10.1371/journal.pone.0015004.

15. Blake CM, Sullenger B a, Lawrence D a, Fortenberry YM. Antimetastatic potential of PAI-1-specific RNA aptamers. *Oligonucleotides*. 2009;19(2):117-128. doi:10.1089/oli.2008.0177.

16. Ii JOM, Kolonias D, Pastor F, et al. Multivalent 4-1BB binding aptamers costimulate CD8 + T cells and inhibit tumor growth in mice. *J Clincal Investig*. 2008;118(1):376-386. doi:10.1172/JCI33365.376.

17. Wang J, Yu J, Yang Q, et al. Multiparameter Particle Display (MPPD): A Quantitative Screening Method for the Discovery of Highly Specific Aptamers. *Angew Chemie Int Ed*. 2017;56(3):744-747. doi:10.1002/anie.201608880.

18. Bradley J. TNF-mediated inflammatory disease. *J Pathol*. 2008;214(2):149-160. doi:10.1002/path.2287.

19. Liu Y, Yang G, Zhang J, et al. Anti-TNF- α monoclonal antibody reverses psoriasis through dual inhibition of inflammation and angiogenesis. *Int Immunopharmacol*. 2015;28(1):731-743. doi:10.1016/j.intimp.2015.07.036.

20. Peluso I, Palmery M. The relationship between body weight and inflammation : Lesson from anti-TNF- a antibody therapy. *Hum Immunol*. 2016;77(1):47-53. doi:10.1016/j.humimm.2015.10.008.

21. Iliuk AB, Hu L, Tao WA. Aptamer in Bioanalytical Applications. *Anal Chem*. 2011;83(12):4440-4452. doi:10.1021/ac201057w.

22. Vanderlugt CL, Miller SD. Epitope Spreading in Immune-Mediated Diseases: Implications for Immunotherapy. *Nat Rev Immunol*. 2002;2(2):85-95. doi:10.1038/nri724.

23. Shi H, Fan X, Sevilimedu A, Lis JT. RNA aptamers directed to discrete functional sites on a single protein structural domain. *Proc Natl Acad Sci*. 2007;104(10):3742-3746. doi:10.1073/pnas.0607805104.

24. Cho M, Oh SS, Nie J, et al. Array-based discovery of aptamer pairs. *Anal Chem*. 2015;87(1):821-828. doi:10.1021/ac504076k.

25. Csordas AT, Jørgensen A, Wang J, et al. High-Throughput Discovery of Aptamers for Sandwich Assays. *Anal Chem*. 2016:acs.analchem.6b03450. doi:10.1021/acs.analchem.6b03450.

26. Meltzer ME, Lisman T, De Groot PG, et al. Venous thrombosis risk associated with plasma hypofibrinolysis is explained by elevated plasma levels of TAFI and PAI-1. *Blood*. 2010;116(1):113-121. doi:10.1182/blood-2010-02-267740.

27. Peng Y, Liu H, Liu F, et al. Atherosclerosis is associated with plasminogen activator inhibitor type-1 in chronic haemodialysis patients. *Nephrology*. 2008;13(7):579-586. doi:10.1111/j.1440-1797.2008.00987.x.

28. Qu H, Csordas AT, Wang J, Oh SS, Eisenstein MS, Soh HT. Rapid and Label-Free Strategy to Isolate Aptamers for Metal Ions. *ACS Nano*. 2016;10(8):7558-7565. doi:10.1021/acsnano.6b02558.

29. McKeague M, Derosa MC. Challenges and opportunities for small molecule aptamer development. *J Nuc Acids*. 2012;2012:748913. doi:10.1155/2012/748913.

30. Chung CH, Kim JH, Jung J, Chung BH. Nuclease-resistant DNA aptamer on gold nanoparticles for the simultaneous detection of Pb2+ and Hg2+ in human serum. *Biosens Bioelectron*. 2013;41(1):827-832. doi:10.1016/j.bios.2012.10.026.

31. Li T, Dong S, Wang E. Label-free colorimetric detection of aqueous mercury ion (Hg2+) using Hg 2+-modulated G-quadruplex-based dnazymes. *Anal Chem*. 2009;81(6):2144-2149. doi:10.1021/ac900188y.

32. Long F, Zhu A, Shi H, Wang H, Liu J. Rapid on-site/in-situ detection of heavy metal ions in environmental water using a structure-switching DNA optical biosensor. *Sci Rep*. 2013;3:2308. doi:10.1038/srep02308.

33. Mido Y, Satake M. *Chemicals in the Environment*. New Delhi: Discovery Publishing House; 1995.

34. Ono A, Togashi H. Highly selective oligonucleotide-based sensor for mercury(II) in aqueous solutions. *Angew Chemie - Int Ed*. 2004;43(33):4300-4302. doi:10.1002/anie.200454172.

Chapter II. Screening for aptamers to tumor biomarker, p32

A. Introduction

Biomarkers provide an indication of a specific biological state, and they can be used to diagnose, monitor, and treat disease.[1] Biomarkers have been identified for cancer, acute kidney injury, Alzheimer's disease, and many other diseases.[2–4] However, identification of biomarkers is not useful without ways to reliably measure them in patients. Affinity reagents targeting biomarkers are essential for applications in disease detection, imaging, and treatment. In many cases, the goal is to detect the biomarker of interest in a blood sample.[5] This requires an affinity reagent capable of sensitive and specific detection. Affinity reagents also have potential for imaging to monitor the progress of disease.[6–8] Targeted drug delivery is another important area of interest. There are many examples of affinity reagents used for active targeting of a particle or drug to a precise location in the body.[9]

Antibodies are considered the gold standard for molecular recognition; however, they have many limitations,[10] as discussed in the previous chapter. Aptamers are promising therapeutic candidates, but there is currently only one FDA approved aptamer drug, pegaptanib (Macugen), targeting vascular endothelial growth factor (VEGF) for the treatment of age-related macular degeneration,[11] and this treatment has been largely replaced by anti-VEGF monoclonal antibodies.[12] Aptamers do not yet exist for many known biomarkers. Once aptamers for a desired target are found, they still face critical challenges for functioning *in vivo*, including nuclease degradation, renal filtration, and toxicity.[13] Because aptamer discovery is only one step of the difficult process of generating useful affinity reagents for detecting and curing disease, it is essential that efficient and reliable aptamer generation methods exist.

Particle display, an aptamer discovery platform developed in our group, enables more efficient isolation of high affinity aptamers.[14] Using high-throughput quantitative screening, we can rapidly identify high affinity aptamers. Here, we demonstrate the use of particle display to discover aptamers for an important tumor biomarker, p32.

B. Overview of p32 screen

We used particle display to screen for high affinity aptamers to p32. Cell surface protein p32 was selected as a target for this screen because it has been found to be differentially expressed in human cancer cells and healthy cells, and it does not have any published nucleic acid aptamers.[15] This protein was identified by the Ruoslahti lab as a molecular target for a tumor homing peptide, LyP-1.[15] LyP-1 exhibits tumor homing and antitumor activity, despite its modest affinity to p32 (3 μM).[15,16] We used the method previously developed in our lab,[14] as described in Chapter I, Section C (**Fig. 1.1**).

C. Results and discussion

Four rounds of particle display were performed. The p32 was expressed with a his-tag, and a fluorescently-labeled anti-his-tag antibody was used to label the bound p32 after incubation with the aptamer particles. In each round, the aptamer particles with the highest fluorescence intensity (top 0.2%) were collected using FACS (**Fig. 2.1**, gate P3). After significant enrichment of the aptamer pool was observed (**Fig. 2.2**), the fourth round aptamer pool was cloned into *E. coli* and sequenced using Sanger sequencing. Eleven colonies were sequenced, and three unique sequences were identified: p32-1, -2, and -3 (**Table 2.1**).

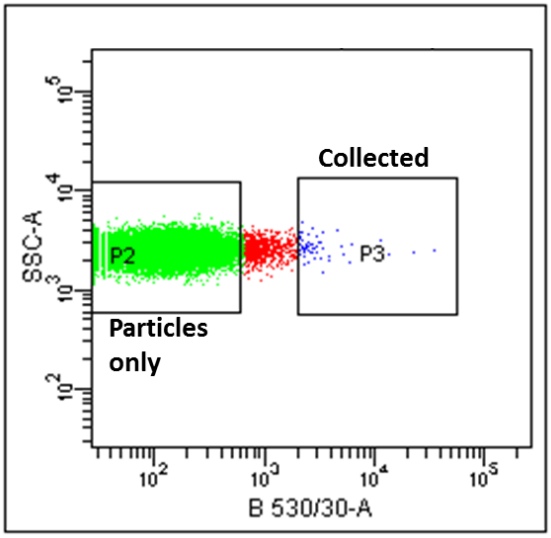

Figure 2.1. Sort gate (P3) for the round 3 pool, set to collect the aptamer particles with the highest affinity to p32 (top 0.2% of singlets). Gate P2 was set using aptamer particles with no p32 as a negative control.

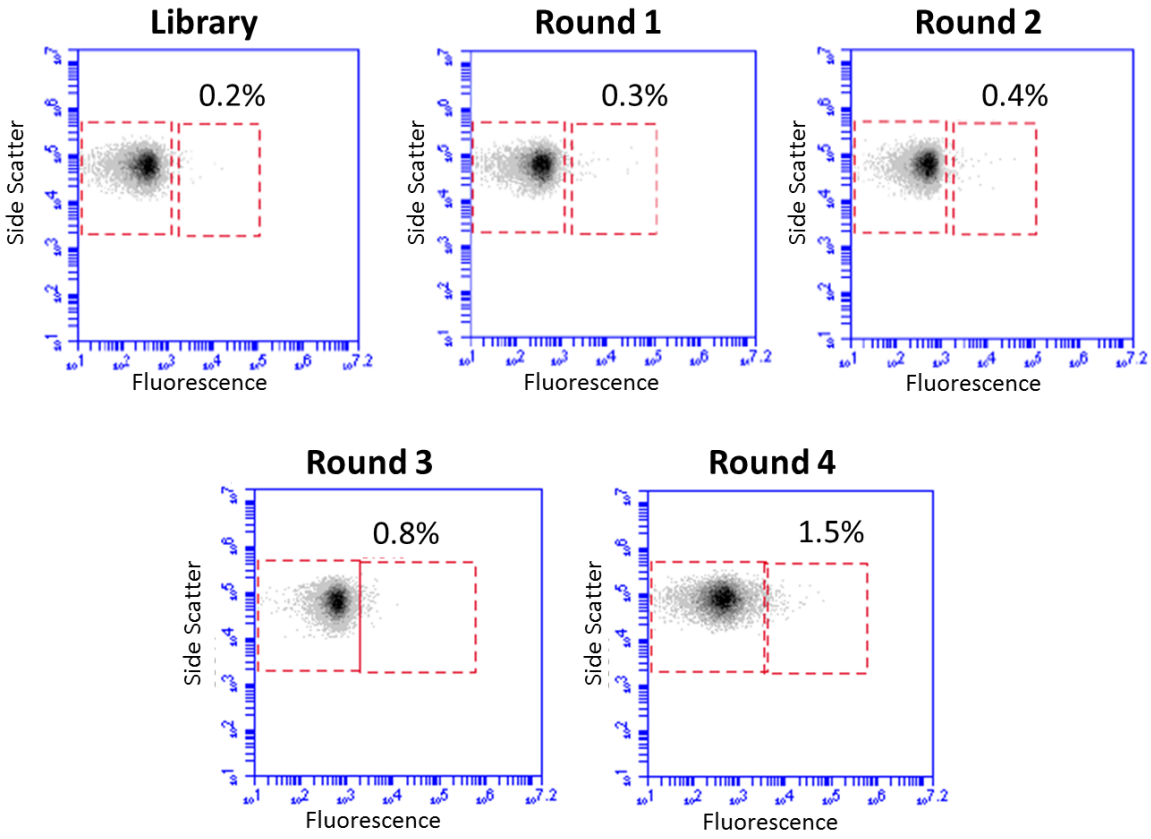

Figure 2.2. Enrichment of high affinity p32 aptamers from the naïve library to the round 4 pool. The concentration of p32 was 100 nM for each measurement.

Aptamer particles displaying each of the three sequences were generated, and binding to p32 was measured. Aptamer p32-2 showed the highest affinity binding to p32 (**Fig. 2.3a**), with a K_d of 7.6 ± 2.8 nM. This is significantly higher than the binding affinity of the tumor-homing peptide LyP-1 (3 μM). The predicted secondary structure of this sequence is shown in **Figure 2.3b**. Testing the function of p32-2 in cells and *in vivo* must still be done to determine if this aptamer shows tumor homing behavior, but its high binding affinity to tumor maker p32 is promising.

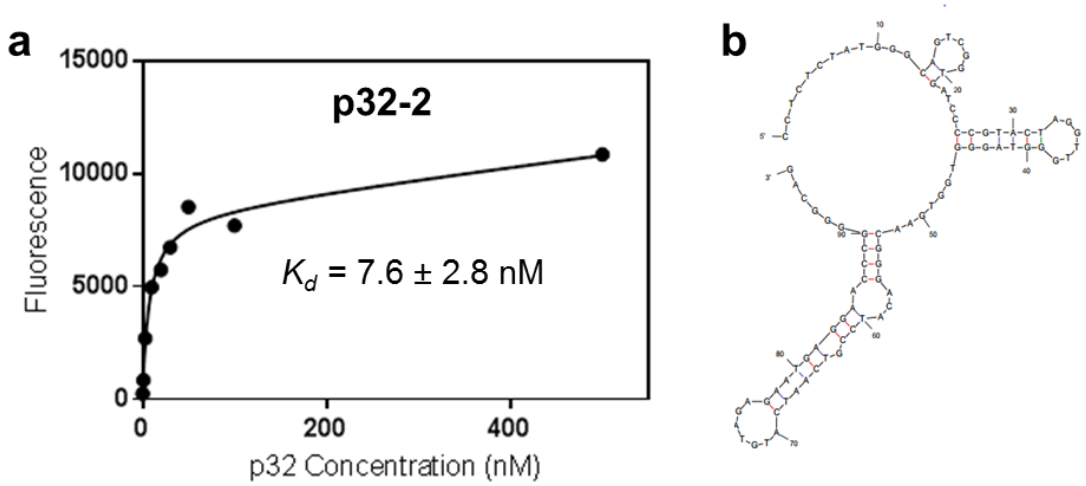

Figure 2.3. (a) Binding curve of aptamer p32-2 to target protein p32, from a bead-based fluorescence assay (K_d = 7.6 ± 2.8 nM). (b) Secondary structure of p32-2, predicted by Mfold.

As next generation sequencing has become more accessible since this screen was completed, we are currently re-analyzing the aptamer pools from each round. Next generation sequencing was performed on the aptamer pools from rounds 1 to 4. The top twenty-five sequences by reads (or copy number) in round 4 are shown in **Table 2.2**. These results support the results from the initial Sanger sequencing; the three aptamers identified are ranked 1, 2, and 4 by copy number in the round four pool. Sequence p32-1 was the most abundant sequence in the round 4 pool, with ten times as many reads as the next most abundant sequence (**Table 2.3**). Forty-eight of the top one hundred sequences in round 4

were closely related to p32-1 (**Fig. 2.4**), demonstrating significant convergence of the pool over the four rounds of screening. The most abundant sequences in the final pool were enriched significantly, 2,000- to almost 16,000-fold, from round 1 to round 4. Interestingly, despite the high abundance of p32-1, p32-2 had significantly higher enrichment from round 1 to round 4 than p32-2 did. Investigation of the additional aptamer candidates identified by NGS is ongoing. Through deeper analysis and characterization of these sequences, we can potentially identify aptamers with higher affinity to p32.

Figure 2.4. Aptamer p32-1 sequence family identified by NGS. Of the top 10 sequences by copy number in round 4, 48 were closely related to p32-1.

D. Conclusions

We have discovered an aptamer that binds to p32, a cancer biomarker, with low nanomolar affinity. Because p32 has been identified as a receptor for tumor-homing reagents, this aptamer is a promising candidate for testing for further testing. Analysis of the aptamer pools from each round using NGS is ongoing. By identifying and characterizing highly enriched and highly abundant sequences, we may discover aptamers with higher affinity to p32. High quality affinity reagents for disease markers are essential for the detection, monitoring, and treatment of disease. This work demonstrates that particle display is an efficient method for generating high affinity aptamers to important biological targets.

E. Experimental section

1. Reagents

Purified, his-tagged p32 was provided by the Ruoslahti lab. The 96 nucleotide library, including a 50 nucleotide random region, and primers were ordered from IDT. The library sequence is shown in **Table 2.1**. The library was synthesized with hand mixing and was PAGE purified. Mineral oil, Span 80, Tween 80, and Triton X-100 were purchased from Sigma-Aldrich. GoTaq Hot Start Polymerase, master mix, and nucleotides were purchased from Promega.

Name	Sequence
Forward primer	CCTCTCTATGGGCAGTCGGTGAT
Reverse primer	CTGCCCCGGGTTCCTCATTCTCT
Library	CCTCTCTATGGGCAGTCGGTGAT-N50-AGAGAATGAGGAACCCGGGGCAG
p32-1	CGCCAAGTAGGTTGGGTAGGGTGGTCTGCGAGTACAGCATGCGCAGTAGC
p32-2	CCCCGTACTAGGTTGGGTAGGGTGGTGAACGGGACATCCGTCAATCATGT
p32-3	AGAACTCTAGGTTGGTGTGGTTGGATGAGTTTTATGCCGAATACGCTGCC

Table 2.1. DNA sequences used in p32 study. Aptamers p32-1, -2, and -3 are shown without primer binding regions. Sequences are shown 5' to 3'.

2. Coupling forward primers to magnetic particles

Amino modified forward primers were conjugated to MyOne carboxylic acid magnetic particles (Life Technologies) using EDC-NHS chemistry. The reaction was incubated on a rotator overnight at room temperature. After the reaction, the particles were capped with amino modified PEG12 in a 2 hour incubation at room temperature to passivate the surface. After the PEG capping, the reaction was quenched by washing the forward primer-conjugated particles in 10 mM Tris three times for 15 minutes each. The particles were stored in 10 mM Tris at 4 °C.

3. Generating monoclonal aptamer particles using emulsion PCR

Monoclonal aptamer particles were generated by emulsion PCR. The oil phase was made up of 4.5% Span 80, 0.45% Tween 80, and 0.05% Triton X-100 in mineral oil. The aqueous phase consisted of 1x PCR mix, 0.1 U/µL GoTaq Hot Start DNA polymerase, 25

mM $MgCl_2$, 0.28 mM of each dNTP, 40 nM forward primer, 3 µM fluorescently labeled reverse primer, ~1 pM template DNA, and ~10^8 1 µm FP-conjugated magnetic beads in a total volume of 1 mL. The aqueous phase was added dropwise to 7 mL of oil phase and emulsified at 620 rpm for 5 min in an IKA DT-20 tube using the IKA Ultra-Turrax device. The emulsion was pipetted into 100 µL reactions in a 96 well PCR plate. The following PCR conditions were used: 95 °C, 5 min + [93 °C, 15s + 62 °C, 30s + 72 °C, 75s]*45 + 72 °C, 7 min.

After PCR, the emulsions were collected into an emulsion collection tray (Life Technologies) by centrifuging at 300 x g for 2 min. The emulsion was broken by adding 10 mL 2-butanol to the tray, and the sample was transferred to a 50 mL tube. The tube was vortexed for 30s, and the particles were pelleted by centrifugation at 3,000 x g for 5 min. The oil phase was carefully removed, and the particles were resuspended in 1 mL of emulsion breaking buffer (100 mM NaCl, 1% Triton X-100, 10 mM Tris-HCl, pH 7.5, and 1 mM EDTA) and transferred to a new 1.5 mL tube. After vortexing for 30s and 90s of centrifugation at 15,000 × g, the supernatant was removed. The tube was placed on a magnetic separator (MPC-S, Life Technologies), and the remaining supernatant was removed. The particles were washed three times with 1x PBS buffer using magnetic separation, then stored in 200 µL PBST at 4 °C.

To generate single-stranded DNA, the particles were resuspended in 200 µL 0.1 M NaOH solution and incubated for 2 min at room temperature. The supernatant was removed using the magnetic separator, and the particles were incubated in 200 µL 0.1 M NaOH twice more for 2 min each. The supernatant was removed using the magnetic separator, and the

particles were resuspended in 200 µL TE buffer. The particles were washed three times with TE buffer and resuspended in 200 µL 10 mM Tris.

4. Particle display screening

The aptamer particles were incubated with purified p32 for 1-2 hours at room temperature on a rotator. For the first three rounds, 100 nM p32 was used. The p32 concentration was decreased to 50 nM for the fourth round. After incubation, a magnetic rack was used to wash the particles and remove unbound p32. The particles were incubated with an anti-his-tag antibody-FITC (fluorescein isothiocyanate) conjugate for 15 minutes. Samples were then washed twice and resuspended resuspended in selection buffer. Samples were analyzed with FACS (Aria I), and sort gates were set to collect aptamer particles with the highest fluorescent signal (top 0.2%). The sequences on the collected particles were then amplified to generate a pool for the next round of screening. A pilot PCR was performed first to select the correct cycle number, and then full scale amplification was performed. After Qiagen purification, this pool was used as the template for the next round of screening.

5. Cloning and sequencing

After four rounds of screening, the resulting aptamer pool was cloned into *E. coli* and sequenced. Of the eleven colonies sequenced, three unique sequences were found (**Table 2.1**).

6. Particle PCR

The three aptamer candidates were ordered from IDT with HPLC purification. The sequences of each candidate are shown in **Table 2.1**. Each sequence was amplified onto forward primer coated beads.

7. Characterization of individual aptamers

For each of the three sequences, aptamer particles were incubated with p32 for 1 hour at RT on a rotator. After the incubation, unbound p32 was removed using a magnetic rack, and bound p32 was labeled with FITC-labeled anti-his antibody. After labeling, the beads were washed once and resuspended in selection buffer. The fluorescence of the aptamer particles was measured using an Accuri C6 flow cytometer. Aptamer p32-2 gave the largest fluorescence signal, so it was chosen for further characterization. Binding assays were performed to measure the fluorescence intensity of p32-2 aptamer particles to varying concentrations of p32 to create a binding curve. The equilibrium dissociation constant was calculated using GraphPad Prism 7 to fit the results using a saturation binding model (one site—total and nonspecific binding).

8. Next generation sequencing of aptamer pools

The aptamer pools from all four rounds were indexed and prepared for sequencing according to the *16S Metagenomic Sequencing Library Preparation* guide by Illumina. Adaptor sequences were ordered from IDT. NGS was performed using an Illumina MiSeq system. The FASTAptamer toolkit was used to calculate the copy number and enrichment of each sequence. The image in **Figure 2.4** was created using Geneious version 11.1.2 (http://www.geneious.com).[17]

Rank in R4	Sequence
1	CGCCAAGTAGGTTGGGTAGGGTGGTCTGCGAGTACAGCATGCGCAGTAGC
2	AGAACTCTAGGTTGGTGTGGTTGGATGAGTTTTATGCCGAATACGCTGCC
3	AGACTTCGGTTGGTTAGGTTGGTGTCATGTTCGATCCGTTTACTTTGCAC
4	CCCCGTACTAGGTTGGGTAGGGTGGTGAACGGGACATCCGTCAATCATGT
5	CGCCAAGTAGGTTGGGTAGGGTGGTCTGCGAGTACAGCATGCGCAGTTGC
6	AGAACTCTAGGTTGGTGTGGTTGGATGAGTTTTATGCCGAATACGCTGAC
7	AGACTTCGGTTGGTTAGGTTGGTGTCATGTTCGATCCGGTTACTTTGCAC
8	CGCCAAGTAGGTTGGGTAGGGTGGTCTGCGGGTACAGCATGCGCAGTAGC
9	CGCCAAGTAGGTTGGGTAGGGTGGTCTGCGAGTACGGCATGCGCAGTAGC
10	CGCCAAGTAGGTTGGGTAGGGTGGTCTGCGAGTACAGCATGCACAGTAGC
11	CGCCAAGTAGGTTGGGTAGGGTGGTCTGCGAGTACAGCATGCGCGGTAGC
12	CGCCAAGTAGGTTGGGTAGGGTGGTCCGCGAGTACAGCATGCGCAGTAGC
13	CGCCAAGTAGGTTGGGTAGGGTGGTCTGCGAGTACAGCACGCGCAGTAGC
14	CGCCAAGTAGGCTGGGTAGGGTGGTCTGCGAGTACAGCATGCGCAGTAGC
15	CGCCAAGTAGGTTGGGTAGGGTGGTCTGCGAGTACAGCATGCGCAGTGGC
16	CGCCAAGTAGGTTGGGTAGGGTGGCCTGCGAGTACAGCATGCGCAGTAGC
17	CGCCAAGTAGGTTGGGTAGGGTGGTCTGCGAGTACAGCGTGCGCAGTAGC
18	CGCCAAGTAGGTTGGGTAGGGCGGTCTGCGAGTACAGCATGCGCAGTAGC
19	CGCCAAGTAGGTTGGGTAGGGTGGTCTGCGAGTACAGTATGCGCAGTAGC
20	CGCCAAGTAGGTTGGGTAGGGTGGTCTGCGAGCACAGCATGCGCAGTAGC
21	CGCCAAGTAGGTTGGGTAGGGTGGTCTGCGAGTACAGCATGTGCAGTAGC
22	CGCCAAGTAGGTTGGGTAGGGTGGTCTGTGAGTACAGCATGCGCAGTAGC
23	CGCCAAGTAGGTCGGGTAGGGTGGTCTGCGAGTACAGCATGCGCAGTAGC
24	CGCCAAGTAGGTTGGGTAGGGTGGTCTGCGAGTACAGCATGCGCAGTAGT
25	CGCCAAGTGGGTTGGGTAGGGTGGTCTGCGAGTACAGCATGCGCAGTAGC

Table 2.2. Top 25 sequences by number of reads in round 4 pool from next generation sequencing. Aptamers previously identified by Sanger are highlighted in orange. Aptamers p32-1, p32-2, and p32-3 are ranked first, fourth, and second, respectively, in the R4 pool.

Rank in R4	Reads in R4	Enrichment (R1 to R4)
1	1,561,752	4,170.0
2	163,958	3,727.6
3	54,436	2,682.2
4	54,017	15,913.0
5	23,020	2,918.1
6	19,860	3,520.3
7	16,464	2,087.0
8	14,887	13,250.1
9	14,301	2,534.9
10	8,775	3,905.1

Table 2.3. NGS results for selected sequences. Reads in R4 and the enrichment (reads in R4/reads in R1) are shown for the top 10 sequences. Aptamers previously identified by Sanger are highlighted in orange. Aptamers p32-1, p32-2, and p32-3 are ranked first, fourth, and second, respectively, in the R4 pool.

F. References

1. Rifai N, Gillette MA, Carr SA. Protein biomarker discovery and validation: The long and uncertain path to clinical utility. *Nat Biotechnol*. 2006;24(8):971-983. doi:10.1038/nbt1235.

2. O'Connor JPB, Aboagye EO, Adams JE, et al. Imaging biomarker roadmap for cancer studies. *Nat Rev Clin Oncol*. 2017;14(3):169-186. doi:10.1038/nrclinonc.2016.162.

3. Parikh CR, Mishra J, Thiessen-Philbrook H, et al. Urinary IL-18 is an early predictive biomarker of acute kidney injury after cardiac surgery. *Kidney Int*. 2006;70(1):199-203. doi:10.1038/sj.ki.5001527.

4. Sattlecker M, Kiddle SJ, Newhouse S, et al. Alzheimer's disease biomarker discovery using SOMAscan multiplexed protein technology. *Alzheimer's Dement*. 2014;10(6):724-734. doi:10.1016/j.jalz.2013.09.016.

5. Stern E, Vacic A, Rajan NK, et al. Label-free biomarker detection from whole blood. *Nat Nanotechnol*. 2010;5(2):138-142. doi:10.1038/nnano.2009.353.Label-free.

6. Artemov D, Mori N, Okollie B, Bhujwalla ZM. MR molecular imaging of the Her-2/neu receptor in breast cancer cells using targeted iron oxide nanoparticles. *Magn Reson Med*. 2003;49(3):403-408. doi:10.1002/mrm.10406.

7. Javier DJ, Nitin N, Levy M, Ellington A, Richards-kortum R. Aptamer-Targeted Gold Nanoparticles As Molecular-Specific Contrast Agents for Reflectance Imaging Aptamer-Targeted Gold Nanoparticles As Molecular-Specific Contrast Agents for Reflectance Imaging. *Bioconjug Chem*. 2008;19:1309-1312. doi:10.1021/bc8001248.

8. Song Y, Zhu Z, An Y, et al. Selection of DNA aptamers against epithelial cell

adhesion molecule for cancer cell imaging and circulating tumor cell capture. *Anal Chem*. 2013;85(8):4141-4149. doi:10.1021/ac400366b.

9. Steichen SE, Caldorera-Moore M, Peppas NA. A review of current nanoparticle and targeting moieties for the delivery of cancer therapeutics. *Eur J Pharm Sci*. 2013;48(3):416-427. doi:10.1016/j.ejps.2012.12.006.

10. Liu JKH. The history of monoclonal antibody development - Progress, remaining challenges and future innovations. *Ann Med Surg*. 2014;3(4):113-116. doi:10.1016/j.amsu.2014.09.001.

11. Ng EWM, Shima DT, Calias P, Cunningham ET, Guyer DR, Adamis AP. Pegaptanib, a targeted anti-VEGF aptamer for ocular vascular disease. *Nat Rev Drug Discov*. 2006;5(2):123-132. doi:10.1038/nrd1955.

12. Ferrara N, Adamis AP. Ten years of anti-vascular endothelial growth factor therapy. *Nat Rev Drug Discov*. 2016;15(6):385-403. doi:10.1038/nrd.2015.17.

13. Zhou J, Rossi J. Aptamers as targeted therapeutics: Current potential and challenges. *Nat Rev Drug Discov*. 2017;16(3):181-202. doi:10.1038/nrd.2016.199.

14. Wang J, Gong Q, Maheshwari N, et al. Particle Display: A Quantitative Screening Method for Generating High-Affinity Aptamers. *Angew Chemie*. 2014;126(19):4896-4901. doi:10.1002/ange.201309334.

15. Fogal V, Zhang L, Krajewski S, Ruoslahti E. Mitochondrial/cell-surface protein p32/gC1qR as a molecular target in tumor cells and tumor stroma. *Cancer Res*. 2008;68(17):7210-7218. doi:10.1158/0008-5472.CAN-07-6752.

16. Laakkonen P, Akerman ME, Biliran H, et al. Antitumor activity of a homing peptide that targets tumor lymphatics and tumor cells. *Proc Natl Acad Sci U S A*. 2004;101(25):9381. doi:10.1073/pnas.0403317101.

17. Kearse M, Moir R, Wilson A, et al. Geneious Basic: An integrated and extendable desktop software platform for the organization and analysis of sequence data. *Bioinformatics*. 2012;28(12):1647-1649. doi:10.1093/bioinformatics/bts199.

Chapter III. Developing a method for the discovery of non-natural aptamers

A. Introduction

Natural DNA aptamers can achieve strong and specific binding to many targets, but the chemical diversity of the four natural nucleotides is limited. The incorporation of non-natural nucleotides can expand the chemical space covered by the aptamer library, resulting in greater structural and chemical diversity. Some modifications, including amino acid-like side chains, increase the affinity of the aptamers to many different protein targets.[1] Other modifications can be incorporated that are known to mediate binding to a particular target of interest.

Several groups have developed strategies for generating and screening libraries of non-natural aptamers. For example, Gold and colleagues at SomaLogic have developed SOMAmers (Slow Off-rate Modified Aptamers), a class of aptamers with nucleotides that are modified at the 5-position of uridine with functional groups that mimic amino acids.[2] These modifications have been shown to greatly improve the success rate of aptamer selections, as the chemical diversity of the modified libraries is increased dramatically compared to natural DNA libraries. Recently, SomaLogic screened a variety of combinations of modifications and identified pairs of modifications that can be used in SELEX to improve the performance of the resulting aptamers.[3] Holliger, Chaput, and others have developed XNA (xeno-nucleic acid) aptamers, synthetic nucleic acids with backbone modifications, capable of specific base pairing with DNA.[4–6] XNAs generally cannot be amplified with typical DNA or RNA polymerases, so polymerase engineering is required. Compartmentalized self-tagging is one method that has been developed in order to identify XNA-compatible polymerases.[4] Chaput has reported a complete replication system for

threose nucleic acid (TNA), enabling aptamer selections with TNA.[7] Hirao's group has used a different strategy, generating high affinity aptamers using a third, unnatural base pair.[8,9] This enabled the introduction of a highly hydrophobic base (Ds) into aptamers. By introducing only a few Ds bases at predetermined positions, the authors were able to generate aptamers with picomolar affinity to vascular endothelial growth factor-165 and interferon-γ, more than 100-fold higher than existing aptamers with natural bases.[8] They went on to perform a SELEX experiment with the unnatural base in randomized positions, rather than predetermined positions.[10] Highly modified aptamers have advantages over natural DNA and RNA aptamers, such as improved chemical diversity and stability *in vivo*; however, significant work is often required to engineer and express polymerases that can incorporate non-natural nucelotides.[11] Despite the extensive research that has been performed in this area, many existing mutant polymerases would need further improvements to have sufficient processivity and fidelity to be used effectively for aptamer selections.[12]

As an alternative, the Mayer group has developed an approach called click-SELEX, in which the library molecules incorporate subtly-modified non-natural nucleotides that can subsequently be modified with other functional groups in a separate click chemistry reaction.[13] This enables the use of modifications that are bulky or chemically incompatible with polymerases while also minimizing the amount of polymerase development and optimization required. However, click-SELEX is subject to the same limitations as other SELEX methods. Round-to-round enrichment is limited and can lead to the failure of the selection. This method also requires the modified DNA strands to be reverse transcribed, which limits modifications to those which can be substrates for available polymerases.

By combining a click chemistry-based DNA modification approach with particle display, we have developed Click-particle display (Click-PD), a general strategy for the rapid and efficient selection of non-natural aptamers. Critically, our method is compatible with standard, commercially-available polymerases and can be used to incorporate a wide variety of chemical modifications. This chapter will describe the development of this method and the results of a screen for non-natural aptamers for the carbohydrate-binding protein, concanavalin A (Con A). We generated and screened large libraries of mannose-modified aptamers to identify high affinity binders for the carbohydrate-binding protein, concanavalin A (Con A). We picked Con A because it is widely used as a model to study the molecular mechanisms of protein-carbohydrate interactions.[14,15] To generate highly specific aptamers, we used another carbohydrate-binding protein as a competitor. We generated particles that display aptamers incorporating a modified nucleotide with an alkyne click handle during emulsion PCR, and then performed a Huisgen copper-catalyzed azide alkyne cycloaddition click reaction to conjugate mannose groups to the DNA. We then performed two color sorting to screen for affinity and specificity simultaneously. After three rounds of screening, we identified an aptamer with high affinity and specificity to Con A that also has strong biological activity.

B. Overview of Click-PD

Click-PD has two key differences from the method used in Chapter 2. First, the DNA is modified with mannose to increase the affinity of the aptamers to Con A, a mannose-binding protein. Second, the target and competitor proteins are labeled with two different fluorophores to enable screening for aptamers that bind specifically to the target.

The mannose modification was performed in two steps: PCR incorporation of an alkyne modified nucleotide and subsequent addition of mannose using click chemistry. For the entire aptamer pool, we replaced deoxythymidine (dT) with an alkyne-bearing deoxyuridine derivative (**1**; **Fig. 3.1**). Mayer and coworkers previously showed that the resulting alkyne-bearing product can be readily modified through copper(I)-catalyzed azide-alkyne cycloaddition (CuAAC) click chemistry,[16] and we used this approach to subsequently introduce monosaccharide moieties. Extensive flexible carbohydrate modifications on the nucleic acid backbone can increase the entropic penalty for forming a stable protein-aptamer complex, particularly when exposed to solvent, so we incorporated a second modified nucleobase to improve folding. We chose to replace deoxycytidine (dC) with a pyrimidine 5-formyl-deoxycytidine (**2**; **Fig. 3.1**) bearing an electrophilic aldehyde group, to confer potential interactions with nucleophilic groups, both intramolecular and on the target molecule. Although **2** occurs in nature as an epigenetic marker, to our knowledge it has never been used as a building block for functional aptamers. This procedure gives rise to a large and diverse collection of three-dimensional aptamer structures that display mannose in a wide range of positions and orientations.

In order to screen these libraries of non-natural aptamers, we developed Click-PD (**Fig. 3.1**), which is based on the particle display approach previously developed by our group for the discovery of conventional DNA aptamers.[17,18] Click-PD begins with the generation of particles that display aptamers containing non-natural nucleic acids **1** and **2** via emulsion PCR, as described previously. For this study, we generated our non-natural aptamer particles from a library of 80 nt DNAs comprising a 40 nt random region flanked by 20 nt primer-binding sites at both ends. Briefly, water-in-oil emulsions were prepared with forward primer

(FP) coated magnetic beads, PCR reagents and templates comprising both modified and canonical deoxynucleotide triphosphates (dNTPs), such that each droplet contains (in most cases) one DNA template and one bead (**Fig. 3.1**, step 1). Details of this process are provided in the Experimental section. We specifically selected non-natural nucleotides **1** and **2** because these nucleotide analogues can be incorporated by commercial DNA polymerases during the PCR procedure.[19–23] Emulsion PCR amplification yields a library of monoclonal particles displaying sequences that bear both alkyne and aldehyde groups (**Fig. 3.1**, step 2). After breaking the emulsion and removing the PCR reagents, the particles are isolated (**Fig. 3.1**, step 3) and conjugated with an azido-substituted mannose side chain (**3**) through click chemistry (**Fig. 3.1**, step 4). The monosaccharide-modified, double-stranded PCR products are subsequently treated with NaOH and ammonium hydroxide to remove the antisense strand and deprotect the monosaccharide moiety, resulting in particle-displayed non-natural aptamers that incorporate monosaccharide-conjugated nucleotides (**4**) (**Fig. 3.1**, step 5). It should be noted that conjugation is performed while the products are still double-stranded. We opted for this approach because the alkyne side chain at the 5-position of uracil adopts an outward-pointing conformation in the major groove of the double helix,[22] which prevents steric hindrance caused by single-stranded nucleic acid folding and thus allows for more efficient and uniform modification.

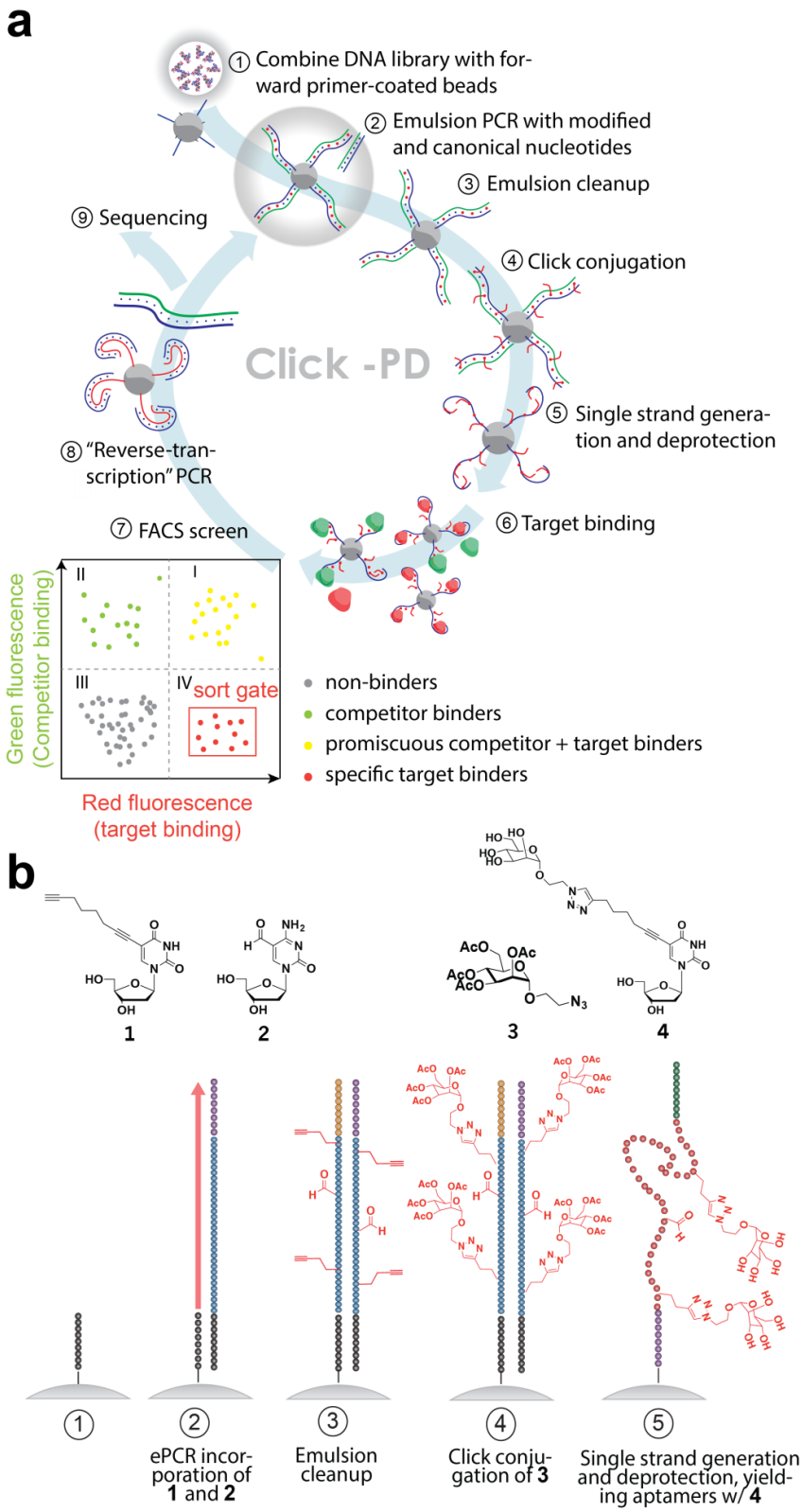

Figure 3.1. Click-PD strategy for the synthesis and screening of non-natural aptamers. (a) After conjugating the initial DNA library to forward primer-coated magnetic beads (step 1), we perform emulsion PCR (step 2) to produce monoclonal aptamer particles in which dT and

dC are substituted with non-natural pyrimidine nucleotides **1** and **2**, respectively. We then break the emulsions (step 3) and use a click chemistry approach (step 4) to conjugate carbohydrate azides (**3**) to the alkyne group on 1. These are converted to single-stranded aptamers (step 5) containing carbohydrate-modified deoxyuridine (**4**), and then combined with both target and non-target lectins, each labeled with a distinct fluorophore (step 6). FACS screening allows us to isolate the aptamers that exhibit strong binding to the target but not the non-target lectin (step 7). The selected non-natural aptamers are then converted back to natural DNA by a "reverse transcription"-like PCR reaction (step 8) and subjected either to sequencing analysis (step 9) or further screening. (b) Structures of non-natural pyrimidine nucleotides and carbohydrate azides, and illustration of the non-natural aptamer synthesis process.

Once the library of non-natural aptamer-displaying particles was prepared, we incubated the particles with both target and non-target carbohydrate-binding proteins (**Fig. 3.1**, step 6). The two proteins were labeled with different fluorophores to enable simultaneous measurement of on- and off-target binding. We chose the lectin Con A as the target for our initial screen, because this protein is widely used as a model to understand the molecular mechanisms of protein-carbohydrate interactions and has been extensively studied in structural biology.[15,24,25] For the non-target competitor, we selected *Pisum sativum* agglutinin (PSA), which is another mannose-binding lectin with considerable structural homology to Con A. [26,27] Con A and PSA were labeled with Alexa Fluor 647 and fluorescein isothiocyanate (FITC), respectively. After incubating our particles with both Con A and PSA, we used FACS to sort individual particles that simultaneously exhibit high Alexa 647 fluorescence (and thus high Con A affinity) and weak FITC fluorescence (and thus low PSA affinity) (**Fig. 3.1**, step 7). Finally, we performed a "reverse transcription"-like PCR reaction to convert the selected non-natural aptamers back to natural DNA (**Fig. 3.1**, step 8), with the enriched pool used for either a new round of screening or sequencing (**Fig. 3.1**, step 9).

C. Results and discussion

1. Click-PD development and optimization

We performed a series of experiments to optimize the efficiency of key steps of the Click-PD procedure. All DNA sequences used in the optimization experiments are shown in **Table 3.1**. First, we screened several DNA polymerases to identify a candidate that allows effective replacement of dT and dC with **1** and **2**, respectively, during PCR (**Fig. 3.2**). We tested KOD-XL, Pwo, and Deep Vent DNA polymerases. A series of test PCR reactions showed that KOD-XL provided the highest yield and purity.

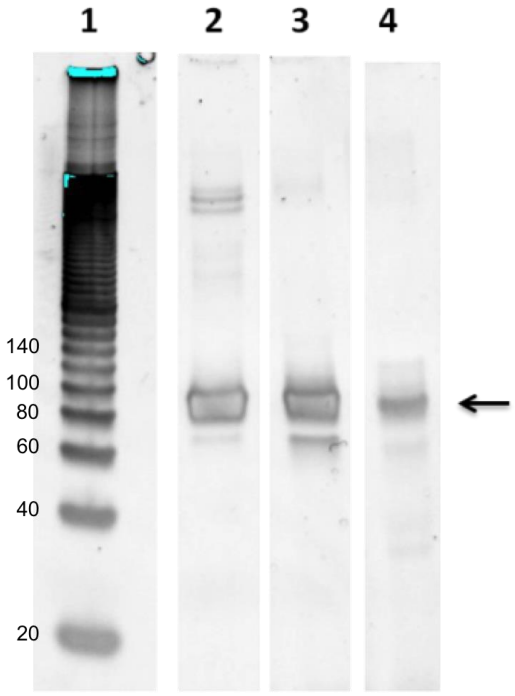

Figure 3.2. Screen for polymerase-mediated incorporation of modified pyrimidine deoxyribonucleotides **1** and **2**. PCR template: an 81 nt DNA oligonucleotide, T1. Lane 1: DNA ladder; lane 2: KOD-XL; lane 3: Pwo; lane 4: Deep Vent. The arrow indicates the full-length product. KOD-XL DNA polymerase gives the highest yield without a major byproduct.

Next, we optimized reaction conditions for coupling mannose to **1** via click chemistry. After screening various reaction conditions for the click conjugation of monosaccharides with azido substitutions at different positions, we determined that a reaction with 2,3,4,6-tetra-O-acetyl-protected, 2-azidoethyl derivatives, such as **3**, performed with copper(I) bromide and tris[(1-benzyl-1H-1,2,3-triazol-4-yl)methyl]amine (TBTA), achieved quantitative yield of the fully-conjugated product (**Fig. 3.3**). We confirmed the successful and efficient PCR incorporation of **1** and **2** and subsequent click chemistry modification by denaturing polyacrylamide gel electrophoresis (PAGE; **Fig. 3.4a**) and electrospray ionization mass spectrometry (ESI-MS, **Fig. 3.4b**).

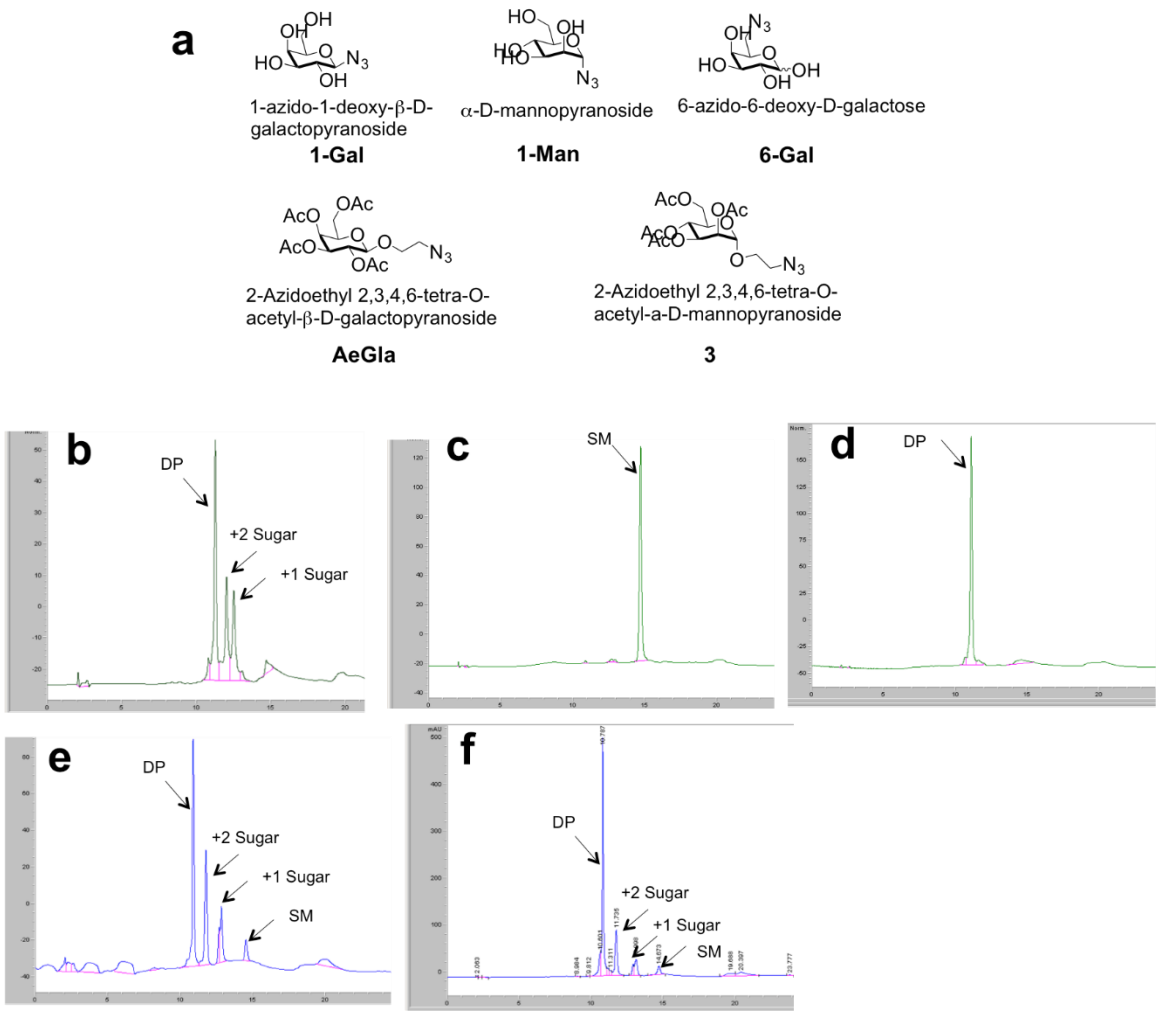

Figure 3.3. Optimization of click chemistry using a 21 nt oligonucleotide substrate with three consecutive alkyne side chains. (a) Structures of azido-sugars screened for click conjugation to alkyne-bearing 21 nt DNA oligonucleotide with three consecutive **1**s, S1. (b)-(f) HPLC analysis of click conjugation under different conditions with different substrates. Click chemistry conditions are as follows: (b) conjugation of **3** 0.4 mM $CuSO_4$ + 2 mM THPTA + 4 mM sodium ascorbate; (c) conjugation of **3** with 0.4 mM $CuSO_4$ + 0.4 mM TBTA + 0.8 mM TCEP; (d) conjugation of **3** with 0.4 mM CuBr + 0.4 mM TBTA; (e) conjugation of 1-Man with 0.4 mM CuBr + 0.4 mM TBTA; (f) conjugation of 6-Gal with 0.4 mM CuBr + 0.4 mM TBTA. DP: desired product. SM: starting material. +1 sugar and +2 sugar: products with one or two carbohydrate substrates conjugated. Only click conjugation of substrates **3** and AeGla (results not shown) with 0.4 mM CuBr + 0.4 mM TBTA gave quantitative yield of the desired product without major byproducts.

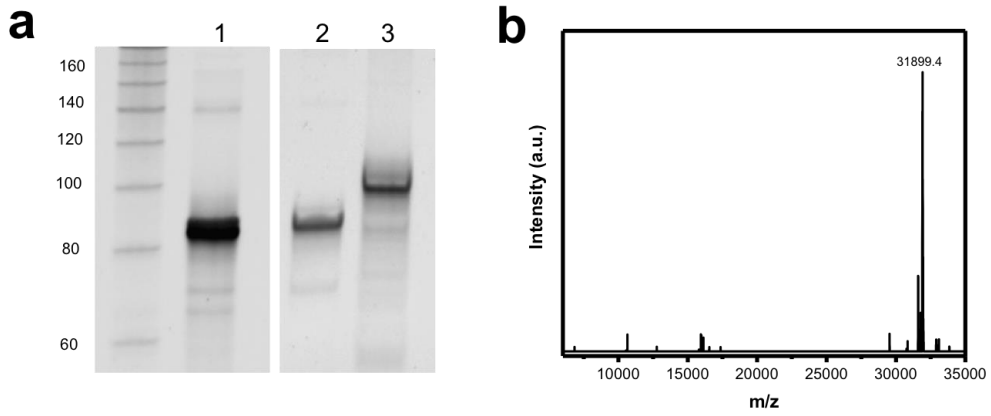

Figure 3.4. Optimization of click conjugation. (a) Click chemistry reaction efficiently modified the T1-derived PCR product (after removing the antisense strand), M1, which contains numerous **1** and **2** nucleotides. Gel lanes represent the template before (lane 1) and after strand separation either immediately after PCR (lane 2) or after subsequent click conjugation with **3** (lane 3). (b) ESI-MS characterization of M1 (expected: 31901.2 Da, observed: 31899.4 Da).

We then confirmed that these non-natural aptamers are efficiently displayed on the particle surface by fluorescently labeling the 3'-end of the non-natural aptamers to allow for characterization by flow cytometry after emulsion PCR. A cleavable disulfide linker was incorporated between the aptamer and the particle to allow cleavage of the modified DNA for electrophoretic analysis (**Fig. 3.5**). The slightly lower mobility of the cleaved non-natural aptamer was attributed to the extra mass from the "scar" of the disulfide linker.

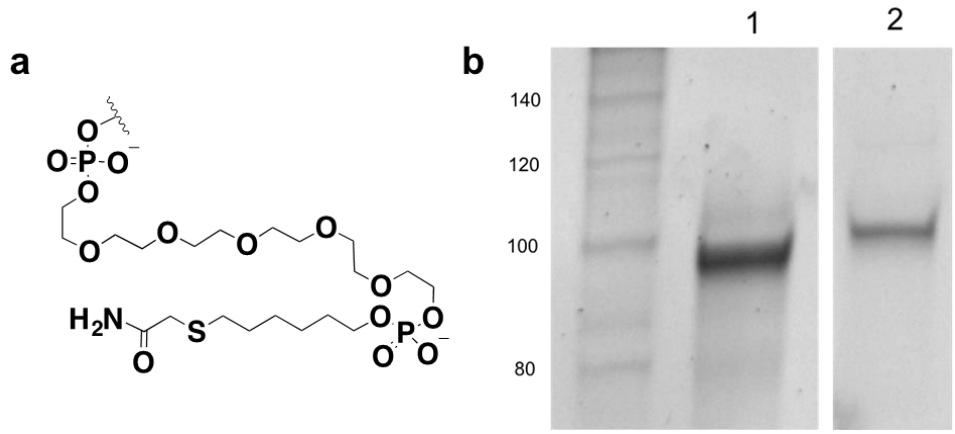

Figure 3.5. Confirmation of the generation of particle-displayed non-natural aptamers. (a) structure of the "scar" of the disulfide linker after non-natural aptamer cleavage. The disulfide linker between the forward primer and the particle is cleaved by TCEP treatment followed by alkylation using iodoacetamide. (b) Click chemistry reaction conditions efficiently modified particle-coupled non-natural aptamers. Lane 1 contains the reaction product M1 formed in solution (see **Fig. 3.4a**), and lane 2 contains non-natural aptamer cleaved from beads after emulsion PCR and on-bead click reaction.

Finally, we optimized the "reverse transcription" process to convert the carbohydrate-modified DNA back to natural DNA molecules with the same nucleotide sequence. After testing four different DNA polymerases (Taq, KOD-XL, Pwo, Deep Vent, **Fig. 3.6a**), we found that Taq efficiently generated DNA of the correct length from the non-natural aptamers (**Fig. 3.6b**). This is consistent with previous findings that family B DNA polymerases such as Taq are particularly suited for primer extension along modified nucleic acid templates.[28,29]. Sanger sequencing showed that the product generated by Taq polymerase was identical to the starting template, confirming the fidelity of the reverse transcription process (**Fig. 3.6c**).

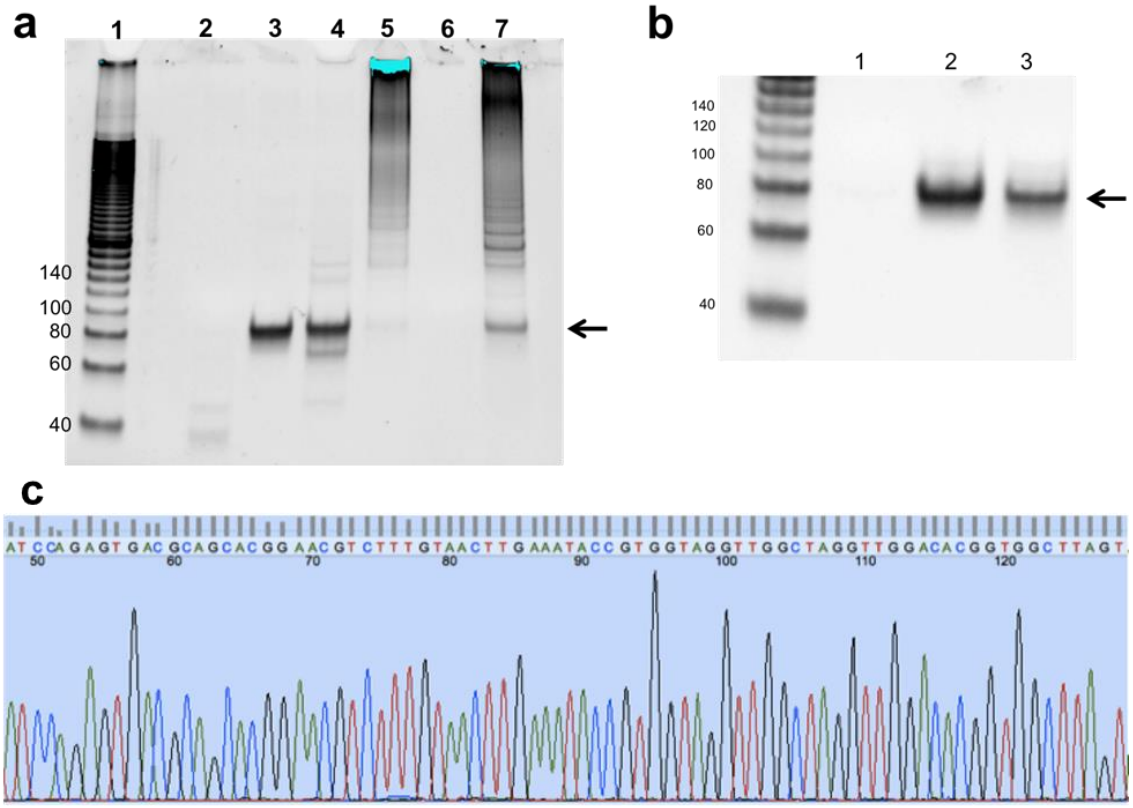

Figure 3.6. Taq polymerase efficiently converts non-natural aptamers back to natural DNA by a "reverse transcription" PCR process. (a) Polymerase screen for the reverse transcription step. Lane 1: DNA ladder; lane 2: Taq polymerase, without template; lane 3: Taq polymerase, using canonical DNA template T1; lane 4: Taq polymerase, using non-natural aptamer particles as template; lane 5: KOD-XL, using non-natural aptamer particles as template; lane 6: Pwo, using non-natural aptamer particles as template; lane 7: Deep Vent, using non-natural aptamer particles as template. The arrow indicates the full-length product. (b) Confirmation of the reverse-transcription using Taq DNA polymerase. Lane 1: PCR without template; lane 2: PCR using natural DNA, T1, as the template; lane 3: PCR using non-natural aptamer M1 displayed on beads as template. (c) Sanger sequencing of the product of reverse-transcription**.** PCR products from reverse-transcription were cloned into a TOPO vector and transfected into TOP10 chemically competent *E. coli*. Colonies were harvested and sent for Sanger sequencing. All 20 colonies sequenced were either matched or complementary to the sequence of T1, demonstrating good fidelity for the reverse-transcription reaction.

2. Screen for mannose-modified aptamers targeting concanavalin A

Once the method was optimized, we began the screen for high affinity aptamers for concanavalin A (Con A). DNA sequences used in the screen are shown in **Table 3.2**. We started the screen with ~10^8 non-natural aptamer particles. A fraction of this starting

population already had strong affinity for Con A at a concentration of 1 nM (**Fig. 3.7**); however, the majority of the sequences in the initial pool were lacking in specificity, as shown by the significant binding to PSA. This lack of specificity was expected, given that both lectins bind strongly to mannose. We performed three rounds of screening, collecting only the particles that exhibited strong Con A binding without binding PSA. We observed a clear increase in the specificity of the selected particles from round to round, and by the end of Round 3, 17.8% of the population bound strongly to 1 nM Con A without binding to PSA, even in the presence of a 250-fold higher concentration of the competitor (**Fig. 3.7)**.

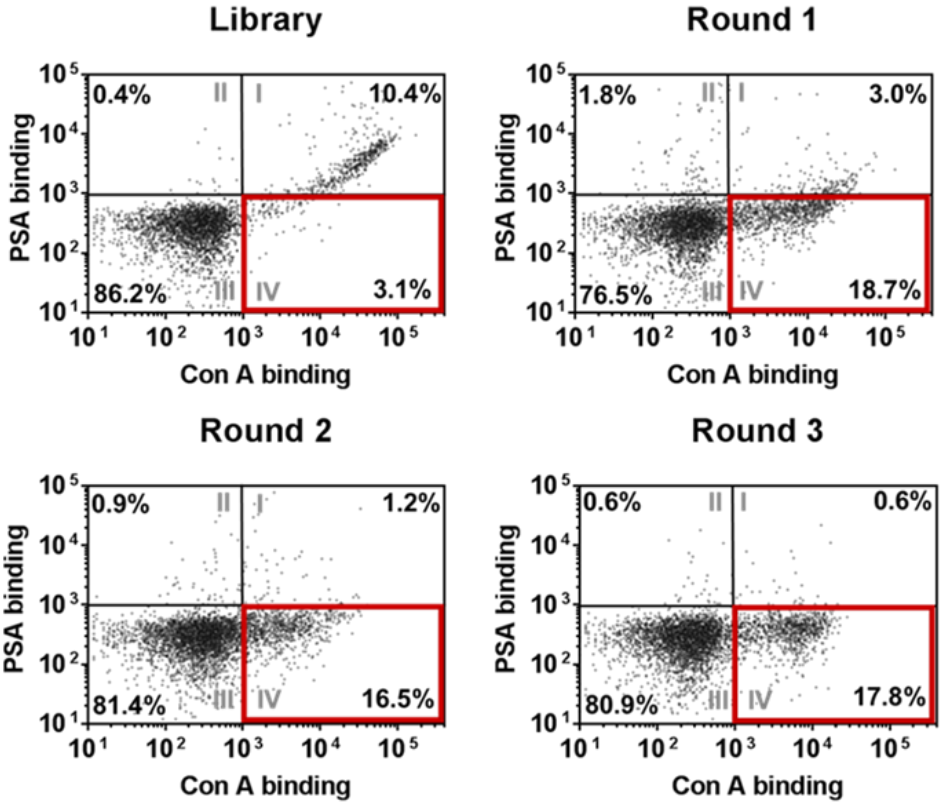

Figure 3.7. Click-PD screening generates non-natural aptamers with high affinity and specificity for Con A. FACS plots of non-natural aptamer-displaying particles from the starting library and Rounds 1–3, where [Con A] = 1 nM and [PSA] = 250 nM. Percentages represent the subpopulation of particles in each quadrant. Quadrant IV (outlined in red) represents aptamers with high Con A and low PSA affinity, which were collected in each round.

We then performed next generation sequencing of the Round 1, 2, and 3 pools to identify sequences that were highly enriched during the Click-PD screen. After filtering out low-quality sequences (where >10% of bases had a quality score ≤20) using Galaxy NGS tools (see Experimental section), we obtained 182,499 unique sequences (684,179 reads) in the Round 1 pool, 150,680 unique sequences (643,462 reads) in the Round 2 pool, and 2,867 unique sequences (470,426 reads) in the Round 3 pool. We identified 132 sequence clusters, defined as groups of closely-related sequences that differ from one another by two or fewer mutations,[30] in the Round 3 pool. The degree of enrichment from Round 1 to Round 3 varied for the sequences within each cluster, with some of the most enriched clusters containing sequences that had undergone 100-fold to >1000-fold enrichment (**Fig. 3.8a**). We selected 14 sequences exhibiting >100-fold enrichment for further testing, synthesizing particles displaying each of these sequences and measuring their fluorescence intensity after incubating with 1 nM Con A (see **Table 3.3**). Sequence 3-1 was selected for further characterization due to its strong binding to Con A and the fact that it belonged to a highly enriched (>2,000-fold) sequence cluster (**Fig. 3.8b**).

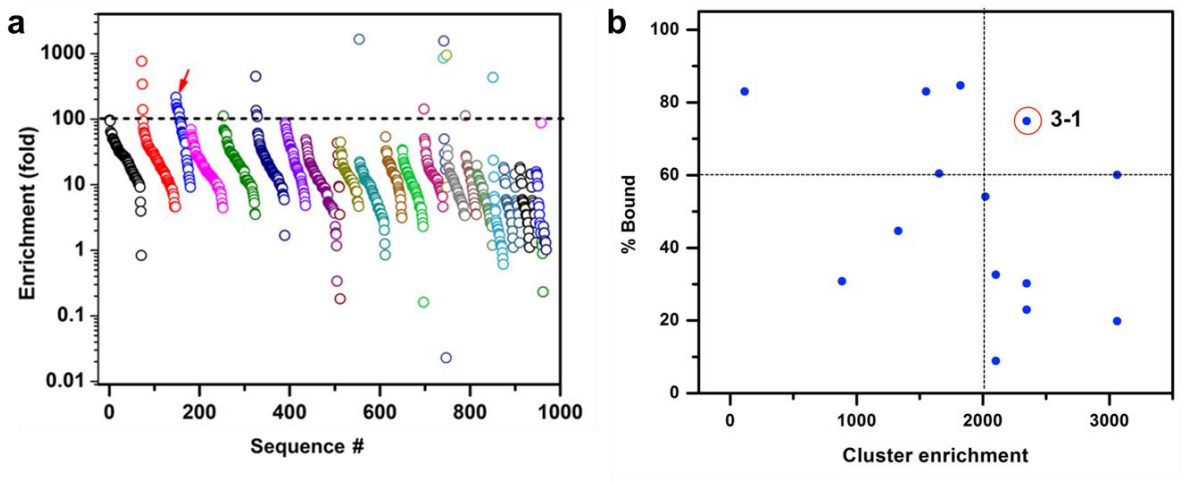

Figure 3.8. (a) Next generation sequencing shows several highly-enriched clusters of closely related sequences in the Round 3 pool. Each circle represents one enriched sequence, with colors indicating related clusters. The dotted line depicts our threshold for the most highly-enriched sequences (>100-fold). Aptamer 3-1 (red arrow) was selected for further characterization. (b) Binding of selected sequences to fluorescently labeled Con A in a particle-based assay. Two criteria were considered to identify the top-performing non-natural aptamer: binding of each sequence to Con A in a particle-based fluorescence assay, and enrichment of the cluster from which each sequence originated. Aptamer 3-1 performed well according to these metrics.

3. Characterizing aptamer affinity and mutation studies

Aptamer 3-1 bound strongly to Con A and exhibited remarkably high specificity for this lectin. We incubated particles displaying 3-1 with different concentrations of fluorescently-labeled Con A and PSA and measured the fluorescence intensity of the particles using flow cytometry. This revealed strong affinity for Con A (K_d = 20 nM), with a much weaker affinity for PSA (K_d > 1000 nM), clearly demonstrating the excellent specificity of this molecule (**Fig. 3.9a).**

Apatamer 3-1 contains multiple types of modifications, so our next objective was to determine the extent to which each of these modifications contributed to its strong and specific interaction with Con A. We synthesized particles displaying various mutant sequences based on 3-1 with different modification profiles (see **Table 3.4**). 3-1a (aldehyde

only) no longer contained **4**, but still had dC substituted with **2**, displaying aldehyde groups. On the other hand, 3-1m (mannose only) lacked **2** but still had dT substituted with **4**. We also prepared a construct composed entirely of canonical bases (3-1n, natural), and a version of 3-1 that was not subjected to subsequent click conjugation of **3** (3-1nc, no click). Finally, to confirm that the affinity of 3-1 is sequence-specific, we prepared a "CT-only" sequence that was the same length as 3-1 but only contained dC and **4**, where the number of **4** nucleotides was equal to that of 3-1 (CT), and a sequence with the same nucleotide composition as 3-1m but in a scrambled order (3-1mscr, scrambled).

3-1a, 3-1n, and 3-1nc showed essentially no binding to 10 nM Con A (**Fig. 3.9b**), indicating that Con A binding was mannose-dependent. Both CT and 3-1mscr showed only low levels of binding to 10 nM Con A, which is most likely attributable to the presence of the mannose functional groups in this polymer. Notably, 3-1m showed only slightly lower levels of binding to 10 nM Con A than 3-1, despite the absence of aldehyde modifications. This unexpected finding prompted us to further investigate 3-1m's binding profile. We determined that the affinity of 3-1m for Con A is in fact slightly superior to 3-1 (K_d = 17 nM), and that the absence of modified nucleotide **2** did not affect 3-1m's specificity against PSA (K_d >1000 nM) (**Fig. 3.9a**). This indicates that the aldehyde functional groups do not contribute meaningfully to 3-1's affinity or specificity, and that only the mannose modifications are required for binding to Con A.

To further determine the extent to which each mannose side chain contributes to 3-1m's interaction with Con A, we generated particles displaying mutants of 3-1m in which either individual occurrences or pairs of nucleotide **4** within the sequence (excluding the primer region) were substituted with dA and screened their affinity for Con A (**Fig. 3.9c**).

The substituted sequences are shown in **Table 3.4**. We determined that essentially all of the mannose groups, with the exception of those at nucleotide positions 45 and 46, are critical for binding, and that the loss of even one mannose side-chain in the sequence significantly reduced the affinity of the mutant (**Fig. 3.9d**).

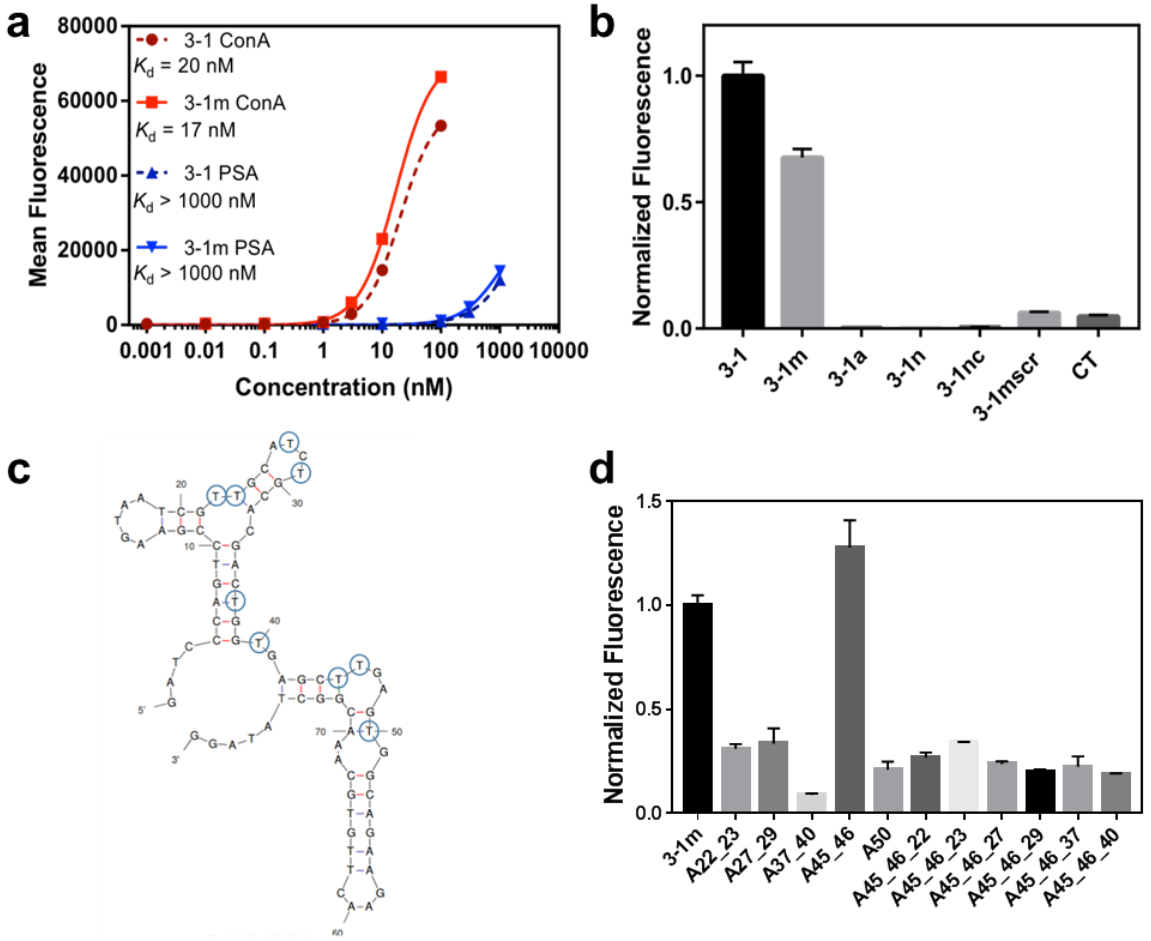

Figure 3.9. Affinity and specificity of Con A aptamers. (a) Binding curves of 3-1 and 3-1m to Con A and PSA based on particle-based fluorescent measurements. (b) Binding activity for various 3-1 derivatives in the presence of 10 nM Con A. Fluorescence intensities were normalized first to particle coating, then to the relative signal of 3-1. (c) Structure-activity relationship of 3-1m. Folding structure of 3-1m predicted by mFold. Note that modified nucleotide **4** has been substituted with dT in the simulation. The circled nucleotide positions were mutated to dA individually or in pairs, and the binding of the mutant non-natural aptamers was characterized in a particle-based fluorescent assay. (d) The relative fluorescence signals of the mutant sequences. The error bars were derived from the standard deviation of three experimental replicates. The fluorescence signals were first normalized to particle coating, and then to the relative signal of 3-1m.

We further validated the binding characteristics of 3-1 and 3-1m by using an alternative measurement method, bio-layer interferometry (BLI).[31] This allowed us to confirm that these binding results are independent of the particles on which the aptamers are immobilized, and to measure association rate (k_{on}) and dissociation rate (k_{off}) constants. Solution-phase non-natural aptamers were prepared using conventional PCR instead of emulsion PCR, with biotinylated FP instead of particle-conjugated FP and with ESI-MS confirmation after click conjugation with **3** (**Fig. 3.10a, b**). We immobilized biotinylated 3-1 and 3-1m onto the streptavidin-coated surface of the biosensor and incubated with Con A at various concentrations, followed by dissociation in blank buffer (**Fig. 3.11a**). For 3-1m, we globally fitted the resulting response curves for each concentration to generate rate constants of $k_{on} = (7.1 \pm 0.3) \times 10^4\ M^{-1}\ s$, and $k_{off} = (2.3 \pm 0.02) \times 10^{-4}\ s^{-1}$, corresponding to a K_d of 3.2 ± 0.2 nM. Notably, the off-rate (k_{off}) of both 3-1 and 3-1m when bound to Con A was comparable to or lower than that of many antibody-antigen interactions.[32,33] We also fitted the maximum response measurements from each concentration to a cooperative binding model, yielding a K_d of 5.3 ± 0.7 nM for 3-1m. These affinity values are in reasonable agreement with the measurement from our particle-based binding assay. In comparison, the K_d of 3-1 for Con A is 5.8 ± 0.8 nM by BLI (**Fig. 3.11b**), confirming that the substitution of dC with **2** does not enhance lectin binding, and indeed slightly reduces affinity in the BLI assay.

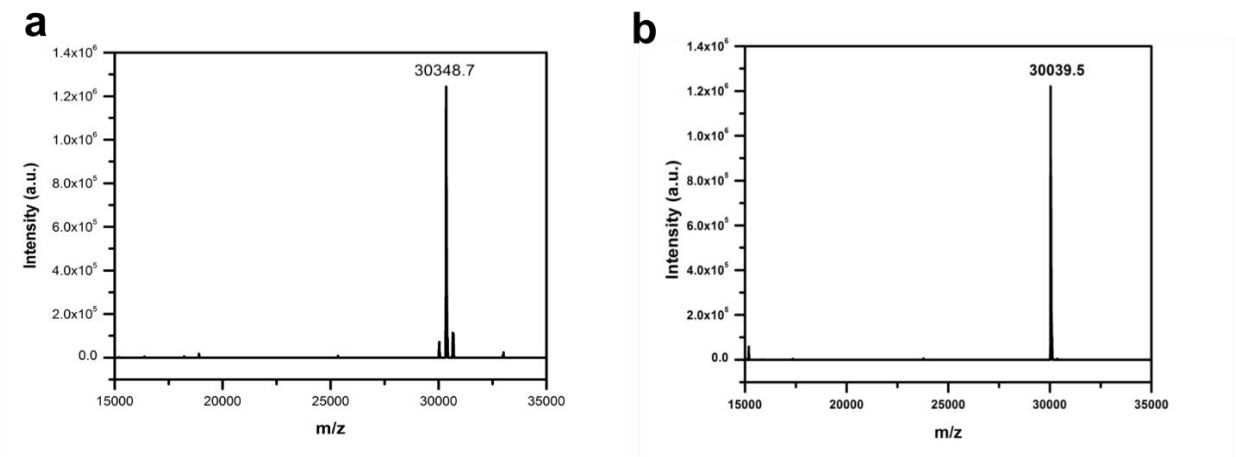

Figure 3.10. ESI-MS characterization of solution-phase 3-1 and 3-1m with 5'-biotinylation. (a) 3-1. Expected mass: 30352.6; observed mass: 30348.7. (b) 3-1m. Expected mass: 30040.5; observed mass: 30039.5.

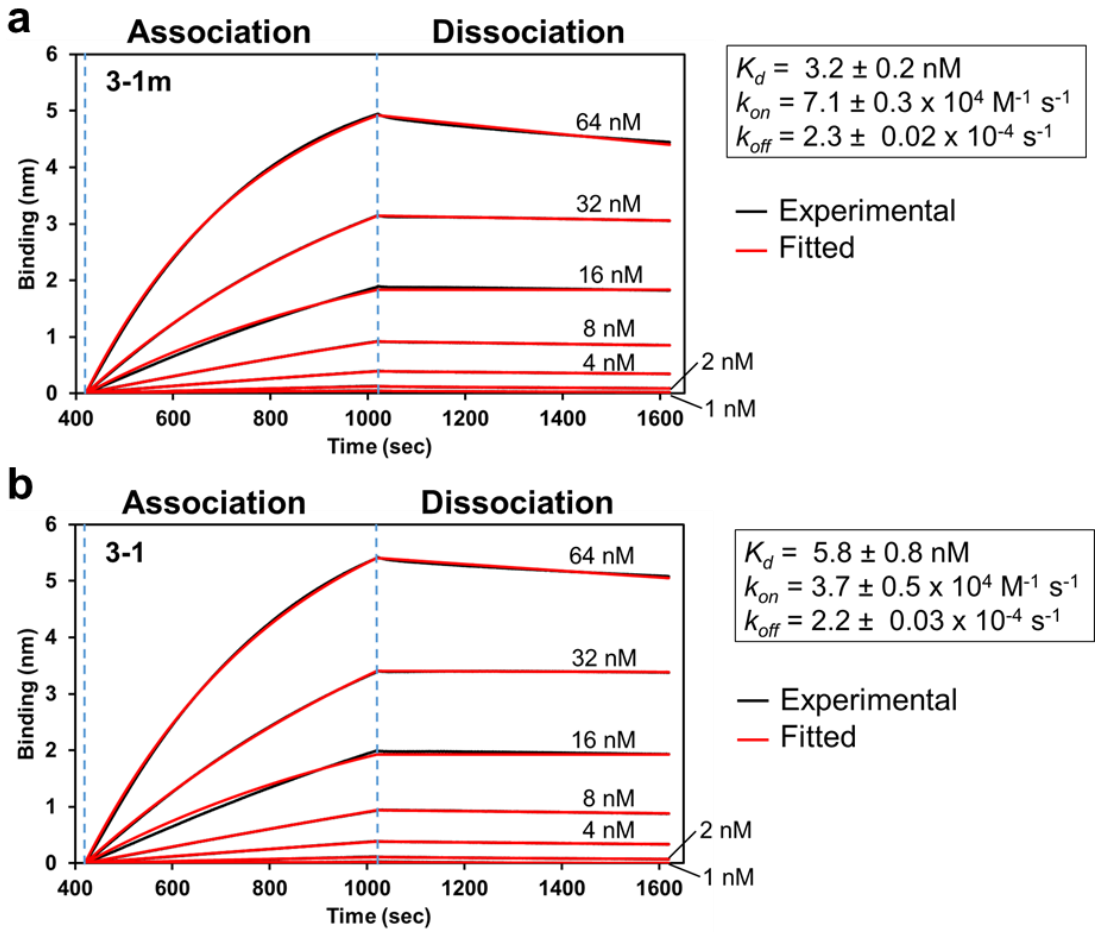

Figure 3.11. BLI analysis of 3-1m and 3-1. Bio-layer interferometry (BLI) measurement of Con A interacting with surface-immobilized (a) 3-1m and (b) 3-1. Global fitting of target association and dissociation at each concentration was performed to generate K_d, k_{on}, and k_{off} values.

4. Testing specificity of aptamer 3-1m to Con A

Having shown 3-1m's strong specificity for Con A versus PSA, we subsequently demonstrated its ability to discriminate against other closely-related lectins that also preferentially bind mannose. Plant-derived mannose-binding lectins such as *Lens culinaris* agglutinin (LcH), *Narcissus pseudonarcissus* lectin (NPA), and *Vicia faba* agglutinin (VFA) all belong to the same carbohydrate specificity group as Con A and PSA and share high structural homology,[34] and are therefore good models for testing specificity. Critically, 3-1m exhibited virtually no binding to LcH, NPA, or VFA at 10 nM. Even at a 100-fold higher concentration (1 μM), 3-1m showed little binding to LcH and NPA, and only modest binding to VFA (**Fig. 3.12a**). This low level of binding to VFA at high concentrations can be attributed to the especially high degree of homology between Con A and VFA.[34]

Next, we expanded our analysis of 3-1m to an extended group of 40 structurally related and unrelated lectins using a lectin array (**Fig. 3.12b**). In addition to the lectins studied above, this array also included lectins belonging to different specificity groups with varying degrees of homology to Con A. A complete list of the lectins on the array is given in **Table 3.5**. This assay further confirmed the remarkable specificity of 3-1m: across a broad range of concentrations from 0.04–400 nM, Con A was the only lectin that generated a strong signal. It should be noted that although VVA showed slightly higher signal than the other non-target lectins, we subsequently determined this to be a false positive. This array feature produced a significant signal even in the absence of 3-1m, and this signal did not increase at higher 3-1m concentrations.

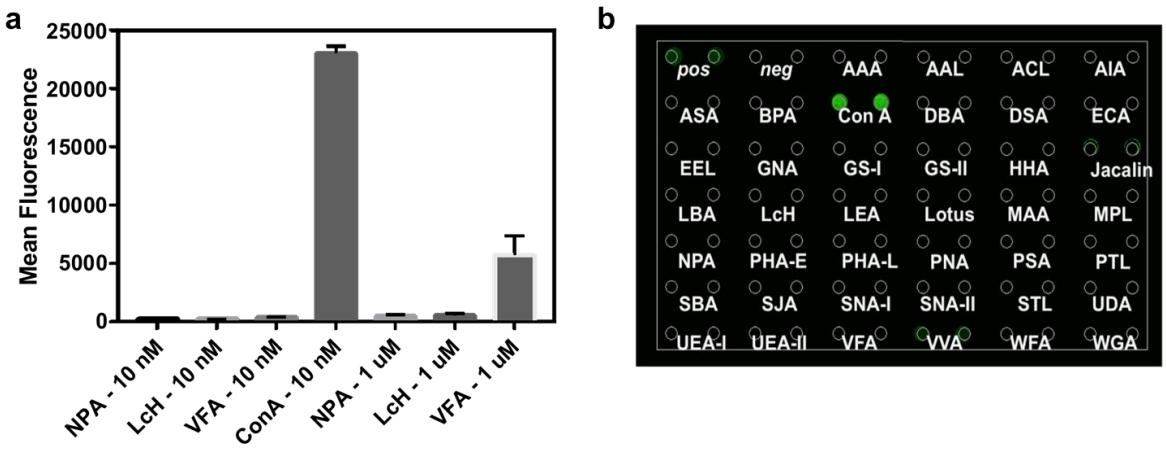

Figure 3.12. Aptamer 3-1m is highly specific to Con A. (a) We incubated particles coated with 3-1m with fluorescently-labeled mannose-binding lectins. These were then washed and analyzed by FACS based on mean fluorescence of the population. Error bars were derived from the standard deviation of three experimental replicates. (b) The strong specificity of 3-1m remains clearly apparent on a larger array of 40 lectins. White open circles show the position of each lectin spot. Each lectin is spotted in duplicate. The short names of the lectins are written under the spots; *pos* and *neg* denote positive and negative controls, respectively.

5. Measuring biological activity of aptamer 3-1m

Given the strong affinity and specificity of aptamer 3-1m to Con A, we hypothesized that it might act as an inhibitor of Con A's biological activity. Con A induces clumping of human erythrocytes in a process known as hemagglutination,[25] and hemagglutination assays are a standard approach for quantifying activity of this lectin. As a baseline, we established that complete hemagglutination occurs at 150 nM Con A, based on visual observation of the deposition of erythrocytes in a 96-well plate. This was confirmed by monitoring absorbance of the cell suspension at 655 nm, which correlates to the size of the agglutinated clump.[35] We then tested the extent to which 3-1m can inhibit this process by incubating various concentrations of 3-1m with 150 nM Con A for 30 min at room temperature before adding erythrocytes at 1% hematocrit. We observed concentration-dependent inhibition of Con A-induced hemagglutination, with complete inhibition at 150 nM and a half-maximal inhibitory

concentration (IC_{50}) of 95 nM (**Fig. 3.13a, b**). We also microscopically monitored inhibition of Con A-induced hemagglutination by 3-1m; the erythrocyte clumps that formed upon the addition of Con A were absent when we incubated Con A with 3-1m beforehand (**Fig. 3.13c–e**).

Aptamer 3-1m inhibits Con A-induced hemagglutination with ~10^7-fold greater potency than methyl α-D-glucopyranoside, a commonly used inhibitor that achieves maximal effect at 50 mM.[36] Furthermore, 3-1m is about three-fold more potent than the best known inhibitor described to date for Con A, a mannose glycopolymer reported by Kiessling et al., which achieves complete inhibition at 500 nM. This is particularly striking given that 3-1m contains 120-fold fewer mannose side chains (14 units) compared with the mannose glycopolymer (~1,700 units), suggesting that its carbohydrate presentation more closely aligns with the active sites of this lectin.[37]

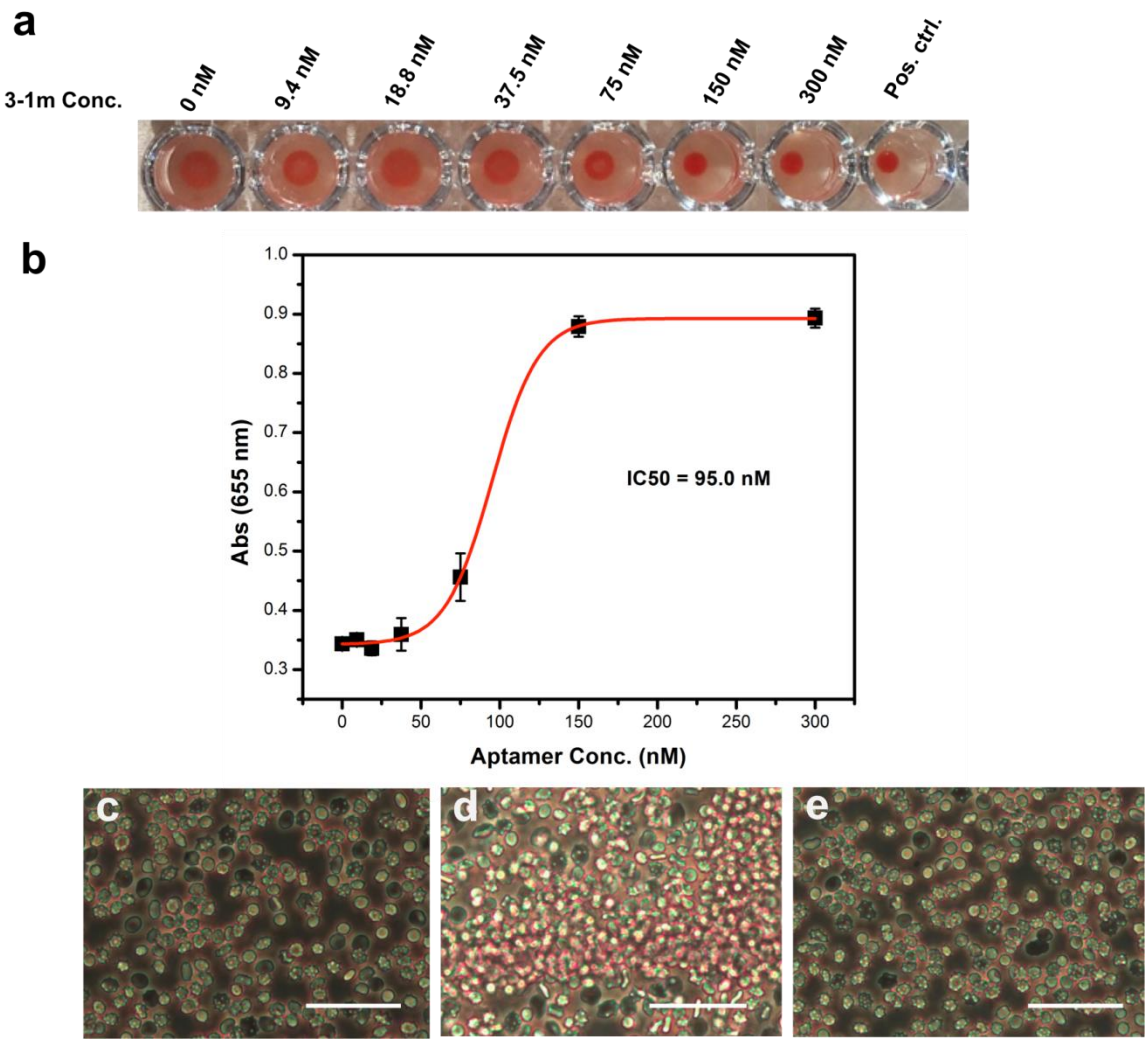

Figure 3.13. 3-1m is a potent inhibitor of Con A-induced hemagglutination. (a) We incubated various concentrations of 3-1m with a human erythrocyte suspension containing 150 nM Con A, a concentration known to induce complete hemagglutination. The deposition of erythrocytes onto the bottom of the wells indicates inhibition of Con A activity. The positive control well contains only human erythrocytes, with no Con A. (b) Inhibition of hemagglutination, as measured by increased absorbance at 655 nm. We observed that 3-1m inhibited 150 nM Con A with an IC_{50} of 95.0 nM. The error bars were derived from the standard deviation of four replicates. (c–e) 40X microscopic images of normal human erythrocytes (c) and human erythrocytes incubated with 0.65 μM Con A (d) or 0.65 μM Con A with 0.8 μM 3-1m (e). Scale bars = 40 μm.

D. Conclusions

We have developed a new method for non-natural aptamer discovery. We used this method to generate mannose-modified aptamers for the target lectin, Con A. The top

aptamer, 3-1m, has high affinity and specificity to Con A. We found that both the mannose modifications and the DNA sequence were essential to the high performance of 3-1m. Finally, we showed that 3-1m has strong biological activity, inhibiting Con A-induced hemagglutination.

Click-PD does not rely on polymerase engineering or synthesis of customized nucleotides. This means that a huge variety of modifications could be readily used in the aptamer discovery process. Modifications that are known to have specific interactions with the target can be used (as shown here). Other work has demonstrated that incorporating amino acid-based modifications can improve the outcome of aptamer selections by generally increasing the potential interactions with the target protein.[1] With this method, we aim to reduce the barrier to discovering non-natural aptamers, enabling the generation of high quality aptamers to a broader range of targets.

E. Experimental section

1. Reagents

All DNA oligonucleotides were purchased from Integrated DNA Technologies. Primers were ordered with standard desalting. PCR templates were ordered with PAGE purification. Other than the exceptions noted below, all commercially available reagents and lab supplies were purchased from Aldrich. 2-azidoethyl 2,3,4,6-tetra-O-acetyl-α-D-mannopyranoside and 2-azidoethyl 2,3,4,6-tetra-O-acetyl-β-D-galactopyranoside were purchased from Synthose Inc. KOD-XL DNA polymerase was purchased from Thermo Fisher Scientific. Taq polymerase was purchased from Promega. Pwo DNA polymerase was purchased from Roche. C8-Alkyne-dUTP was purchased from Axxora Inc. 5-formyl dCTP was purchased from TriLink BioTechnologies. Deep Vent DNA polymerase and standard

dNTPs were purchased from New England Biolabs. Lectin Array 40 was purchased from RayBiotech, Inc. Human erythrocytes were purchased from BioreclamationIVT. Mini-PROTEAN^{TM} native and denaturing PAGE gels (10%) were purchased from Bio-Rad. Dynabeads MyOne carboxylic acid and streptavidin C1 beads for particle display and single-stranded PCR product generation, respectively, were purchased from Thermo Fisher Scientific.

ESI-MS characterization was performed by Novatia. Optical microscopy imaging was performed on an Olympus CKX-41 inverted microscope with color digital camera using 40X objectives. The images were processed with ImageJ software. Reverse-phase HPLC analysis was performed on an Agilent 1100 system using a PLRP-S 4.6×150 mm 5 μm column with 300 Å packing material, with a gradient from 95% 0.1 M triethylammonium acetate (TEAA)/5% acetonitrile to 20% 0.1 M TEAA/65% acetonitrile over 30 min. Flow cytometry assays were performed using a BD Accuri C6 flow cytometer. Fluorescence-based sorting of particles was done using a BD FACSAria III. Bio-Layer Interferometry measurements were performed with a ForteBIO Octet RED384 system, and analysis was performed using Octet Data Analysis software. MicroScale Thermophoresis measurements were carried out by 2bind.

2. Polymerase-mediated incorporation of modified pyrimidine building blocks

We used a PCR mixture containing 1X polymerase buffer, 0.2 mM dATP, 0.2 mM dGTP, 0.2 mM 5fdCTP (2), 0.2 mM C8-Ak-dUTP (1), 0.4 μM T-FP, 0.4 μM T-RP, 0.05 U/μL DNA polymerase, 20 pM PCR template T1, and water for a total volume of 50 μL. The cycling conditions were as follows: 96 °C, 2 min + [96 °C, 15 s + 51 °C, 30 s + 72 °C, 30 s]*30 + 72 °C, 2 min + hold at 4 °C. To screen KOD-XL, Pwo, and Deep Vent DNA

polymerases for the efficiency of modified nucleotide incorporation, we loaded 2 μL of each PCR reaction directly onto a 10% native PAGE gel, which was run at 150 V for 30 min in 1X TBE buffer. Gels were imaged after staining with 1X GelStar Nucleic Acid Stain in TBE buffer.

Name	**Sequence**
S1	5'-CGG AAC GTC /i5OctdU//i5OctdU//i5OctdU/ GTA ACT TGA-3'
T1	5'- ATC CAG AGT GAC GCA GCA CGG AAC GTC TTT GTA ACT TGA AAT ACC GTG GTA GGT TGG CTA GGT TGG ACA CGG TGG CTT AGT -3'
M1	5'- ATC CAG AGT GAC GCA GCA **2**GG AA**2** G**42 444** G**4**A A**24 4**GA AA**4** A**22** G**4**G G**4**A GG**4 4**GG **24**A GG**4 4**GG A**2**A **2**GG **4**GG **244** AG**4** -3'
T-FP	5'- ATC CAG AGT GAC GCA GCA -3'
T-RP	5'- ACT AAG CCA CCG TGT CCA -3'
T-RP-2Bio	5'- /52-Bio/ACT AAG CCA CCG TGT CCA -3'

Table 3.1. DNA sequences used in Click-PD optimization. See Figure 3.1 for the structures of **1**, **2**, and **4**.

3. Optimization of click conjugation reaction

10 μL of 100 μM 21-nt oligonucleotide substrate (containing consecutive three 1 nucleotides), 1 μL 100 mM azido-sugar in DMSO (100 eq), and 14 μL 20 mM sodium phosphate buffer, pH 8 (pre-degassed by bubbling N_2 through) were combined in a 1.5 mL Eppendorf tube. Click chemistry was initiated by one of the following three conditions:

(1) addition of premixed 1 μL 20 mM $CuSO_4$, 1 μL 0.1 M tris(3-hydroxypropyltriazolylmethyl)amine (THPTA), and 20 μL water, followed by 1 μL 0.2 M sodium ascorbate.

(2) addition of premixed 1 μL 20 mM $CuSO_4$ and 1 μL 20 mM tris[(1-benzyl-1H-1,2,3-triazol-4-yl)methyl]amine (TBTA)] in 10 μL of 4:3:1 water:DMSO:t-BuOH, followed by addition of 2 μL 20 mM tris(2-carboxyethyl)phosphine (TCEP).

(3) addition of 10 μL premixed 1:1 Cu:TBTA (2 mM, prepared from 1 mg CuBr + 0.7 mL 10 mM TBTA in 4:3:1 water: DMSO: t-BuOH, then diluted five-fold with the same solvent).

The cap of the tube was then removed, and the de-capped tube was immediately placed in a 20 mL vial equipped with a rubber septum, followed by Ar flushing for 5 min. We incubated the sealed vial in the dark for two hours. The reaction product was purified with a Centri-Spin 10 column (Princeton Separations). 200 μL of concentrated ammonium hydroxide (18 M) was added to the purified product, and the solution was incubated at room temperature for 3 hours. 400 μL n-butanol was then added, vortex mixed, and centrifuged at 16,000 ×*g* at 4 °C for 2 min. The top organic layer was removed and discarded. The bottom aqueous layer was purified by an Oligo Clean and Concentrator spin column (Zymo Research), followed by HPLC analysis.

4. PCR amplification, click conjugation of 3, single strand generation, and acetyl deprotection for an 81-nt non-natural aptamer M1

For PCR incorporation of modified nucleotides, we prepared a PCR mixture containing 1X KOD-XL DNA polymerase buffer, 0.2 mM dATP, 0.2 mM dGTP, 0.2 mM 2, 0.2 mM 1, 0.4 μM T-FP, 0.4 μM 5'-doubly biotinylated T-RP-2Bio, 0.05 U/μL KOD-XL DNA polymerase, 20 pM PCR template T1, and water in a total volume of 5 mL in a 96 well plate. Cycling conditions were as follows: 96 °C, 2min + [96 °C, 15 s + 51 °C, 30 s + 75 °C, 30 s]*12 + 75 °C, 2 min + hold at 4 °C.

PCR reactions were then transferred into a 50 mL conical tube. 0.5 mL 3 M sodium acetate (pH 5.2) and 13.75 mL of 100% ethanol were added, followed by freezing at -80 °C for 30 min. The frozen stock was then centrifuged for 30 min at 5000 RPM at 4 °C to precipitate the DNA. The pellet was dissolved with 600 µL water, followed by purification using MinElute spin columns. The PCR product was eluted with 180 µL of 10 mM Tris buffer, pH 8.0. To this DNA solution, we added 40 µL of 3 M sodium acetate (pH 5.2) and 1.2 mL of 100% ethanol, followed by freezing at -80 °C for 30 min. The frozen stock was then centrifuged for 30 min at 21,000 ×*g* at 4 °C to precipitate the DNA. The material was resuspended in 20 µL 1X PBS buffer.

20 µL 100 mM 3 in DMSO (100 eq) and 40 µL 20 mM sodium phosphate buffer, pH 8 (pre-degassed by bubbling N_2 through) were combined with 20 µL of base-modified DNA solution in a 1.5 mL Eppendorf tube. Click chemistry was initiated by the addition in reaction of 20 µL premixed solution of 1:1 Cu:TBTA (10 mM, prepared from 1 mg CuBr + 0.7 mL 10 mM TBTA in 4:3:1 water:DMSO:t-BuOH). The cap of the tube was removed, and the de-capped tube was immediately placed in a 20 mL vial equipped with a rubber septum, followed by Ar flushing for 5 min. We incubated the sealed vial in the dark for two hours. To this DNA solution, we added 10 µL of 3 M sodium acetate (pH 5.2) and 330 µL of 100 % ethanol, followed by freezing at -80 °C for 30 min. The frozen stock was then centrifuged for 30 min at 21,000 ×*g* at 4 °C to precipitate the DNA. We resuspended the material in 350 µL 1X bind and wash buffer (B&W; 5 mM Tris, 0.5 mM EDTA, 1 M NaCl, pH 7.5).

We then added 350 µL MyOne C1 streptavidin beads to a 1.5 mL Eppendorf tube. We captured the beads on the side of the tube with a magnet and removed the supernatant. The beads were washed three times with 350 µL 1X B&W. The click product sample was

added to the beads and mixed on a rotator for 30 min. The beads were then captured, and the supernatant was discarded. The beads were washed three times with 350 μL 1X B&W, and then treated with 100 μL freshly-prepared 0.25 M NaOH solution to generate single-stranded DNA. The beads were captured by magnet, and the supernatant was collected and desalted using a CENTRI-SEP column (Princeton Separations).

We deprotected the acetyl groups by adding 200 μL concentrated ammonium hydroxide (18 M) to the collected oligos and incubating for 4 hours at room temperature. 450 μL n-butanol was then added to the solution, followed by vortexing, and centrifuging at 21,000 ×*g* at 4 °C for 1 min. The top organic layer was removed and discarded. The resulting non-natural aptamer solution was then desalted by a Centri Spin-10 column (Princeton Separations).

5. General procedure for generating particle-displayed non-natural aptamers

Monoclonal, particle-displayed non-natural aptamers were generated by emulsion PCR. The oil phase was made up of 4.5% Span 80, 0.45% Tween 80, and 0.05% Triton X-100 in mineral oil, and all reagents were purchased from Sigma-Aldrich. The aqueous phase consisted of 1x KOD XL DNA polymerase buffer, 50 u KOD XL DNA polymerase, 0.2 mM dATP, 0.2 mM dGTP, 0.2 mM 2, 0.2 mM 1, 10 nM FP, 1 μM fluorescently labeled RP, ~1 pM template DNA, and ~10^8 1 μm FP-conjugated magnetic beads. For each reaction, 1 mL of aqueous phase was added to 7 mL of oil phase and emulsified at 620 rpm for 5 min in an IKA DT-20 tube using the IKA Ultra-Turrax device. The emulsion was pipetted into 100 μL reactions in a 96 well plate. The following PCR conditions were used: 96 °C, 2 min + [96 °C, 15s + 52 °C, 30s + 75 °C, 60s]*39 + 75 °C, 5 min.

After PCR, the emulsions were collected into an emulsion collection tray (Life Technologies) by centrifuging at 300 x g for 2 min. The emulsion was broken by adding 10 mL 2-butanol to the tray, and the sample was transferred to a 50 mL tube. The tube was vortexed for 30s, and the particles were pelleted by centrifugation at 3,000 x g for 5 min. The oil phase was carefully removed, and the particles were resuspended in 1 mL of emulsion breaking buffer (100 mM NaCl, 1% Triton X-100, 10 mM Tris-HCl, pH 7.5, and 1 mM EDTA) and transferred to a new 1.5 mL tube. After vortexing for 30s and 90s of centrifugation at 15,000 × g, the supernatant was removed. The tube was placed on a magnetic separator (MPC-S, Life Technologies), and the remaining supernatant was removed. The particles were washed three times with 1x PBS buffer using magnetic separation, then stored in 200 µL PBST at 4 °C.

For the click conjugation of 3, the particles were resuspended in 10 µL PBS. 20 mM sodium phosphate buffer, pH 7.3 was degassed for at least 15 min with N_2 before preparing the reaction. The 10 µL bead suspension was combined with 25 µL 20 mM Na_2HPO_4 and 5 µL 10% Tween 20 in a 1.5 mL Eppendorf tube. The click reaction was initiated by the addition of 5 µL 2-azidoethyl 2,3,4,6-tetra-O-acetyl-a-D-mannopyranoside (AeMan, 100 mM in methanol) and 2.5 µL premixed solution of Cu:TBTA (10 mM, 1 mg Cu(I)Br + 10 mM TBTA in 3:1 DMSO:tBuOH). The reaction was vortexed briefly, placed in a 20 mL vial with a septum, flushed with N_2 for 5 min, and incubated in the dark with constant vortexing for 2 hours. The reaction tube was placed on the magnetic separator, and the supernatant was removed. The particles were washed 5 times with 50 µL TE buffer.

To generate single-stranded DNA, the particles were resuspended in 200 µL 0.1 M NaOH solution and incubated for 5 min at room temperature. The supernatant was removed

using the magnetic separator, and the particles were resuspended in 200 µL concentrated ammonium hydroxide (18 M) to deprotect the AeMan. The particles were incubated for three hours on a slow rotator. The particles were washed five times with TE buffer and resuspended in 200 µL 10 mM Tris.

6. Optimization of 'reverse-transcription' of particle-displayed non-natural aptamers

Non-natural aptamer-displayed particles as templates were subjected to PCR with 1X polymerase buffer, 0.2 mM dATP, 0.2 mM dGTP, 0.2 mM dCTP, 0.2 mM dTTP, 0.4 µM T-FP, 0.4 µM T-RP, 0.05 U/µL DNA polymerase, 10^4 non-natural aptamer (M1)-displayed particles, and water in a total volume of 50 µL. Cycling conditions were as follows: 96 °C, 2 min + [96 °C, 15 s + 51 °C, 30 s + 72 °C, 30 s]*30 + 72 °C, 2 min + hold at 4 °C.

We screened four DNA polymerases: Taq, KOD-XL, Pwo, and Deep Vent for the efficiency of reverse transcription, 2 µL of each PCR reaction was loaded directly onto a 10% native PAGE gel and run at 150 V for 30 min in 1X TBE buffer. Gels were imaged after staining with 1X GelStar Nucleic Acid Stain in TBE buffer.

7. Click-PD screening

For each round of screening, we incubated ~10^8 non-natural aptamer particles with 1 nM biotinylated Con A and 250 nM FITC-conjugated PSA in selection buffer (SB; 1 x PBS, 2.5 mM $MgCl_2$, 1 mM $CaCl_2$, 0.1 mM $MnCl_2$, 0.01% Tween 20) for 1 hour in the dark on a rotator. After incubation, the particles were resuspended in a 500-fold dilution of streptavidin-conjugated Alexa Fluor 647 to fluorescently label biotinylated Con A bound to the non-natural aptamer particles, and incubated for 10 min in the dark on a rotator. The particles were washed once and resuspended in SB. The sample was then analyzed with the BD FACS Aria III, and the sort gate was set to collect non-natural aptamer particles in

quadrant IV, the population that exhibits high binding to Con A and low binding to PSA. 0.2-1% of the total singlet population was collected in each round. After sorting, the collected non-natural aptamer particles were resuspended in 20 µL PBS and reverse transcribed into canonical DNA by Taq polymerase.

Name	**Sequence**
C-FP	5'-GAT CCC AGT CCG AAG TAA TC-3'
C-FP-Bio	5'-/5BiotinTEG/GAT CCC AGT CCG AAG TAA TC-3'
C-RP	5'-CCT ATA GCC GTT TGC ACA AG-3'
C-Lib	5'- GAT CCC AGT CCG AAG TAA TC-N40-CTT GTG CAA ACG GCT ATA GG-3'

Table 3.2. DNA sequences used in Con A aptamer screen.

8. Next generation sequencing of the enriched aptamer pools

Preparation of DNA pools for next generation sequencing was done by following the steps described in *16S Metagenomic Sequencing Library Preparation* by Illumina. Overhang adaptor sequences for the forward and reverse primers were ordered from IDT. DNA pools from rounds 1, 2, and 3 were indexed using the Nextera XT DNA Library Preparation Kit (Illumina) and then pooled for sequencing. Sequencing was performed using an Illumina MiSeq at the Stanford Functional Genomics Facility. Sequences with low quality were filtered out using the "Filter by quality" Galaxy NGS tool, accepting only sequences with more than 90% of the bases having a quality score of 20 or above. For each round, 23-27% of the sequences were discarded because of low quality. The FASTAptamer toolkit was used to identify sequence clusters (sequences varying by 2 or fewer bases) and calculate the degree enrichment of each sequence from round to round. The sequences identified as aptamer candidates are shown in **Table 3.3**.

Name	Sequence
1-1	TATCATGGACTATACGGAGGTAGATCGGATATGCGAACCA
2-1	CTCCGCGGATCAATGCAGAGGATTGCAGATCCTCGACATG
2-2	CTTCGCGGATCAATGCAGAGGATTGCAGATCCTCAACATG
3-1	GTTGCATCTGCACGACTGGTGAGCTTGAGTGGCAGAAGAA
3-2	GTTGCATCTGCACTACTGGTGAACTTGAGTGGCAGAAGAA
3-3	GTTGCATCTGCACGACTGGTGAACTTGAGTGGCAGAAGAA
4-1	AGCGATAGGTGCACTGGGGTCCTCTAAGCGCGTTAACGAG
5-1	TAGTACGGAGGAACGTGCGAGCGGTAGCATTATAGCGAGA
6-1	CACGTACTGCTACGGGGGAGGGAGGTATCTGTCGCGGA
6-2	CACGTACTGCTACGGGAAGGGAGGTATCTGTCGCGGA
7-1	TCTGTGACGGTACGTCGCTGGAAGAAGTTGGGACGTATTA
9-1	GAAGCAAGTTGGTCTTTAACGATACAACAGCTTGCGGAAC
11-1	GGAGGTGTTACTGGCCGGGGAAGATTGAGGGTGGCGTGG
17-1	GTTGAATCTGGATACGATTTCTGAGTTCTTAATGGGAAGA

Table 3.3. Aptamer candidates selected for characterization. Primer binding regions are not shown. The first number in each name refers to the sequence cluster that each sequence belongs to.

9. General procedure for particle-based binding assay for fluorescently labeled targets

~10^6 particles were incubated with varying concentrations of fluorescently labeled protein in SB for 1 hour on a rotator. After incubation, the particles were washed once and resuspended in SB. The particles were analyzed using the BD Accuri C6 flow cytometer, and the mean fluorescence and/or percentage of bound particles were measured in the relevant fluorescence channel(s).

Name	Sequence
3-1a	GTTG**2**AT**2**TG**2**A**2**GA**2**TGGTGAG**2**TTGAGTGG**2**AGAAGAA**2**TTGTG**2**AAA**2**GG**2**TATAGG
3-1nc	G**11**G**2**A**121**G**2**A**2**GA**21**GG**1**GAG**211**GAG**1**GG**2**AGAAGAA**211**G**1**G**2**AAA**2**GG**21**A**1**AGG
3-1n	GTTGCATCTGCACGACTGGTGAGCTTGAGTGGCAGAAGAACTTGTGCAAACGGCTATAGG
3-1mscr	AGCAG**44**AA**4**G**44**AGGA**4**GCGGAGGCGCA**4**ACG**4**CG**4**ACGC**44**G**4**GCAAACGGC**4**A**4**AGG
3-1m	G**44**GCA**4**C**4**GCACGAC**4**GG**4**GAGC**44**GAG**4**GGCAGAAGAAC**44**G**4**GCAAACGGC**4**A**4**AGG
A22_23	G**AA**GCA**4**C**4**GCACGAC**4**GG**4**GAGC**44**GAG**4**GGCAGAAGAAC**44**G**4**GCAAACGGC**4**A**4**AGG
A27_29	G**44**GCA**A**C**A**GCACGAC**4**GG**4**GAGC**44**GAG**4**GGCAGAAGAAC**44**G**4**GCAAACGGC**4**A**4**AGG
A37_40	G**44**GCA**4**C**4**GCACGAC**A**GG**A**GAGC**44**GAG**4**GGCAGAAGAAC**44**G**4**GCAAACGGC**4**A**4**AGG
A45_46	G**44**GCA**4**C**4**GCACGAC**4**GG**4**GAGC**AA**GAG**4**GGCAGAAGAAC**44**G**4**GCAAACGGC**4**A**4**AGG
A50	G**44**GCA**4**C**4**GCACGAC**4**GG**4**GAGC**44**GAG**A**GGCAGAAGAAC**44**G**4**GCAAACGGC**4**A**4**AGG
A45_46_22	G**A4**GCA**4**C**4**GCACGAC**4**GG**4**GAGC**AA**GAG**4**GGCAGAAGAAC**44**G**4**GCAAACGGC**4**A**4**AGG
A45_46_23	G**4A**GCA**4**C**4**GCACGAC**4**GG**4**GAGC**AA**GAG**4**GGCAGAAGAAC**44**G**4**GCAAACGGC**4**A**4**AGG
A45_46_27	G**44**GCA**A**C**4**GCACGAC**4**GG**4**GAGC**AA**GAG**4**GGCAGAAGAAC**44**G**4**GCAAACGGC**4**A**4**AGG
A45_46_29	G**44**GCA**4**C**A**GCACGAC**4**GG**4**GAGC**AA**GAG**4**GGCAGAAGAAC**44**G**4**GCAAACGGC**4**A**4**AGG
A45_46_37	G**44**GCA**4**C**4**GCACGAC**A**GG**4**GAGC**AA**GAG**4**GGCAGAAGAAC**44**G**4**GCAAACGGC**4**A**4**AGG
A45_46_40	G**44**GCA**4**C**4**GCACGAC**4**GG**A**GAGC**AA**GAG**4**GGCAGAAGAAC**44**G**4**GCAAACGGC**4**A**4**AGG

Table 3.4. Mutant sequences tested for binding affinity to Con A. Sequences are shown 5' to 3', and the forward primer regions are not shown. See Figure 3.1 for the structures of **1**, **2**, and **4**.

10. Generation of solution-phase non-natural aptamers with 5'-biotinylation.

PCR using modified substrates was performed in a PCR mixture containing 1X KOD-XL polymerase buffer, 0.2 mM dATP, 0.2 mM dGTP, 0.2 mM 2, 0.2 mM 1, 0.4 μM 5'-biotinylated C-FP-Bio, 0.4 μM C-RP, 0.05 U/μL KOD-XL DNA polymerase, 20 pM PCR template, and water in a total volume of 5 mL in a 96 well plate. Cycling conditions were as follows: 96 °C, 2min + [96 °C, 15 s + 52 °C, 30 s + 75 °C, 30 s]*12 + 75 °C, 2 min + hold at 4 °C.

PCR reactions were transferred into a 50 mL conical tube. To this PCR mixture, we added 0.5 mL 3 M sodium acetate (pH 5.2) and 13.75 mL of 100% ethanol were added,

followed by freezing at -80 °C for 30 min. The frozen stock was then centrifuged for 30 min at 5000 RPM at 4 °C to precipitate the DNA. The pellet was dissolved with 600 μL water, followed by purification using MinElute spin columns. The PCR product was eluted with 180 μL of 10 mM Tris buffer, pH 8.0. To this DNA solution we added 40 μL of 3 M sodium acetate (pH 5.2) and 1.2 mL of 100% ethanol, followed by freezing at -80 °C for 30 min. The frozen stock was then centrifuged for 30 min at 21,000 ×*g* at 4 °C to precipitate the DNA. The DNA was resuspended in 20 μL 1X PBS buffer.

We combined 20 μL of the base-modified DNA solution with 20 μL 100 mM 3 in DMSO (100 eq) and 40 μL 20 mM sodium phosphate buffer, pH 8 (pre-degassed by bubbling N_2 through) in a 1.5 mL Eppendorf tube. Click chemistry was initiated by the addition of 20 μL of a premixed solution of 1:1 Cu:TBTA (10 mM, prepared with 1 mg CuBr + 0.7 mL 10 mM TBTA in 4:3:1 water:DMSO:t-BuOH). The cap of the tube was removed, and the de-capped tube was immediately placed a 20 mL vial equipped with a rubber septum, followed by Ar flushing for 5 min. We incubated the sealed vial in the dark for two hours. To this DNA solution, we added 10 μL of 3 M sodium acetate (pH 5.2) and 330 μL of 100% ethanol, followed by freezing at -80 °C for 30 min. The frozen stock was then centrifuged for 30 min at 21,000 ×*g* at 4 °C to precipitate the DNA. We resuspended the DNA in 350 μL 1X B&W.

We added 350 μL MyOne C1 streptavidin beads to a 1.5 mL Eppendorf tube. The beads were captured on the side of the tube with a magnet and the supernatant was removed. The beads were washed three times with 350 μL 1X B&W. The click product sample was added to the beads and mixed on a rotator at room temperature for 30 min. The beads were then captured and the supernatant was discarded. The beads were washed three times with

350 μL 1X B&W, then treated twice with 100 μL 0.25 M freshly prepared NaOH solution to generate single-stranded DNA. The supernatant was discarded. Deprotection of the acetyl group on the mannose was effected by the addition of 300 μL of concentrated ammonium hydroxide (18 M) and incubation at room temperature for three hours. This tube was then sealed tightly before heating on a thermal block at 70 °C for 10 min. The sample was cooled in an ice bath before opening the cap. The tube was placed on the magnet, and the supernatant was transferred to a separate tube. 100 μL more ammonium hydroxide (18 M) was added to the beads, and the heating procedure was repeated once more.

The supernatants from the two ammonium hydroxide treatment steps were combined and then combined with 4.5 mL n-butanol before vortexing and centrifuging at 16,000 ×*g* at 4 °C for 10 min. The supernatant was removed and discarded. The sample was dried over vacuum centrifugation, and then resuspended in 100 μL water. To this solution, we added 50 uL of 5 M NH_4OAc and 415 μL of cold 100% ethanol before freezing at -80 °C for 30 min. We centrifuged for 30 min at 21,000 ×*g* at 4 °C to precipitate the non-natural aptamer. The pellet was washed once with 70% cold ethanol in water, then dissolved in 100 μL water.

11. Bio-layer interferometry measurement of selected non-natural aptamers

3-1 and 3-1m were diluted to 50 nM in SB. Solutions of 0, 1, 2, 4, 8, 16, 32, and 64 nM Con A were prepared in SB. The solutions were loaded into a 384 well plate, with 100 μL of SB, 80 μL of biotinylated aptamer, and 100 μL of Con A solution for each reaction. The following steps were run on the ForteBIO Octet RED384 with Super Streptavidin biosensors: 60s in buffer for equilibration, 5 min in aptamer solution to load the aptamer onto the biosensors, 60s in buffer for a baseline measurement, 10 min in Con A solution to measure association, and 10 minutes in buffer to measure dissociation. Analysis was

performed using Octet Data Analysis software, including the alignment of the different measurements and global fitting of the experimental data to a binding model to extract K_d, k_{on}, and k_{off}.

12. Lectin array assay to probe non-natural aptamer specificity

The following procedure was adapted from the vendor's product manual. First, we dried the glass slide. The slide with the pre-printed lectin array was equilibrated to room temperature inside the sealed plastic bag for 20- 30 minutes. We then annealed 30 μL 0.5 μM 3-1m in 1X PBS by incubating the solution at 95 °C and slowly cooling down to 4 °C at a ramp rate of 0.1 °C/second. We incubated at 4 °C for 5 min. We then added 100 μL sample diluent (included in the lectin array package) into each well of the array and incubated at room temperature for 30 min to block the slides. We removed the buffer from each well. After diluting 3-1m to the desired concentration with SB, we added 100 μL of diluted 3-1m to each well and incubated the arrays at room temperature for 3 hours. We then removed the samples from each well, and washed each well five times (5 min each) with 150 μL of 1X wash buffer I (included in the lectin array package, supplemented with 2.5 mM $MgCl_2$, 1 mM $CaCl_2$, and 0.1 mM $MnCl_2$) at room temperature with gentle shaking. We completely removed the buffer between each wash step. We then washed two times (5 min each) with 150 μL of 1X wash buffer II (included in the lectin array package, supplemented with 2.5 mM $MgCl_2$, 1 mM $CaCl_2$, and 0.1 mM $MnCl_2$) at room temperature with gentle shaking. We completely removed the wash buffer between each wash step. We then briefly spun down the Cy3 equivalent dye-conjugated streptavidin tube (included in the lectin array package), and added 1.4 mL of sample diluent to the tube, mixing gently. We added 80 μL of Cy3 equivalent dye-conjugated streptavidin to each well and incubated in the dark at room

temperature for 1 hour. We decanted the samples from each well, and washed five times with 150 μL of 1X wash buffer I at room temperature with gentle shaking, completely removing the wash buffer after each wash step. We disassembled the slide assembly by pushing the clips outward from the slide side and carefully removing the slide from the gasket. We placed the slide in the slide washer/dryer (a four-slide holder/centrifuge tube included in the lectin array package), adding enough 1x wash buffer I (about 30 mL) to cover the whole slide, and then gently agitated at room temperature for 15 minutes. After decanting wash buffer I, we washed with 1x wash buffer II (about 30 mL) with gentle shaking at room temperature for 5 minutes. Finally, we dried the slide by centrifugation at 200 ×*g* on a microscope slide spinner and scanned the slide on a microarray scanner, monitoring the Cy3 dye channel at PMT 500.

Lectin	Abbreviation	Source	Carbohydrate Specificity
AIA	AIA	Artocarpus integrifolia (Jackfruit) seeds	αGal
Aleuria aurantia	AAL	*Aleuria aurantia* mushrooms	Fucα6GlcNAc
Allium sativum	ASA	*Allium sativum* agglutinin (Garlic)	αMan
Amaranthus caudatus	ACL, ACA	*Amaranthus caudatus* seeds	Galβ3GalNAc
Anguilla anguilla	AAA	*Anguilla anguilla* (Fresh Water Eel)	αFuc
Bauhinia purpurea	BPA, BLP	*Bauhinia purpurea alba* (Camel's Foot Tree) seeds	Galβ3GalNAc
Concanavalin A	Con A	*Canavalia ensiformis* (Jack Bean) seeds	αMan, αGlc
Datura stramonium	DSA, DSL	*Datura stramonium* (Thorn Apple, Jimson Weed) seeds	$(GlcNAc)_{2-4}$
Dolichos biflorus	DBA	*Dolicos biflorus* (Horse Gram) seeds	αGalNAc
Erythrina cristagalli	ECA, ECL	*Erythrina cristagalli* (Coral Tree) seeds	Galβ4GlcNAc
Eunonymus europaeus	EEL	*Eunonymus europaeus* (Spindle Tree) seeds	Galα3Gal
Galanthus nivalis	GNA, GNL	*Galanthus nivalis* (Snowdrop) bulbs	αMan
Griffonia (*Bandeiraea*) *simplicifolia* I	GS-I, GSL-I, BSL-I	*Griffonia* (*Bandeiraea*) *simplicifolia* seeds	αGal, αGalNAc
Griffonia (*Bandeiraea*)	GS-II, GSL-II, BSL-II	*Griffonia* (*Bandeiraea*) *simplicifolia* seeds	α or βGlcNAc
Hippeastrum hybrid	HHA, HHL, AL	*Hippeastrum* hybrid (Amaryllis) bulbs	αMan
Jacalin	Jacalin, AIL	*Artocarpus integrifolia* (Jackfruit) seeds	Galβ3GalNAc
Lens culinaris	LcH, LCA	*Lens culinaris* (lentil) seeds	αMan,αGlc
Lectin	**Abbreviation**	**Source**	**Carbohydrate Specificity**
Lotus tetragonolobus	Lotus, LTL	*Lotus tetragonolobus, Tetragonolobus purpurea* (Winged Pea, Asparagus Pea) seeds	αFuc
Lycopersicon esculentum	LEA, LEL, TL	Lycopersicon esculentum (tomato) fruit	$(GlcNAc)_{2-4}$
Maackia amurensis I	MAA, MAL, MAL-I	*Maackia amurensis* seeds	Galβ4GlcNAc
Maclura pomifera	MPL, MPA	*Maclura pomifera* (Osage Orange) seeds	Galβ3GalNAc
Narcissus pseudonarcissus	NPA, NPL, DL	Narcissus pseudonarcissus (Daffodil) bulbs	αMan
Peanut	PNA	*Arachis hypogaea* peanuts	Galβ3GalNAc
Phaseolus lunatus	LBA	*Phaseolus lunatus* (Lima Bean) seeds	GalNAcα(1,3)[Fucα(1,2)]Gal
Phaseolus vulgaris Erythroagglutinin	PHA-E	*Phaseolus vulgaris* (Red Kidney Bean) seeds	Galβ4GlcNAcβ2Manα6(GlcNAcb4)(GlcNAcβ4Manα3)Manβ4
Leucoagglutinin	PHA-L	*Phaseolus vulgaris* (Red Kidney Bean) seeds	Galβ4GlcNAcβ6(GlcNAcβ2Manα3)Manα3
Pisum sativum	PSA, PEA	*Pisum sativum* (Pea) seeds	αMan, αGlc
Psophocarpus	PTL, PTL-I, WBA-I	*Psophocarpus tetragonolobus* (Winged Bean) seeds	GalNAc, Gal
Sambucus nigra I	SNA-I	*Sambucus nigra* (Elderberry) bark	NANAα(2,6)GalNAc > GalNAc = Lac > GalNANAα(2,6)Gal
Sambucus nigra II	SNA-II	*Sambucus nigra* (Elderberry) bark	GalNAc > Gal
Solanum tuberosum	STL, PL	*Solanum tuberosum*, (potato) tubers	$(GlcNAc)_{2-4}$
Sophora japonica	SJA	*Sophora japonica* (Japanese Pagoda Tree) seeds	βGalNAc
Soybean	SBA	*Glycine max* (soybean) seeds	α > βGalNAc
Ulex europaeus I	UEA-I	*Ulex europaeus* (Furze Gorse) seeds	αFuc
Ulex europaeus II	UEA-II	*Ulex europaeus* (Furze Gorse) seeds	Poly β(1,4)GlcNAc
Urtica dioica	UDA	*Urtica dioica* (Stinging Nettle) seeds	GlcNAc
Vicia faba	VFA	*Vicia faba* (Fava Bean) seeds	αMan
Vicia villosa	VVA, VVL	*Vicia villosa* (Hairy Vetch) seeds	GalNAc
Wheat Germ	WGA	*Triticum vulgaris* (wheat germ)	GlcNAc
Wisteria floribunda	WFA	*Wisteria floribunda* (Japanese Wisteria) seeds	GalNAc

Sugar Abbreviations

Fuc: L-Fucose	Gal: D-Galactose	GalNAc: *N*-Acetylglactosamine	Glc: D-Glucose
GlcNAc: *N*-Acetylglucosamine	Lac: Lactose	Man: Mannose	

Table 3.5. Complete list of lectins on lectin array. This information is replicated from the Lectin Array 40 product manual.

13. Determining Con A concentration to induce complete hemagglutination

Human erythrocytes were washed and resuspended in 1X PBS in a 96-well U-shaped well plate at 1% hematocrit, with Con A concentrations ranging from 2 μg/mL to 250 μg/mL.

We let the plate stand at room temperature for 1 hour before visualizing the deposition of erythrocytes at the bottom of the well. The optical densities at 655 nm of the cell suspensions were then measured on a plate reader.

14. Hemagglutination inhibition assay

We annealed 30 μL 0.5 μM 3-1m in 1X PBS by heating the solution to 95 °C and slowly cooling down to 4 °C at a ramp rate of 0.1 °C/second, followed by incubation at 4 °C for 5 min. We incubated the annealed non-natural aptamer at a range of concentrations from 9.6 nM to 300 nM with 150 nM Con A in 1X PBS for 30 min in a 96-well U-shaped well plate. Human erythrocytes were added to produce a cell suspension of 1% hematocrit in a total volume of 50 μL per well. After 1 hour of incubation at room temperature, the hemagglutination status of the samples was visualized, and the optical densities of the cell suspensions at 655 nm were monitored by a plate reader.

15. Microscopic characterization of human erythrocyte agglutination

We annealed 2 μL of 4 μM 3-1m in 1X PBS by incubating the solution at 95 °C and slowly cooling down to 4 °C at a ramp rate of 0.1 °C/second, and then incubated at 4 °C for 5 min. To this non-natural aptamer solution, we added 1 μL of 6.5 μM Con A and incubated for 30 min at room temperature. We prepared an erythrocyte suspension to a final hematocrit of 20% in PBS. 7 μL of each erythrocyte suspension was combined either with the Con A-non-natural aptamer complex or 3 μL 1X PBS. 10 μL of this mixture was loaded onto glass slides, covered with coverslips, and immediately visualized using 10X and 40X objective lenses on a microscope.

F. References

1. Rohloff JC, Gelinas AD, Jarvis TC, et al. Nucleic Acid Ligands With Protein-like Side Chains: Modified Aptamers and Their Use as Diagnostic and Therapeutic Agents. *Mol Ther Nucleic Acids*. 2014;3(August):e201. doi:10.1038/mtna.2014.49.

2. Gold L, Ayers D, Bertino J, et al. Aptamer-based multiplexed proteomic technology for biomarker discovery. *PLoS One*. 2010;5(12). doi:10.1371/journal.pone.0015004.

3. Gawande BN, Rohloff JC, Carter JD, Carlowitz I Von, Zhang C, Schneider DJ. Selection of DNA aptamers with two modified bases. 2017;(25):1-6. doi:10.1073/pnas.1615475114.

4. Pinheiro VB, Taylor AI, Cozens C, et al. Synthetic genetic polymers capable of heredity and evolution. 2012;336(6079):341-344. doi:10.1126/science.1217622.Synthetic.

5. Ferreira-bravo IA, Cozens C, Holliger P, Destefano J. Selection of 2 -deoxy-2 -fluoroarabinonucleotide (FANA) aptamers that bind HIV-1 reverse transcriptase with picomolar affinity. 2015;43(20):9587-9599. doi:10.1093/nar/gkv1057.

6. Kuwahara M, Obika S, Kuwahara M, Obika S. In vitro selection of BNA (LNA) aptamers. 2017;968(August). doi:10.4161/adna.25786.

7. Yu H, Zhang S, Dunn MR, Chaput JC. An efficient and faithful in vitro replication system for threose nucleic acid. *J Am Chem Soc*. 2013;135(9):3583-3591. doi:10.1021/ja3118703.

8. Kimoto M, Yamashige R, Matsunaga K, Yokoyama S, Hirao I. Generation of high-affinity DNA aptamers using an expanded genetic alphabet. *Nat Biotechnol*. 2013;31(5):453-457. doi:10.1038/nbt.2556.

9. Okamoto I, Miyatake Y, Kimoto M, Hirao I. High Fidelity, Efficiency and Functionalization of Ds-Px Unnatural Base Pairs in PCR Amplification for a Genetic Alphabet Expansion System. *ACS Synth Biol*. 2016;5(11):1220-1230. doi:10.1021/acssynbio.5b00253.

10. Matsunaga KI, Kimoto M, Hirao I. High-affinity DNA aptamer generation targeting von Willebrand factor A1-domain by genetic alphabet expansion for systematic evolution of ligands by exponential enrichment using two types of libraries composed of five different bases. *J Am Chem Soc*. 2017;139(1):324-334. doi:10.1021/jacs.6b10767.

11. Nikoomanzar A, Dunn MR, Chaput JC. Engineered Polymerases with Altered Substrate Specificity: Expression and Purification. *Curr Protoc Nucleic Acid Chem*. 2017;(June):4.75.1-4.75.20. doi:10.1002/cpnc.33.

12. Loakes D, Holliger P. Polymerase engineering: towards the encoded synthesis of unnatural biopolymers. *Chem Commun*. 2009;(31):4619. doi:10.1039/b903307f.

13. Tolle F, Brandle GM, Matzner D, Mayer G. A Versatile Approach Towards Nucleobase-Modified Aptamers. *Angew Chemie - Int Ed*. 2015;54(37):10971-10974.

doi:10.1002/anie.201503652.

14. Glenney JR, Hixson DC, Walborg EF. Inhibition of concanavalin A-induced agglutination of Novikoff tumor cells by cytochalasins and metabolic inhibitors. Role of cell-surface morphology and the distribution of concanavalin A receptors. *Exp Cell Res*. 1979;118(2):353-364. doi:10.1016/0014-4827(79)90159-9.

15. Zand R, Agrawal BB, Goldstein IJ. pH-dependent conformational changes of concanavalin A. *Proc Natl Acad Sci U S A*. 1971;68(9):2173-2176. doi:10.1073/pnas.68.9.2173.

16. Tolle F, Brändle GM, Matzner D, Mayer G. A Versatile Approach Towards Nucleobase-Modified Aptamers. *Angew Chem Int Ed Engl*. July 2015. doi:10.1002/anie.201503652.

17. Wang J, Gong Q, Maheshwari N, et al. Particle Display: A Quantitative Screening Method for Generating High-Affinity Aptamers. *Angew Chemie*. 2014;126(19):4896-4901. doi:10.1002/ange.201309334.

18. Wang J, Yu J, Yang Q, et al. Multiparameter Particle Display (MPPD): A Quantitative Screening Method for the Discovery of Highly Specific Aptamers. *Angew Chemie Int Ed*. 2017;56(3):744-747. doi:10.1002/anie.201608880.

19. Gramlich PME, Wirges CT, Gierlich J, Carell T. Synthesis of modified DNA by PCR with alkyne-bearing purines followed by a click reaction. *Org Lett*. 2008;10(19):249-251. doi:10.1021/ol7026015.

20. Fischler M, Simon U, Nir H, et al. Formation of bimetallic Ag-Au nanowires by metallization of artificial DNA duplexes. *Small*. 2007;3(6):1049-1055. doi:10.1002/smll.200600534.

21. Gierlich J, Burley G, Gramlich PME, Hammond DM, Carell T. Click chemistry as a reliable method for the high-density postsynthetic functionalization of alkyne-modified DNA. *Org Lett*. 2006;8(6):3639-3642. doi:10.1021/ol0610946.

22. Gierlich J, Gutsmiedl K, Gramlich PME, Schmidt A, Burley G, Carell T. Synthesis of highly modified DNA by a combination of PCR with alkyne-bearing triphosphates and click chemistry. *Chem Eur J*. 2007;13(34):9486-9494. doi:10.1002/chem.200700502.

23. Gramlich PME, Wirges CT, Manetto A, Carell T. Postsynthetic DNA modification through the copper-catalyzed azide-alkyne cycloaddition reaction. *Angew Chemie - Int Ed*. 2008;47:8350-8358. doi:10.1002/anie.200802077.

24. Obata F, Sakai R, Sfflokawa H. Carbohydrate-Binding Activity of Concanavalin A Containing Various Numbers of Calcium and Manganese Ions 1. 1981;89(5):1475-1482.

25. Glenney JR, Hixson DC, Walborg EF. Inhibition of Concanavalin A-induced agglutination of Novikoff tumor cells by cytochalasins and metabolic inhibitors. *Exp Cell Res*. 1979;118:353-364.

26. Schwarz FP, Puri KD, Bhat RG, Surolia A. Thermodynamics of monosaccharide

binding to concanavalin A, pea (Pisum sativum) lectin lentil (Lens culinaris) lectin. *J Biol Chem*. 1993;268(11):7668-7677.

27. Richardson C, Behnke WD, Freisheim JH, Blumenthal KM. The complete amino acid sequence of the a-subunit of pea lectin, Pisum Sativum. *Biochim Biophys Acta*. 1986;537:310-319.

28. Jager S, Rasched G, Kornreich-Leshem H, Engeser M, Thum O, Famulok M. A versatile toolbox for variable DNA functionalization at high density. *J Am Chem Soc*. 2005;127(43):15071-15082. doi:10.1021/ja051725b.

29. Hili R, Niu J, Liu DR. DNA ligase-mediated translation of DNA into densely functionalized nucleic acid polymers. *J Am Chem Soc*. 2013;135(1):98-101. doi:10.1021/ja311331m.

30. Khalid K Alam JLC and DHB. FASTAptamer: A Bioinformatic Toolkit for High-throughput Sequence Analysis of Combinatorial Selections. *Mol Ther Nucleic Acids*. 2015;4:e230.

31. Abdiche Y, Malashock D, Pinkerton A, Pons J. Determining kinetics and affinities of protein interactions using a parallel real-time label-free biosensor, the Octet. *Anal Biochem*. 2008;377(2):209-217. doi:10.1016/j.ab.2008.03.035.

32. Steckbeck JD, Orlov I, Chow A, et al. Kinetic Rates of Antibody Binding Correlate with Neutralization Sensitivity of Variant Simian Immunodeficiency Virus Strains Kinetic Rates of Antibody Binding Correlate with Neutralization Sensitivity of Variant Simian Immunodeficiency Virus Strains †. *J Virol*. 2005;79(19):12311-12320. doi:10.1128/JVI.79.19.12311.

33. Ernst B, Magnani JL. From carbohydrate leads to glycomimetic drugs. *Nat Rev Drug Discov*. 2009;8(8):661-677. doi:10.1038/nrd2852.

34. Hemperly JJ, Hopp P, Becker JW, Cunningham BA. The chemical characterization of Favin, a Lectin Isolated from Vicia faba. *J Biol Chem*. 1979;254(14):6803-6810.

35. Martins VP, Morais SB, Pinheiro CS, et al. Sm10.3, a member of the micro-exon gene 4 (MEG-4) family, induces erythrocyte agglutination in vitro and partially protects vaccinated mice against schistosoma mansoni infection. *PLoS Negl Trop Dis*. 2014;8(3):e2750. doi:10.1371/journal.pntd.0002750.

36. Mortell KH, Gingras M, Kiessling LL. Synthesis of cell agglutination inhibitors by aqueous ring-opening metathesis polymerization. *J Am Chem Soc*. 1994;116(26):12053-12054. doi:10.1021/ja00105a056.

37. Mortell KH, Weatherman R V., Kiessling LL. Recognition specificity of neoglycopolymers prepared by ring-opening metathesis polymerization. *J Am Chem Soc*. 1996;118(9):2297-2298. doi:10.1021/ja953574q.

Chapter IV. Developing a method to generate pH switching aptamers

A. Introduction

Differences in pH are strictly maintained both inside and outside of cells. This is essential for cellular functions, including energy generation and maintenance of protein structure and function.[1] Extracellular pH is typically around 7.4 at physiological conditions, while intracellular pH, in the cytosol, is slightly more acidic, pH 7.2.[1] The pH of intracellular compartments varies widely. For example, early and late endosomes are roughly pH 6.3 and pH 5.5, respectively. By engineering pH sensitive reagents, we can take advantage of these carefully regulated cellular conditions. One important example of this is pH-triggered drug delivery.[2,3] Because pH is lower in endosomes than in the extracellular area, delivery systems can be programmed to selectively release drugs once they have been internalized and are exposed to a pH change. Other anticancer delivery systems exploit the more acidic tumor microenvironment (pH 6.5-7.2) to deliver drugs to tumors and not to healthy tissue.[3] Intracellular imaging and pH sensing are also important applications for pH sensitive reagents.[4,5]

Despite the utility of pH sensitive reagents, strategies for making them are limited. There are two common approaches: designing pH sensitive polymers and modifying existing aptamers with pH active motifs. Polymers have been developed that collapse or swell based on the pH of their environment.[6] Polymer systems can be tuned to release drugs under acidic or basic conditions.[7–10] Aptamers and other targeting or imaging agents can be tethered to the polymer to create multifunctional nanostructures for drug delivery. The advantage of these systems is that targeting or other function can be performed independently from the pH switching action. Modular approaches enable faster development of nanostructures for new targets. However, polymers are not well-suited for all applications requiring pH switching

reagents. Once an aptamer is identified, it can be used for many different applications. For polymers, however, design requirements are highly dependent on the applications, so the same pH sensitive polymer could not be used in biosensors and drug delivery, for example.

The second strategy for developing pH switching reagents is directly engineering a biomolecule to perform pH switching. Aptamers are promising candidate molecules, since selection conditions can be varied to match the assay the aptamer is ultimately intended for. Parameters like salt concentration, pH, and temperature are frequently adjusted; however, it is less common to select directly for a desired function other than binding. Strategies exist for engineering pH switching aptamers without selection. Some groups have modified existing aptamers with an i-motif or other pH sensitive structure to engineer in pH dependent activity.[11,12] However, testing post-selection modifications can be cumbersome, as the best location for adding a pH sensitive structure is not obvious and any modification can reduce or eliminate the aptamer's binding activity.[13,14] Ideally, aptamers with the desired pH behavior would be directly chosen during the selection. With conventional SELEX methods, however, this requires many rounds of selection, which greatly increases the likelihood of the emergence of biases and failure of the selection. Our lab previously reported the selection of pH-activated DNA nanostructures.[15] This was the first example of *de novo* selection for pH active motifs. However, this system used DNA hybridization and displacement of the nucleic acid target (rather than aptamer binding) and required twelve rounds of selection using conventional SELEX. An urgent need remains for a method to efficiently generate pH sensitive aptamers.

Here, we demonstrate the first reported screen for pH switching aptamers. By screening for binding to the target protein, streptavidin, at pH 7.4 and against binding at pH

5.2, we isolated pH switching aptamers in only three rounds. For the top performing aptamer, we identified the pH active domain and were able to modulate its pH behavior through single point mutations.

B. Overview of screen for pH switching

The objective of this work was to directly screen for aptamers with pH dependent binding, eliminating the need for the addition of a pH sensitive motif post-selection. We incorporated a short existing aptamer sequence in the library, so the starting library would bind to the target (**Fig. 4.1**). An adjacent 20 nucleotide random region was included, so successful pH switching sequences would disrupt the aptamer sequence. We then screened for aptamers that retained target binding at pH 7.4 but lost binding at pH 5.2. We chose streptavidin as the target because it is stable across a wide pH range and it has a short, well-characterized aptamer, SBA29.[16–18] SBA29 was selected by Bing and coworkers and has a reported K_d of 40 ± 18 nM.[16] This screen was performed using a variation on the previously described particle display platform.[19] The experimental scheme is shown in **Figure 4.2**. First, a pool of monoclonal aptamer particles were created using emulsion PCR (**Fig. 4.2**, step 1). Here, the key difference from the method described in Chapter II is that two sequential sorts were performed each round without amplification in between. For the first sort, we incubated the aptamer particles with streptavidin in pH 7.4 selection buffer (**Fig. 4.2**, step 2) and collected all particles that bound streptavidin (**Fig. 4.2**, step 3). For the second sort, we re-incubated the aptamer particles with streptavidin in pH 5.2 selection buffer (**Fig. 4.2**, step 4) and collected all aptamer particles that did not bind streptavidin (**Fig. 4.2**, step 5). This was considered one round of screening, and the aptamer particles collected in the second sort were amplified to create the aptamer pool for the next round (**Fig. 4.2**, step 6). After three

rounds, the aptamer pools from all three rounds were sequenced using next generation sequencing (**Fig. 4.2**, Step 7).

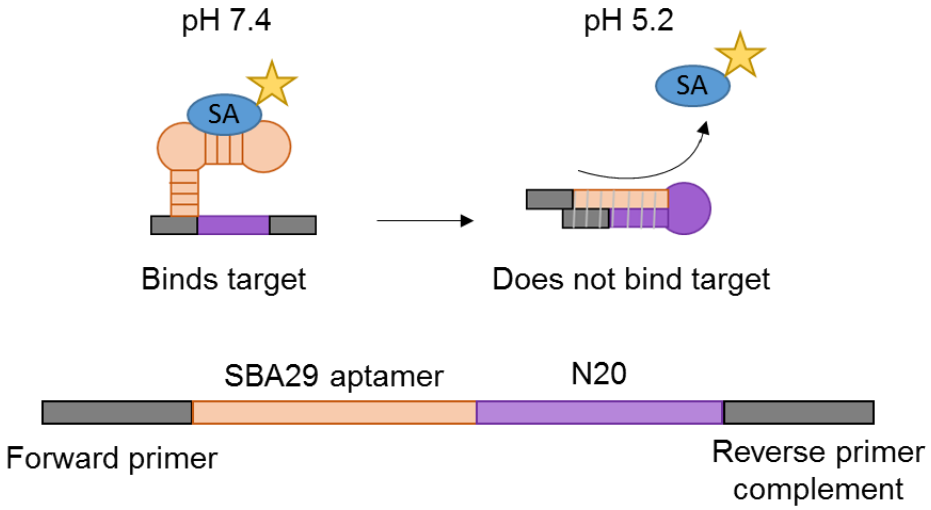

Figure 4.1. Library designed to include a streptavidin aptamer domain (SBA29) and a 20 nucleotide random region. The objective of the screen is to identify sequences that bind to the target (streptavidin) at pH 7.4 but disrupt the SBA29 aptamer domain at pH 5.2 to eliminate target binding.

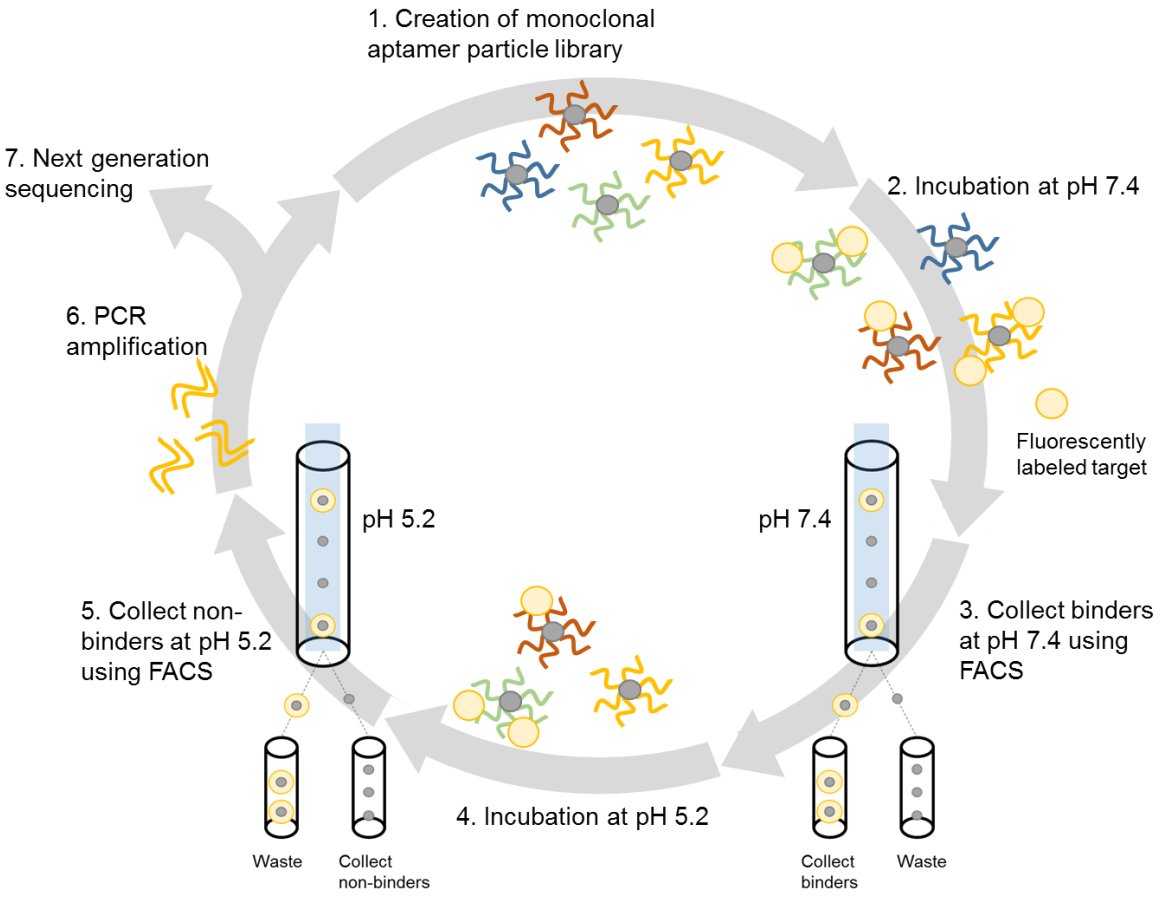

Figure 4.2. Scheme for pH switching particle display screen. Monoclonal aptamer particles were created. Two incubation and sorting steps were performed to isolate pH switching aptamers. First, aptamer particles that bound the target at pH 7.4 were collected. Second, aptamer particles that did not bind the target at pH 5.2 were collected. Aptamers from the collected particles were amplified to enrich the pool for pH switching sequences. After three rounds of screening, the aptamer pools from all rounds were sequenced.

C. Results and discussion

Three rounds of particle display screening were performed. The gates used for each sort are shown in **Figure 4.3**. In the first sort, all of the sequences that bound streptavidin at pH 7.4 were collected (**Fig. 4.3**, gate P2). In the second sort, all of the sequences that did not bind streptavidin at pH 5.2 were collected (**Fig. 4.3,** gate P1). After three rounds, the pH switching behavior of the aptamer pool was significantly enriched (**Table 4.1**). There was a small decrease in the ratio of binding at pH 7.4 to binding at pH 5.2 in round 2, but the ratio

increased significantly in round 3. With a large majority of the sequences in the round 3 pool demonstrating the desired pH switching, we performed next generation sequencing of the three aptamer pools. The aptamers with the highest copy number in round 3 and the high enrichment from round 1 to round 3 were identified (**Figure 4.4a**). Ten candidate sequences were synthesized and tested individually. Particles displaying each sequence were incubated with a streptavidin-phycoerythrin conjugate (SA-PE). Results from testing of the aptamer candidates are shown in **Figure 4.4b**. Eight of the ten sequences had higher binding to streptavidin at pH 7.4 than at pH 5.2, and two of the sequences had similar or higher binding at pH 5.2. The two sequences that showed the largest decrease in binding from pH 7.4 to pH 5.2, S3 and S8, were chosen for further testing.

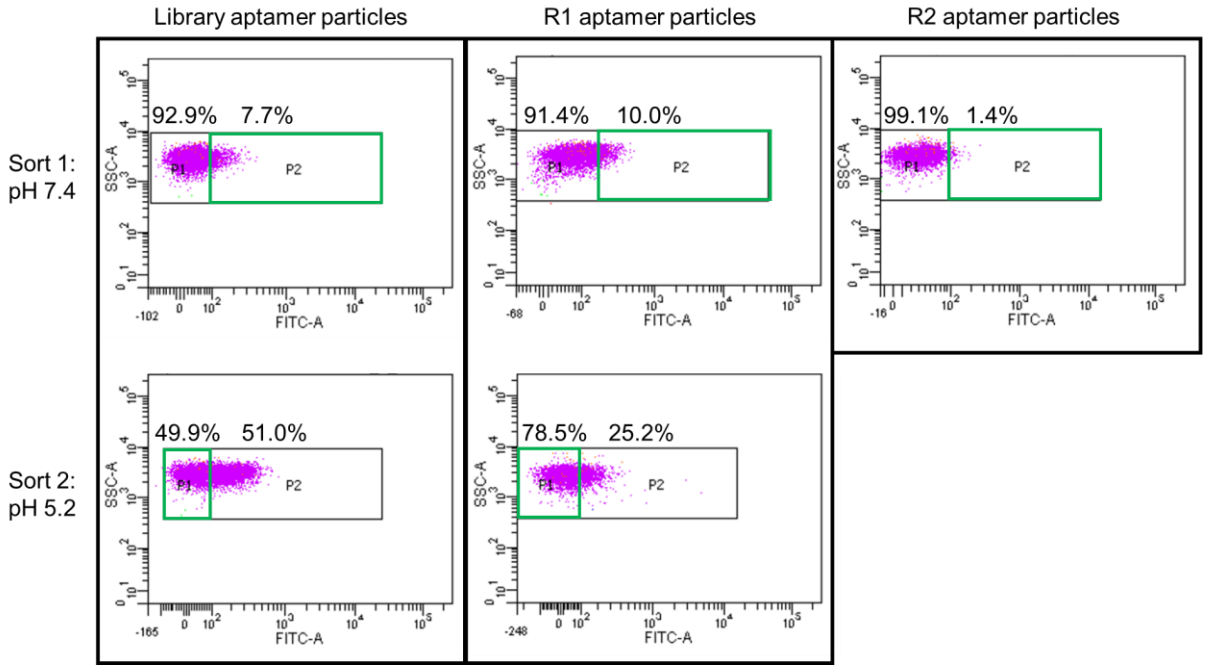

Figure 4.3. Sort gates for the first and second sort for the library, round 1, and round 2 aptamer particles (outlined in green). In the top graphs, high fluorescence particles (gate P2) in pH 7.4 selection buffer were collected. In the bottom graphs, low fluorescence particles (gate P1) in pH 5.2 selection buffer were collected. Binding at pH 7.4 was lower for the round 2 particles, so only the first sort was performed.

DNA pool	% binding at pH 7.4	% binding at pH 5.2	Ratio of binding at pH 7.4 to binding at pH 5.2
Library	3.0	1.2	2.5
Round 1	14.1	4.0	3.5
Round 2	9.4	3.8	2.5
Round 3	5.2	0.8	6.5

Table 4.1. Percentage of particles that bound to streptavidin at pH 7.4 and pH 5.2 in each round.

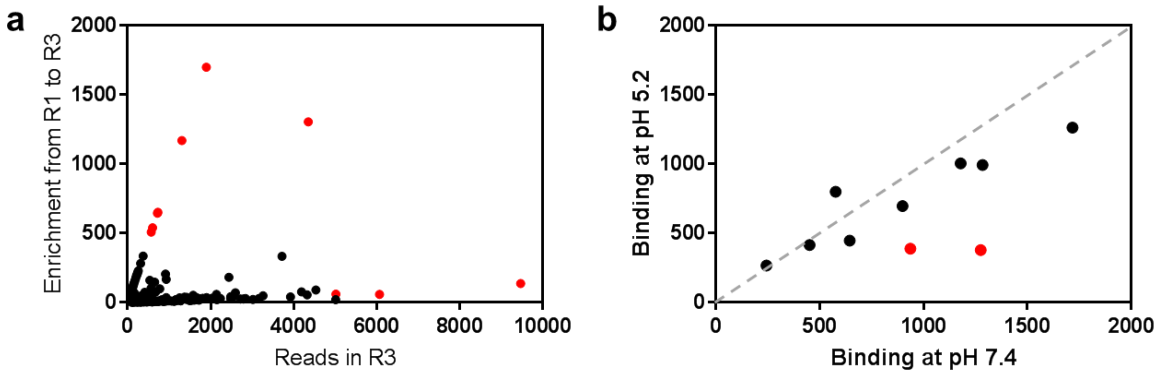

Figure 4.4. (a) Identification of aptamer candidates with NGS. The top 1000 sequences by number of reads in R3 are shown (after filtering out low quality reads and sequences with incorrect length). The seven sequences with highest enrichment from R1 to R3 and the three sequences with the highest number of reads in R3 were chosen for testing (shown in red). (b) Screening of aptamer candidates for pH-dependent binding. Each sequence was conjugated to beads and binding to streptavidin (50 nM) was measured at pH 7.4 and pH 5.2. The two sequences with the biggest difference in binding at pH 7.4 and pH 5.2 were chosen for further characterization (shown in red).

Compared to the original aptamer (SBA29), the pH switching aptamers S3 and S8 demonstrated significantly more pH sensitivity (**Fig. 4.5**). Particles displaying each sequence were generated, and the fluorescence intensity of the aptamer particles was measured across a range of streptavidin concentrations at both pH 7.4 and pH 5.2. The equilibrium dissociation constant, K_d, was determined for each sequence using a saturation binding model (one site, total binding) in GraphPad Prism. SBA29 has a similar K_d under both pH conditions, 10.4 ± 1.5 nM at pH 7.4 and 3.50 ± 0.46 at pH 5.2. pH switching aptamers S3 and S8 bound

strongly to streptavidin at pH 7.4 (K_d of 24.2 ± 3.4 nM and 112 ± 19 nM, respectively), but both aptamers had much weaker binding at pH 5.2. We were not able to test the binding at high enough target concentrations to reach a stable bound plateau for either S3 or S8 at pH 5.2, so K_d could not be determined reliably.

The binding affinity of SBA29 and S8 to streptavidin was confirmed using another method, microscale thermophoresis (MST). These results also demonstrated that SBA29 is pH insensitive, with similar K_d values at pH 7.4 and at pH 5.2 (6.1 nM and 27 nM, respectively) (**Fig 4.6a**, **4.6b**). Again, aptamer S8 demonstrated significant pH sensitivity, with approximately 2 orders of magnitude higher binding affinity at pH 7.4 than at pH 5.2. At pH 7.4, S8 has a K_d of 10 nM (**Fig 4.6c**). At pH 5.2, the K_d could not be determined because the highest practical target concentrations did not give a stable binding plateau (**Fig 4.6d**). From the observed binding response, we estimate that the K_d is in the high nanomolar to low micromolar range.

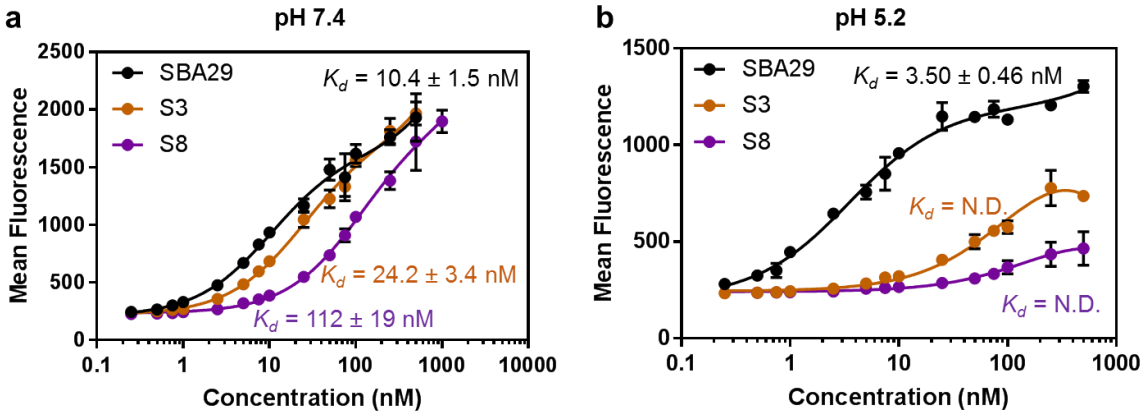

Figure 4.5. Bead-based binding measurements at (a) pH 7.4 and (b) pH 5.2, for aptamer SBA29 and pH switching aptamers, S3 and S8. Aptamer particles for each sequence were incubated with streptavidin-phycoerythrin and fluorescence intensity was measured using flow cytometry. The error bars were determined from the standard deviation of experimental replicates (n = 2 for SBA29, pH 5.2, n = 3 for all other samples). (N.D. = not determined)

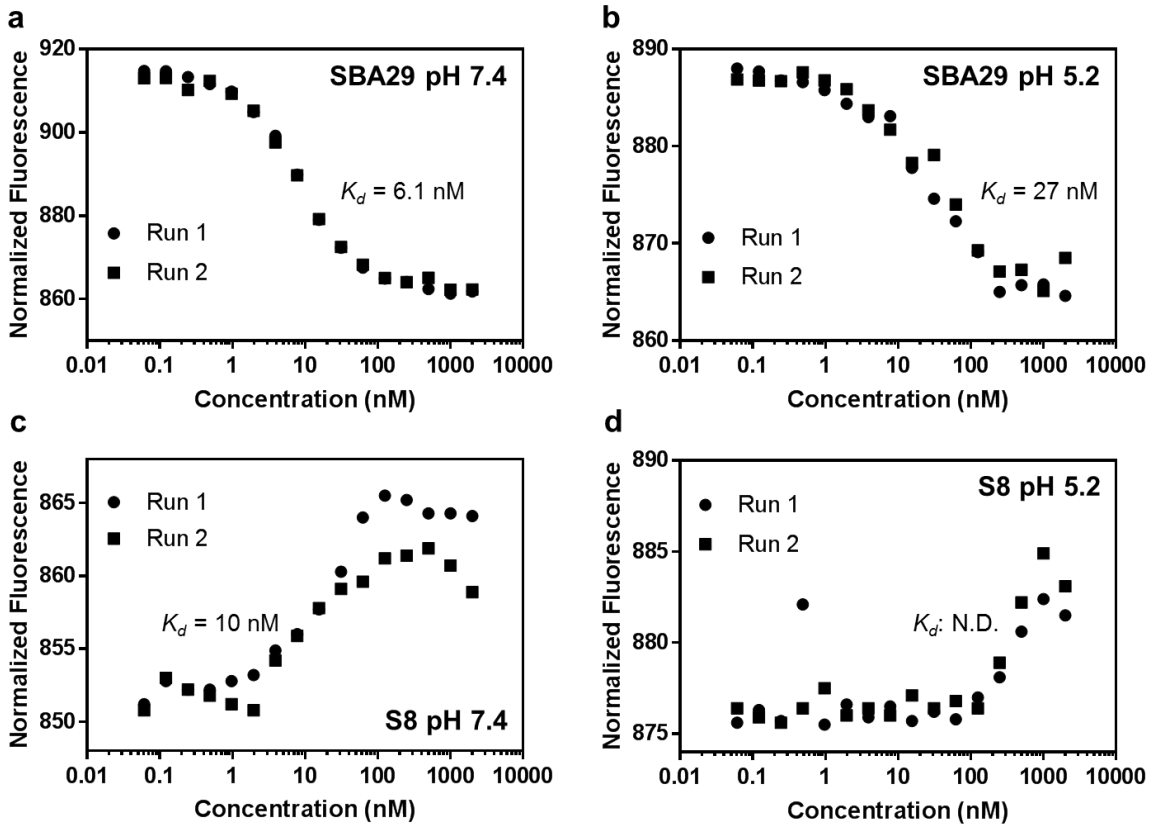

Figure 4.6. Binding measurements by microscale thermophoresis for (a) SBA29 at pH 7.4, (b) SBA29 at pH 5.2, (c) S8 at pH 7.4, and (d) S8 at pH 5.2. No bound plateau was reached for S8 binding measured at pH 5.2, so the K_d could not be determined reliably.

Predicted secondary structures for aptamer S8 are shown in **Figure 4.7** (obtained using Mfold).[20] The structure with the lowest free energy shows correct folding of the SBA29 aptamer region (**Fig. 4.7a**). However, in the structure with the second lowest free energy, the random region hybridizes with the SBA29 aptamer region, preventing the original aptamer domain from folding (**Fig. 4.7b**). We hypothesize that the first structure is more stable at pH 7.4, and that the second (blocked) structure is stabilized at pH 5.2. The blocked structure has a predicted G-A mismatch, a pairing which has been shown to be stabilized at acidic pH, both experimentally and computationally.[21–23] There is a second predicted mismatch (C-T), which has been shown to be pH insensitive.[21]

To identify the pH active domain, we tested the S8 aptamer with various point mutations predicted to affect the stability of the blocked structure (**Fig. 4.8a**). The mutated positions are shown in **Figure 4.8b**. Three types of mutations were introduced: (1) mismatch replaced with base pair, (2) mismatch replaced with another mismatch, and (3) base pair replaced with mismatch stabilized at low pH. We expected that replacing the mismatches at positions 61 and 62 with correctly matched base pairs would stabilize the blocked structure, leading to low binding at both pH 7.4 and pH 5.2. These two mutations (G61 and T62) greatly reduced binding at pH 7.4. This supports the hypothesis that the random region of S8 is hybridizing to the SBA29 domain, preventing binding to streptavidin. Replacing the mismatches at positions 61 and 62 with other mismatches (A61, A62, C62) also reduced the binding at pH 7.4. Notably, replacing the G-A mismatch with a C-A mismatch significantly reduces binding at pH 7.4, even though C-A is also stabilized at acidic pH.[21,23] The last three mutations replaced a G-C pair with a C-A or G-A mismatch (A59, A65, A67). Sequence A59 had high binding at both pH conditions, likely because the elimination of the G-C pair significantly destabilized the stem of the blocked structure and caused the SBA29 domain to fold at both pH values. The sequences with a second G-A mismatch added to the stem of the blocked structure (A65, A67) retained high binding at pH 7.4, but also had higher binding at pH 5.2. This is likely because the G-C pair is more stable than the G-A mismatch, even at acidic pH, so the stem is less stable. Despite this, some pH sensitivity remains for these sequences.

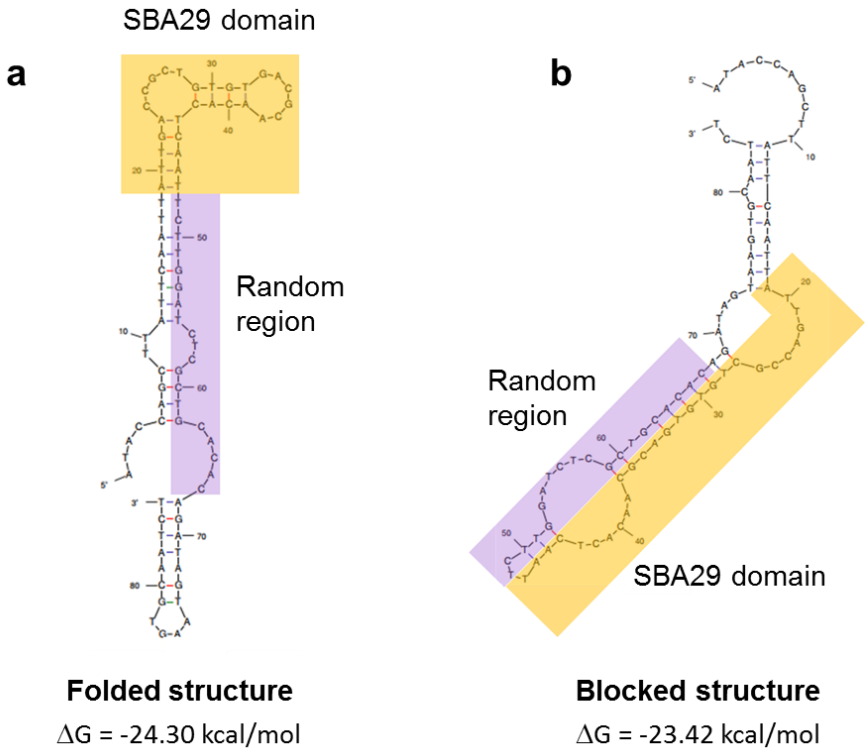

Figure 4.7. Predicted secondary structures for pH switching aptamer S8. (a) The SBA29 aptamer domain (highlighted in yellow) is folded correctly in the lowest free energy structure and does not interact with the random region (purple). (b) Another predicted low free energy structure for the same sequence (right) shows the SBA29 domain (yellow) blocked by the random region domain (purple).

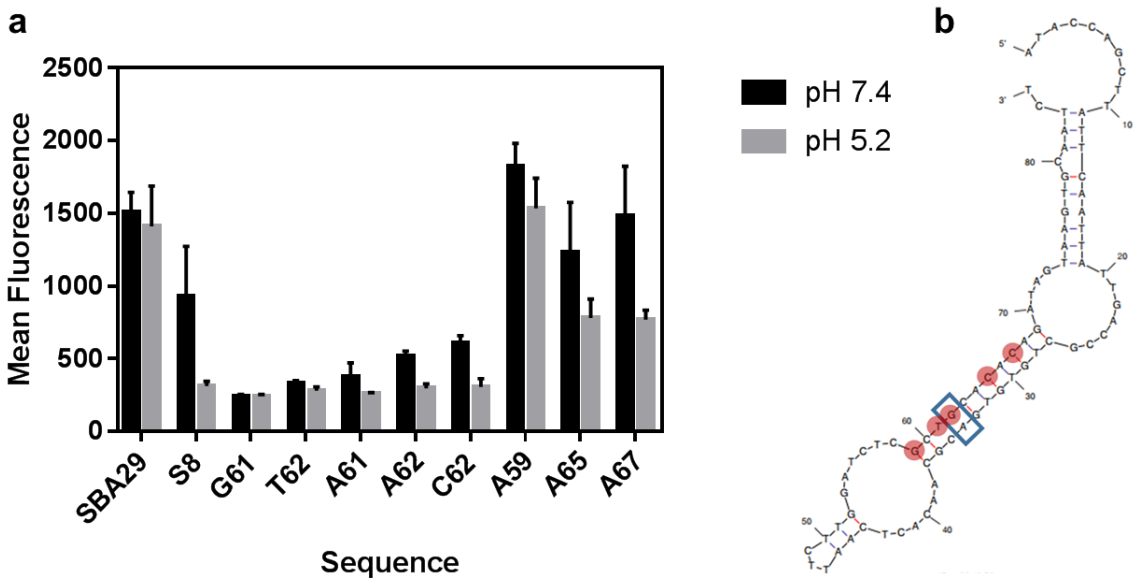

Figure 4.8. (a) Bead-based binding assay of S8 mutant sequences at 50 nM streptavidin. Three experimental replicates were performed, and mean + SD is shown. (b) Predicted blocked structure of pH switching aptamer S8 with mutation positions shown in red. The G-A mismatch predicted to stabilize this structure at pH 5.2 is outlined in blue.

D. Conclusions

In this work, we have developed the first method to isolate pH switching aptamers using directed evolution. We have discovered pH sensitive aptamers for streptavidin. For the top aptamer, S8, we have identified the pH active domain and proposed a mechanism for its pH switching behavior. Interestingly, the pH switching behavior of S8 is driven by a completely different interaction than the commonly used i-motif. The i-motif is made up of intercalated C-C^+ pairs, while S8 undergoes significant structural changes based on the pH stability of a G-A pair. Particle display for pH switching aptamers can be readily adapted to isolate aptamers for other targets in order to produce highly functional aptamers for use in drug delivery and pH sensing applications.

E. Experimental section

1. Reagents

Oligos were purchased from IDT with standard desalting. Streptavidin Alexa Fluor 488 conjugate was purchased from ThermoFisher Scientific, and streptavidin-phycoerythrin was purchased from Invitrogen.

The SBA29 aptamer sequence used was 5'-ATT GAC CGC TGT GTG ACG CAA CAC TCA AT-3'. The library sequence was 5'- ATA CCA GCT TAT TCA ATT ATT GAC CGC TGT GTG ACG CAA CAC TCA AT- N20 – AGA TAG TAA GTG CAA TCT-3'.

2. Screen conditions

Forward primer conjugated magnetic particles and monoclonal aptamer particles were made as described previously (Chapter II, Section E). Prior to incubation, the aptamer particles were annealed in the thermocycler using the following conditions: 95^{o}C for 5 min, 5% ramp, 4^{o}C for 5 min. The aptamer particles were incubated with 200 nM streptavidin Alexa Fluor 488 (SA-AF488) conjugate (same concentration for all three rounds) in pH 7.4 selection buffer (PBSMCT: 1x PBS, 2.5 mM $MgCl_2$, 1 mM $CaCl_2$, 0.01% Tween 20) in a final volume of 1 mL for 1-2 hours on a rotator in the dark at room temperature. After incubation, the particles were washed once and resuspended in 1 mL selection buffer, pH 7.4. The sample was sonicated and then measured on the flow cytometer (BD, FACSAria III). Aptamer particles with high fluorescence intensity were collected in each round (430,000 events in the first round, 65,000 events in the second round, and 18,000 events in the third round). For the first round, all aptamer particles with fluorescence intensity above the background were collected. The stringency was increased in the next round; the sort gate was shifted to the right, and the top 10% of aptamer particles were collected in the second round.

In the third round, binding to the target was lower, so all particles with fluorescence above the background were collected (1.4%). The collected particles were transferred to a 1.5 mL tube and placed on a magnetic rack for 5 min and the supernatant was removed. In the first two rounds, the particles were resuspended in 200 nM SA-AF488 in pH 5.2 selection buffer (PBSMCT, adjusted to pH 5.2 with NaOH) in a final volume of 250-500 µL, and incubated on a rotator in the dart at room temperature for 30 min. The particles were washed once and resuspended in 1 mL selection buffer, pH 5.2. The sample was sonicated and then measured on the flow cytometer. For the second sort, all "dark" beads were collected, so any aptamer particles that bound SA-AF488 at pH 5.2 were eliminated. In the second sort, 40,000 and 3,000 events were collected in the first and second rounds, respectively. Aptamer particles collected from the second sort were amplified to regenerate the aptamer pool for the following round. A second sort was not performed for the third round, so the aptamer particles were amplified immediately after the first sort.

3. Next generation sequencing of the enriched aptamer pools

The aptamer pools from all three rounds were indexed and prepared for sequencing according to the *16S Metagenomic Sequencing Library Preparation* guide by Illumina. Adaptor sequences were ordered from IDT. NGS was performed using an Illumina MiSeq system. The FASTAptamer toolkit was used to calculate the copy number and enrichment of each sequence.

4. Screening aptamer candidates

Ten candidate sequences were ordered from IDT (**Table 4.2**). Aptamer particles were generated for each sequence. Bead-based fluorescence assays were performed to measure the binding affinity of each aptamer to streptavidin. A different streptavidin conjugate

(Phycoerythrin) was used to characterize the binding that was used during the screen to ensure the aptamer was not interacting with the Alexa Fluor 488.

S1	ATTGACCGCTGTGTGACGCAACACTCAATTATTATGTCTTTTTTGTTTT
S2	ATTGACCGCTGTGTGACGCAACACTCAATATTCCCATCTCATGACGTCG
S3	ATTGACCGCTGTGTGACGCAACACTCAATACCTTCTCAACGTTCTCTGT
S4	ATTGACCGCTGTGTGACGCAACACTCAATCCCCTCTATCCGTCCGTCTG
S5	ATTGACCGCTGTGTGACGCAACACTCAATGTCCTCGTCCCGCAGACTAA
S6	ATTGACCACTGTGTGACGCAACACTCAATATATGCAGAAGCCTCCCCGT
S7	ATTGACCGCTGTGTGACGCAACACTCAATCGTCTAAGTAGAGATGGTCT
S8	ATTGACCGCTGTGTGACGCAACACTCAATTCTTGGATCTCGCTGCACAC
S9	ATTGACCGCTGTGTGACGCAACACTCAATACATTGCGAAATGGTTCCCG
S10	ATTGACCGCTGTGTGACGCAACACTCAATAAATTCTGGCACTCTACCGT

Table 4.2. Sequences of aptamer candidates synthesized and tested for pH switching. Primer binding regions are not shown. The SBA29 domain is shown in black, and the random region is shown in red.

5. Binding affinity measurement of pH switching aptmaers

Binding curves were generated using bead based fluorescence assays for the aptamer candidates, S3 and S8, and for the original aptamer, SBA29. K_d was determined based on a saturation binding model (one site-total binding) using GraphPad Prism 7.

Microscale thermophoresis was performed by 2bind to measure the binding affinity of S8 and SBA29 to streptavidin at pH 7.4 and pH 5.2. For each experiment, a serial dilution of the streptavidin was prepared (final concentration 61 pM to 2 µM) and mixed with Cy5-labeled aptamer (final concentration held constant at 5 nM). The samples were analyzed on a Monolith NT.115 Pico at 25 ^{o}C, with 5% LED power and 60% laser power.

6. Mutation study to identify pH active motif for aptamer S8

The predicted structures were generated using mfold, with salt conditions similar to the selection buffer (137 mM Na^+, 2.5 nM Mg^{2+}). S8 point mutants were ordered from IDT. Bead-based fluorescent measurements were performed to test the binding of each sequence to streptavidin.

G61	ATTGACCGCTGTGTGACGCAACACTCAATTCTTGGATCTCGCGGCACAC
T62	ATTGACCGCTGTGTGACGCAACACTCAATTCTTGGATCTCGCTTCACAC
A61	ATTGACCGCTGTGTGACGCAACACTCAATTCTTGGATCTCGCAGCACAC
A62	ATTGACCGCTGTGTGACGCAACACTCAATTCTTGGATCTCGCTACACAC
C62	ATTGACCGCTGTGTGACGCAACACTCAATTCTTGGATCTCGCTCCACAC
A59	ATTGACCGCTGTGTGACGCAACACTCAATTCTTGGATCTCACTGCACAC
A65	ATTGACCGCTGTGTGACGCAACACTCAATTCTTGGATCTCGCTGCAAAC
A67	ATTGACCGCTGTGTGACGCAACACTCAATTCTTGGATCTCGCTGCACAA

Table 4.3. Sequences of aptamer S8 mutants. Primer binding regions are not shown. The mutated base for each sequence is shown in red.

F. References

1. Casey JR, Grinstein S, Orlowski J. Sensors and regulators of intracellular pH. *Nat Rev Mol Cell Biol*. 2010;11(1):50-61. doi:10.1038/nrm2820.
2. Schmaljohann D. Thermo- and pH-responsive polymers in drug delivery. *Adv Drug Deliv Rev*. 2006;58(15):1655-1670. doi:10.1016/j.addr.2006.09.020.
3. Mura S, Nicolas J, Couvreur P. Stimuli-responsive nanocarriers for drug delivery. *Nat Mater*. 2013;12(11):991-1003. doi:10.1038/nmat3776.
4. Modi S, Nizak C, Surana S, Halder S, Krishnan Y. Two DNA nanomachines map pH changes along intersecting endocytic pathways inside the same cell. *Nat Nanotechnol*. 2013;8(6):459-467. doi:10.1038/nnano.2013.92.
5. Chakraborty K, Leung KH, Krishnan Y. High lumenal chloride in the lysosome is critical for lysosome function. *Elife*. 2017;6:1-21. doi:10.7554/eLife.28862.
6. Kuhn W, Hargitay B, Katchalsky A, Eisenberg H. Reversible dilation and contraction by changing the state of ionization of high-polymer acid networks. *Nature*. 1950;165(4196):514-516. doi:10.1038/165514a0.

7. Luppi B, Cerchiara T, Bigucci F, Orienti I, Zecchi V. pH-sensitive polymeric physical-mixture for possible site-specific delivery of ibuprofen. *Eur J Pharm Biopharm*. 2003;55(2):199-202. doi:10.1016/S0939-6411(02)00190-X.

8. Lee ES, Gao Z, Kim D, Park K, Kwon IC, Bae YH. Super pH-sensitive multifunctional polymeric micelle for tumor pHe specific TAT exposure and multidrug resistance. *J Control Release*. 2008;129(3):228-236. doi:10.1016/j.jconrel.2008.04.024.

9. Du JZ, Du XJ, Mao CQ, Wang J. Tailor-Made dual pH-sensitive polymer-doxorubicin nanoparticles for efficient anticancer drug delivery. *J Am Chem Soc*. 2011;133(44):17560-17563. doi:10.1021/ja207150n.

10. Wu H, Zhu L, Torchilin VP. pH-sensitive poly(histidine)-PEG/DSPE-PEG co-polymer micelles for cytosolic drug delivery. *Biomaterials*. 2013;34(4):1213-1222. doi:10.1016/j.biomaterials.2012.08.072.

11. Day HA, Pavlou P, Waller ZAE. I-Motif DNA: Structure, stability and targeting with ligands. *Bioorganic Med Chem*. 2014;22(16):4407-4418. doi:10.1016/j.bmc.2014.05.047.

12. Shi L, Peng P, Du Y, Li T. Programmable i-motif DNA folding topology for a pH-switched reversible molecular sensing device. *Nucleic Acids Res*. 2017;45(8):4306-4314. doi:10.1093/nar/gkx202.

13. Ni X, Castanares M, Mukherjee A, Lupold SE. Nucleic Acid Aptamers: Clinical Applications and Promising New Horizons. *Curr Med Chem*. 2011;18(27):4206-4214. doi:10.2174/092986711797189600.

14. Sundaram P, Kurniawan H, Byrne ME, Wower J. Therapeutic RNA aptamers in clinical trials. *Eur J Pharm Sci*. 2013;48(1-2):259-271. doi:10.1016/j.ejps.2012.10.014.

15. Fong FY, Oh SS, Hawker CJ, Soh HT. In Vitro Selection of pH-Activated DNA Nanostructures. *Angew Chemie - Int Ed*. 2016;55(49):15258-15262. doi:10.1002/anie.201607540.

16. Bing T, Yang X, Mei H, Cao Z, Shangguan D. Conservative secondary structure motif of streptavidin-binding aptamers generated by different laboratories. *Bioorganic Med Chem*. 2010;18(5):1798-1805. doi:10.1016/j.bmc.2010.01.054.

17. Jørgensen AS, Hansen LH, Vester B, Wengel J. Improvement of a streptavidin-binding aptamer by LNA- and α-l-LNA-substitutions. *Bioorganic Med Chem Lett*. 2014;24(10):2273-2277. doi:10.1016/j.bmcl.2014.03.082.

18. Ouellet E, Lagally ET, Cheung KC, Haynes CA. A simple method for eliminating fixed-region interference of aptamer binding during SELEX. *Biotechnol Bioeng*. 2014;111(11):2265-2279. doi:10.1002/bit.25294.

19. Wang J, Gong Q, Maheshwari N, et al. Particle Display: A Quantitative Screening Method for Generating High-Affinity Aptamers. *Angew Chemie*. 2014;126(19):4896-4901. doi:10.1002/ange.201309334.

20. Zuker M. Mfold web server for nucleic acid folding and hybridization prediction. *Nucleic Acids Res*. 2003;31(13):3406-3415. doi:10.1093/nar/gkg595.

21. Brown T, Leonard GA, Booth ED, Kneale G. Influence of pH on the conformation and stability of mismatch base-pairs in DNA. *J Mol Biol*. 1990;212(3):437-440. doi:10.1016/0022-2836(90)90320-L.

22. Lee JA, DeRosa MC. A pH-driven DNA switch based on the A+·G mispair. *Chem Commun*. 2010;46(3):418-420. doi:10.1039/B918725A.

23. Jissy AK, Datta A. Designing molecular switches based on DNA-base mispairing. *J Phys Chem B*. 2010;114(46):15311-15318. doi:10.1021/jp106732u.

Chapter V. Conclusion

High quality affinity reagents are essential for molecular recognition in many contexts, including biological research and diagnosis, monitoring, and treatment of disease. The three projects discussed here demonstrate that particle display is an effective method for discovering highly functional aptamers. A high affinity aptamer was identified for a tumor biomarker, p32, using the existing particle display method. Two methods were developed that expanded the capabilities of the particle display platform: Click-PD and PD for pH switching aptamers. Click-PD allows screening for non-natural aptamers, using only commercially available nucleotides and polymerases. Using this method, we generated a non-natural DNA aptamer with extremely high affinity and specificity to Con A. Aptamers with pH dependent binding to streptavidin were generated, and a mechanism for pH switching was proposed and evaluated for the top aptamer. Together, these methods offer a significant improvement over traditional aptamer discovery techniques. This chapter will briefly highlight potential future directions for each of these projects.

For the p32 screen, analysis and characterization is ongoing. Next generation sequencing offers much deeper information about the progress of the experiment and the resulting aptamers. We plan to identify other aptamer candidates for testing. We also plan to study the evolution of the aptamer pool from round to round and investigate strategies for streamlining the aptamer discovery process. To determine if p32-2 or another aptamer is functional *in vivo*, several stages of work are still required. Cell binding assays must be performed *in vitro* to ensure that the aptamer binds membrane bound p32. Developing aptamers for cell surface receptors can be challenging, as the soluble form of the protein used for selection can have a very different structure than the native protein. Second, the aptamer

must be tested for binding *in vivo*. The aptamer must bind to p32 on tumor cells and avoid any problematic off-target binding. Finally, the aptamer must be tested for efficacy. To be an effective reagent, the aptamer needs to either bind p32 and deliver a payload to the cell or to act as a therapeutic itself. Beyond this project, there is great potential for using particle display to generate aptamers for other disease biomarkers. In the future, better methods for performing selections with cells or tissues are needed to more reliably generate functional aptamers and to discover new biomarkers.

Click-PD has great potential to be used to incorporate countless modifications. We are currently studying amino acid-like modifications as well as short peptides. Work is ongoing in our lab to isolate non-natural aptamers to lectins, glycans, and other small molecules of great biological interest. Future work is needed to continue to develop strategies for choosing the most effective modification for a particular target. Another potential direction is performing two orthogonal chemical reactions after PCR to further increase the chemical diversity of DNA.

For pH switching PD, we are continuing to validate this method to demonstrate that it is a versatile platform for generating pH switching aptamers. For the next phase of this work, we plan to use this method to generate aptamers for other targets with biological applications. The two classes of targets that would be most interesting are drugs and cell surface receptors. A pH sensitive aptamer for a drug, such as doxorubicin, could release the drug once it is internalized into the more acidic endosome. pH sensitive aptamers for cell surface receptors could bind to the receptor and be released upon internalization. This would be interesting for drug delivery or for measuring the pH along different cellular pathways.

In this work, we have demonstrated solutions to several critical problems with traditional aptamer discovery methods. By developing better methods, we enable the isolation of high quality affinity reagents for a broader range of targets. Ultimately, this will provide valuable tools for detecting and curing disease.